LUNA VIGGIANO DE ALVARENGA

DESMONOSTOC SALINUM CCM-UFV059, A NOVEL CYANOBACTERIA FROM A SALINE-ALKALINE LAKE: MOLECULAR AND PHYSIOLOGICAL RESPONSES TO LIGHT, DESICCATION AND SALT STRESS

Thesis submitted to the Plant Phisiology Program of the Universidade Federal de Viçosa as part of the requirements for obtaining the degree of *Doctor Scientiae.*

VIÇOSA
MINAS GERAIS - BRASIL
2019

Ficha catalográfica preparada pela Biblioteca Central da Universidade Federal de Viçosa - Câmpus Viçosa

T
A473d
2019

Alvarenga, Luna Viggiano de, 1989-
Desmonostoc salinum CCM-UFV059, a novel cyanobacteria froma saline-alkaline lake : molecular and physiological responses to light, desiccation and salt stress / Luna Viggiano de Alvarenga. – Viçosa, MG, 2019.
viii, 112 f. : il. (algumas color.) ; 29 cm.

Texto em inglês.
Orientador: Wagner Luiz Araújo.
Tese (doutorado) - Universidade Federal de Viçosa.
Inclui bibliografia.

1. Cianobactéria. 2. Stress (Fisiologia). 3. Biomassa. I. Universidade Federal de Viçosa. Departamento de Biologia Vegetal. Programa de Pós-Graduação em Fisiologia Vegetal. II. Título.

CDD 22. ed. 579.82

LUNA VIGGIANO DE ALVARENGA

DESMONOSTOC SALINUM CCM-UFV059, A NOVEL CYANOBACTERIA FROM A SALINE-ALKALINE LAKE: MOLECULAR AND PHYSIOLOGICAL RESPONSES TO LIGHT, DESICCATION AND SALT STRESS

Thesis submitted to the Plant Phisiology Program of the Universidade Federal de Viçosa as part of the requirements for obtaining the degree of *Doctor Scientiae*.

APPROVED: February 22th, 2019.

Marcelo Gomes Marçal Vieira Vaz
(Co-Adviser)

Alberto Abrantes Esteves Ferreira

Dimas Mendes Ribeiro

Marcio Arêdes Martins

Wagner Luiz Araújo
(Adviser)

ACKNOWLEDGEMENTS

My first and greatest thanks always goes to God, who, even though I do not deserve, gives me his merciful grace in a daily basis.

To my father Roberto, thank you for your patience, guidance and unconditional love. He is my rock, and he rocks!

To my sisters Duda, Carmem, Marina and Maria, I'm so thankful for having you in my life. I cannot imagine life without my four little sis.

To my grandparents, Lea and José, for respecting my choices and making me feel loved in the most decisive phase of my life, they gave me roots and for that I will always be grateful.

To my grandparents, Sonia and Diogenes, for teaching me the value of affection and the daily dedication in life.

My aunt Zana, thanks for being such a strong person. I am extremely grateful to have her in my life and every day I learn a little more with her.

To my dearest friends Priscila Schultz, Karla Gasparini, Rodolfo Santos and Raphael Wakin, thanks for staying by my side during hard times. 'A faithful friend is a powerful protection: whoever found it, discovered a treasure.' Ec. 6:14

To Professor Wagner L. Araújo, for the orientation, friendship and dedication. We had quite a journey together and it was essential for my growth.

To Professor Martin Hagemann, for making this last year possible and for always being willing to help and sharing his wisdom with me.

To Professors Adriano Nunes Nesi, Agustin Zsögön and Dimas Ribeiro for the friendship and all support given during this period.

To the Professor and coordinator of the program, Fábio M. DaMatta, for the friendship and to make available the structure of his laboratory whenever required.

To Dr. Marcelo Vaz and Dr. Alberto Abrantes, thanks for all the support, scientific discussion and patience during all these years. I feel very lucky for having both during this period.

To Allan, Naira and Jean, for the friendship. The Cyanotops rocks!

To friends and colleagues of the UCP research group, for the companionship and attention, making my days funnier.

To the PUR friends, Stefan Lucius, Dr. Eva Brouwer, Shanshan Song, Maria Wittmiß, Manja Henneberg, Kris Hippler, Dr. Stefan Timm, Saskia Schwab and Ole Reinholdt for the friendship, barbecues, "Schnaps" and coffee breaks. Thanks for welcoming me with open arms and for making the year of 2018 memorable.

To the technicians and plant physiology workers, Rogério Gomide, Carlos Raimundo, Antônio Cordeiro, Mercês, Marcele and Luciene for always helping me with a smile on their face.

To the Universidade Federal de Viçosa and the Plant Physiology Graduate Program for the support during my PhD.

To FAPEMIG and CNPq/DAAD for granting the scholarships, allowing this research to happen. This study was also partially financed by the Coordenação de Aperfeiçoamento de Pessoal de Nível Superior – Brasil (CAPES) – Finance code 001.

BIOGRAPHY

Luna Viggiano de Alvarenga, daughter of Roberto Coelho de Alvarenga and Lucia Maria Viggiano, was born on June 10th, 1989, in Viçosa, Minas Gerais, Brazil. In 2007 she completed elementary education at the Marista Dom Silvério in Belo Horizonte.

In August of 2013 she graduated in Biological Sciences at the Universidade Federal de Viçosa. In the same month, she began her Masters studies at Plant Physiology Graduate Program in the same university.

In February of 2015 she obtained the title of *Master Scientiae*, beginning her PhD studies in March of 2015 at the Plant Physiology Graduate Program, at the Universidade Federal de Viçosa. Between February of 2018 and January of 2019 she perform part of her research as a guest PhD under a PhD sandwich program at the Universität Rostock, Germany. In February 2019 she defended her *Doctor Scientiae* thesis.

INDEX

ABSTRACT

ALVARENGA, Luna Viggiano de, D.Sc., Universidade Federal de Viçosa, February, 2019. ***Desmonostoc salinum* CCM-UFV059, a novel cyanobacteria from a saline-alkaline lake: Molecular and physiological responses to light, desiccation and salt stress.** Adviser: Wagner Luiz Araújo. Co-Adviser: Marcelo Gomes Marçal Viera Vaz.

Cyanobacteria are widespread photosynthetic prokaryotes and are among the oldest organisms on Earth. During their long evolution, cyanobacteria developed an enormous diversity in terms of morphology, metabolic plasticity and molecular properties, which seems to be important factors to cope with limiting environmental conditions and allowed their ecological success in almost all known photic ecosystems. The first part of this work consisted of the taxonomic characterization, using the polyphasic approach, of the strain *Desmonostoc salinum* CCM-UFV059, a filamentous heterocytous cyanobacterium isolated from a hypersaline lake. Taken together, our data allowed the description of a new species and the first strain of the *Desmonostoc* genus from a saline environment. The second part of this work aimed to decipher the main salt acclimation mechanisms present in *Desmonostoc salinum* CCM-UFV059, because most studies on cyanobacterial salt acclimation have been carried out on unicellular strains, which cannot fix N_2. We performed a comparative study using the model strain *Nostoc* PCC7120, and we could observe a remarkable high salt tolerance displayed by *Desmonostoc salinum* CCM-UFV059. In cells of *Desmonostoc salinum* CCM-UFV059 the intracellular sodium content was significantly lower than in *Nostoc* PCC7120 and these cells were able to sustain photosynthetic activity up to 0.5 M NaCl while *Nostoc* PCC7120 cells were not. Moreover, *Desmonostoc salinum* CCM-UFV059 induced sucrose over-accumulation under desiccation stress conditions, which allowed this strain to survive harsh desiccation stress. Together with the presence of highly unsaturated lipids in the membrane, the high sucrose production and the intense export of sodium could explain, at least partially, how *Desmonostoc salinum* CCM-UFV059 is capable of acclimate to high salinities and to resist longer desiccation periods. Collectively, our results provide the first insights into the physiological adaptations explaining the remarkable high salt and desiccation tolerance presented by this strain. Furthermore, given that cyanobacteria have several biotechnological applications, such as the production of biomass for human and animal consumption, and metabolites of industrial interest, the third part of this work was performed to analyze the physiological and metabolic responses of *Desmonostoc*

salinum CCM-UFV059 submitted to different light availabilities, aiming at finding the light regime suitable for maximal biomass production as well as to better understand how distinct growth conditions may interfere within the basal metabolism. Collectively our results indicate that *Desmonostoc salinum* CCM-UFV059 display a highly plastic metabolism and the ability to grow in a large range of light regimes, that open the possibility to outdoor cultivation and commercial use of this species that has a great biotechnological potential. Notwithstanding, further research is clearly required in order to enable a large scale cultivation of *Desmonostoc salinum* CCM-UFV059.

RESUMO

ALVARENGA, Luna Viggiano de, D.Sc., Universidade Federal de Viçosa, Fevereiro de 2019. ***Desmonostoc salinum*** **CCM-UFV059, uma nova cianobactéria: Respostas moleculares e fisiológicas a luz, dessecação e stress salino.** Orientador: Wagner Luiz Araújo. Coorientador: Marcelo Gomes Marçal Viera Vaz.

Cianobactérias são procariotos fotossintetizantes e estão entre os organismos mais antigos da Terra. Durante sua longa evolução, as cianobactérias desenvolveram uma enorme diversidade em termos de morfologia, plasticidade metabólica e propriedades moleculares, fatores importantes para lidar com condições ambientais limitantes e que permitiram o sucesso ecológico deste grupo em quase todos os ambientes. A primeira parte deste trabalho consistiu na caracterização taxonômica da cepa *Desmonostoc salinum* CCM-UFV059, uma cianobactéria filamentosa heterocitada isolada de um ambiente hipersalino. Em conjunto, os dados obtidos permitiram a descrição da primeira cepa do gênero *Desmonostoc* oriunda de um ambiente salino. Como a maioria dos estudos sobre aclimatação ao sal em cianobactérias foi realizada em linhagens unicelulares, que não podem fixar N_2, a segunda parte deste trabalho focou na identificação dos principais mecanismos de aclimatação ao sal empregados por *Desmonostoc salinum* CCM-UFV059. Para tanto, foi realizado um estudo comparativo utilizando a cepa modelo *Nostoc* PCC7120. Com efeito, células de *Nostoc* PCC7120 apresentaram teor intracelular de sódio quatro vezes maior que células de *Desmonostoc salinum* CCM-UFV059, sendo estas últimas capazes de sustentar a atividade fotossintética até 0,5 M de NaCl, concentração essa na qual *Nostoc* PCC7120 não mais apresentava atividade fotossintética. Além disso, *Desmonostoc salinum* CCM-UFV059 produziu grande concentração de sacarose em resposta a limitação hídrica, o que permitiu a sobrevivência dessa cepa ao estresse severo de dessecação. A presença de lipídios altamente insaturados concomitantemente com uma alta produção de sacarose e capacidade de manter o sódio fora das células, explicam, ao menos parcialmente, a capacidade de *Desmonostoc salinum* CCM-UFV059 em se adaptar a altas salinidades e resistir a longos períodos de dessecação. Coletivamente, os resultados obtidos fornecem informações iniciais sobre adaptações fisiológicas que explicariam a notável tolerância ao sal e a dessecação pela espécie *Desmonostoc salinum* CCM-UFV059. Devido as potenciais aplicações biotecnológicas apresentadas por cianobactérias, incluindo a produção de biomassa para consumo humano e animal além de metabólitos de interesse industrial, a terceira parte deste trabalho buscou

investigar as respostas fisiológicas e metabólicas de *Desmonostoc salinum* CCM-UFV059 frente à diferentes disponibilidades de luz e fotoperíodo, visando encontrar o regime de luz adequado para a máxima produção de biomassa e também compreender melhor como distintas condições de crescimento interferem no metabolismo basal dessa cianobactéria. Em síntese, *Desmonostoc salinum* CCM-UFV059 possui uma alta plasticidade metabólica podendo ser cultivada em uma ampla gama de regimes luminosos, o que possibilitaria o cultivo aberto e uso comercial dessa espécie, que apresenta grande potencial biotecnológico. Não obstante, estudos são ainda necessários para viabilizar o cultivo e uso de *Desmonostoc salinum* CCM-UFV059 em larga escala.

GENERAL INTRODUCTION

Cyanobacteria are photosynthetic microorganisms present in almost all environments on Earth, including marine waters, fresh water, desert soils, glaciers, and hot springs. The "Endosymbiotic Theory" attributes to this group the evolution of oxygenic photosynthesis and an essential role for life development, as it is the endosymbionts for photosynthetic plastids in eukaryotic phototrophs (Hohmann-Marriott and Blankenship, 2011). During their long-term evolution, cyanobacteria evolved an enormous diversity in terms of morphology, metabolic plasticity and molecular properties, which seems to be important factors to cope with limiting environmental conditions, allowing their ecological success in photic environments (Beck et al., 2012). It should be kept in mind that in order to survive in diverse habitats comprising various environmental factors such as temperature, light, water availability, pH, and even salts, cyanobacteria should display a highly exquisite metabolic acclimation.

The natural diversity of cyanobacteria and their ability to grow in a variety of habitats, such as areas not suitable for agriculture, always sparks interest in characterizing new strains of this group for their potential of biomass and biofuels production. Furthermore, compared with land plants, cyanobacteria presents higher photosynthetic efficiency, rapid cell growth, basic nutritional requirements (sunlight, water and CO_2 mainly) and the possibility of genetic manipulation (Parmar et al., 2011), making them useful organisms for a number of industrial applications. Cyanobacteria also share physiological traits with land plants beyond photosynthetic reactions (e.g. phytohormones) (Deusch et al., 2008), and thus these microorganisms have been widely recognized as useful model systems for the investigation of environmental stress responses among plants (Orf et al., 2016). Previously to their modern application as industrial substrate, physiological model for plants or resistance gene bank, cyanobacteria have been used for centuries in non-Western culture for nourishment, with several records in history (Farrar, 1966; Ciferri, 1983; Takenaka et al., 1998). Moreover, the implementation of cyanobacteria in Western diets has been strongly discussed during the last decades due to the search for new sources of proteins and there is already both production of and a market for cyanobacteria as food supplements around the world. The genus *Spirulina* is, for instance, the principal cyanobacteria cultivated for these purposes (Sandrin et al., 2009). One of the great

advantages of using *Spirulina* in food is that up to 70 % of its dry weight are proteins that contain all essential amino acids for the human body. In addition to being a source of high quality protein, *Spirulina* is considered a vitamin and mineral "gold mine", presenting high contents of β-carotene, iron, vitamin B12, and glycogen (a natural source of energy) (Soni et al., 2017). These are few reasons why NASA has considered the use of *Spirulina* as a food of choice for space flights and the United Nations (UN) consider *Spirulina* as a possible solution to global protein shortages (Becker, 2007). It is worth to mention that the future mass cultivation of cyanobacteria for biotechnological or feeding purposes should be probably done in saline/brackish waters, avoiding competition with agriculture and human consumption. Notably, cyanobacteria growth in saline media could impact the cellular metabolism and perhaps product yield (Florian et al., 2013; Pade et al., 2016).

Salinity, as the total concentration of dissolved inorganic ions, is a major environmental stress and severely affects aquatic organisms, such as most cyanobacteria (Hagemann, 2011). Increased salt concentrations in the external environment promote increments in the ion concentration inside the cell due to water loss, reducing the water potential and increasing osmotic stress. At the same time, high concentrations of certain ions can have toxic effects on the cellular metabolism. As a result, salt stress always occurs in combination with osmotic stress. Nevertheless, physiological and biochemical aspects of acclimation to salt stress in cyanobacteria are widely recognized and can be commonly distinguished in two strategies namely 'salt-in' and 'salt-out' (Hagemann, 2013). The strategy 'salt-in' is only used by few halophilic organisms, from Archaea and Bacteria, and consists in the accumulation of high internal amounts of inorganic salts (especially KCl), exceeding the external salt concentration. The accumulation of inorganic ions is metabolically cheaper and able to ensure water uptake, turgor pressure, and growth (Oren et al., 2007). However, the presence of high salt concentrations in metabolically active compartments clearly requires an adaptation of all organic macromolecules to this new environment, which was seemingly difficult to achieve during evolution, and this assumption explains, at least partially, why the energetically favorable 'salt-in' strategy is restricted to only a few prokaryotes. The vast majority of organisms, including most cyanobacteria and all eukaryotes, use the "salt-out" strategy for acclimation to saline environments. This strategy maintains a low level of toxic inorganic ions such as Na^+ and Cl^- within the cytoplasm, avoiding damages to the metabolism (Hagemann, 2011). Cyanobacteria

normally use two basic processes in the so-called 'salt-out' strategy: (i) active export of toxic inorganic ions (Fulda et al., 2006; Hagemann, 2013), and (ii) accumulation of organic osmoprotective compounds, which do not interfere with the basal cellular metabolism (Marin et al. 2002; Hagemann, 2011). These osmoprotective compounds, commonly referred to as compatible solutes, help to maintain membrane integrity and stability of the cellular protein apparatus. Cyanobacteria can be distinguished in three groups according to the preferred osmoprotective compound. Cyanobacterial strains with low salt tolerance accumulate sucrose and/or trehalose, whereas moderate halotolerant strains use glucosylglycerol (GG); and halophilic strains, which have an absolute requirement for a minimal salt concentration, synthesize glycine betaine as a characteristic compatible solute (Klähn and Hagemann 2011).

The strain *Desmonostoc salinum* CCM-UFV059 is a filamentous heterocytous cyanobacterium, isolated from a benthic microbial mat occurring at the shore of a hypersaline lake (Laguna Amarga). The work presented here is largely focused on understanding how this strain can cope with high salt concentration. That being said, the main aims of this thesis were: *(i)* obtain a comprehensive metabolic and molecular overview of how and to which extent strain *Desmonostoc salinum* CCM-UFV059 is able to deal with salinity; *(ii)* provide the description of the first *Desmonostoc* strain isolated from a saline-alkaline lake, culminating with the erection of the new species, *Desmonostoc salinum* sp. nov. To reach these goals several different but complementary experimental approaches were undertaken and therefore this thesis is organized as a compilation of three independent stand-alone chapters containing an introduction and discussion as well as details of the methods used.

Thus, the first part of this research initiative consisted of the taxonomic characterization of the strain using the polyphasic approach coupling molecular characterization (16S rRNA phylogeny and 16-23S ITS secondary structures) with morphological, ecological and physiologic data. Taken together, our data allowed the description of the first *Desmonostoc* strain from a saline-alkaline lake, named *Desmonostoc salinum* sp. nov., under the provisions of the International Code of Nomenclature for Algae, Fungi and Plants. This finding extends the ecological coverage of the genus *Desmonostoc*, contributing to a better understanding of cyanobacterial diversity and systematic.

In the second part of this work, we pursued to identify mechanisms and key metabolites associated with the differential halotolerance observed in the strain

Desmonostoc salinum CCM-UFV059, allowing a better understanding of the strategies adopted by cyanobacteria to tolerate high salinity. Briefly, we observed that the LD_{50}, the value that represents the salt concentration capable of killing 50 % of cells after 72 h of exposure, was a concentration nine times higher (890 mM NaCl - de Alvarenga et al, 2018) than found in the model filamentous strain *Nostoc* sp. PCC7120 (Agrawal et al., 2014). Moreover, we observed that the intracellular sodium concentration, sucrose production and metabolite changes in response to salt stress, are responsible for the remarkable halotolerance presented by *Desmonostoc salinum* CCM-UFV059 and, surprisingly, by the desiccation tolerance also presented by this strain.

Once prokaryotes are highly susceptible to environmental fluctuations, they respond with drastic changes in their metabolism to even small variations in light quality and availability, nutrients, and inorganic ions (e.g. NaCl). In this context, in the third part of this work both physiological and metabolic responses of *Desmonostoc salinum* CCM-UFV059 were investigated under different light intensities and photoperiods, as well as under saline conditions. Our main goal was to discover the light regime suitable for maximal biomass production and to further understand how distinct growth conditions may interfere within the basal metabolism of this strain. Our results demonstrate an association between the macroscopic colony architecture of *Desmonostoc salinum* CCM-UFV059 and the predominant cellular type. We also demonstrate that relatively small variations in light intensity are able to modulate the storage metabolism of *Desmonostoc salinum* CCM-UFV059, without impacting the final biomass production.

Finally, in the last chapter of this thesis entitled “Concluding Remarks” I summarize the main findings of this work and provide a relatively brief but up to date discussion about the challenges and perspectives in enhancing our understanding of the taxonomy, physiology, and metabolism of this highly intriguing and specialized cyanobacterial strain, with the practical biotechnological applications of the strain *Desmonostoc salinum* CCM-UFV059.

REFERENCES

Agrawal C., Sen S., Singh S., Rai S., Singh P.K., Singh V.K., Rai L.C. (2014) Comparative proteomics reveals association of early accumulated proteins in conferring butachlor tolerance in three N2-fixing Anabaena spp. J Proteomics 96: 271–290.

Beck C., Knoop H., Axmann I. M. & Steuer R. (2012) The diversity of cyanobacterial metabolism: genome analysis of multiple phototrophic microorganisms. BMC Genomics 13(1): 56.

Becker, E. W. (2007) Micro-algae as a source of protein. Biotechnology Advances, 25(2), 207-210.

Ciferri O. (1983) Spirulina, the edible microorganism. Microbiological reviews 47(4): 551.

Deusch O., Landan G., Roettger M., Gruenheit N., Kowallik K. V., Allen J. F., Martin W. & Dagan T. (2008) Genes of cyanobacterial origin in plant nuclear genomes point to a heterocyte-forming plastid ancestor. Molecular Biology and Evolution 25 (4): 748-761.

Farrar W. (1966) Tecuitlatl; a glimpse of Aztec food technology. Nature, 211, 341-342.

Florian A., Araújo W.L., Fernie A.R. (2013) New insights into photorespiration obtained from metabolomics. Plant Biol 15: 656–666.

Fulda S., Mikkat S., Huang F., Huckauf J., Marin K., Norling B. & Hagemann M. (2006) Proteome analysis of salt stress response in the cyanobacterium Synechocystis sp. strain PCC 6803. Proteomics 6(9): 2733–2745.

Hagemann M. (2013) Genomics of salt acclimation: synthesis of compatible solutes among cyanobacteria. In: Chauvat F, Cassier Chauvat C (eds) Book series: Advances in Botanical Research, vol 65. Elsevier, San Diego, pp 27–55

Hagemann M. (2011) Molecular biology of cyanobacterial salt acclimation. FEMS Microbiology Reviews 35(1): 87-123.

Hohmann-Marriott, M. F., & Blankenship, R. E. (2011) Evolution of photosynthesis. Annual Review of Plant Biology, 62, 515-548.

Klähn, S., & Hagemann, M. (2011) Compatible solute biosynthesis in cyanobacteria. Environmental Microbiology, 13(3), 551-562.

Marin K., Huckauf J., Fulda S. & Hagemann M. (2002) Salt-dependent expression of glucosylglycerol-phosphate synthase, involved in osmolyte synthesis in the cyanobacterium synechocystis sp. strain PCC 6803. Journal of Bacteriology 184: 2870–2877.

Markou, G., & Georgakakis, D. (2011) Cultivation of filamentous cyanobacteria (blue-green algae) in agro-industrial wastes and wastewaters: a review. Applied Energy, 88(10), 3389-3401.

Oren, A. (2007) Diversity of organic osmotic compounds and osmotic adaptation in cyanobacteria and algae. In Algae and Cyanobacteria in Extreme Environments (pp. 639-655). Springer, Dordrecht.

Orf I., Timm S., Bauwe H., Fernie A. R., Hagemann M., Kopka J., & Nikoloski Z. (2016) Can cyanobacteria serve as a model of plant photorespiration?–a comparative meta-analysis of metabolite profiles. Journal of Experimental Botany, 67(10), 2941-2952.

Pade, N., Michalik, D., Ruth, W., Belkin, N., Hess, W. R., Berman-Frank, I., & Hagemann, M. (2016) Trimethylated homoserine functions as the major compatible solute in the globally significant oceanic cyanobacterium Trichodesmium. Proceedings of the National Academy of Sciences, 113(46), 13191-13196.

Parmar A., Singh N. K., Pandey A., Gnansounou E., Madamwar D. (2011) Cyanobacteria and microalgae: A positive prospect for biofuels. Bioresource Technology 102(22): 10163–10172.

Sandrin T. R., Dowd S. E., Herman D. C. & Maier R. M. (2009) Aquatic Environments. In Environment Microbiology. Elsevier Inc.

Sudhakar, K., & Rana, R. S. (2017) Spirulina–From growth to nutritional product: A review. Trends in food science & technology, 69, 157-171.

Takenaka H., Yamaguchi Y., Sakaki S., Watarai K., Tanaka N., Hori M. & Morinaga T. (1998) Safety evaluation of Nostoc flagelliforme (Nostocales, Cyanophyceae) as a potential food. Food and Chemical Toxicology 36(12), 1073-1077.

EXTENDING THE ECOLOGICAL DISTRIBUTION OF *DESMONOSTOC* GENUS: PROPOSAL OF *DESMONOSTOC SALINUM* SP. NOV., A NOVEL CYANOBACTERIA FROM A SALINE-ALKALINE LAKE

Luna Viggiano de Alvarenga; Marcelo Gomes Marçal Vieira Vaz; Diego Bonaldo Genuário; Alberto A. Esteves-Ferreira; Allan V. Martins Almeida; Naira Valle de Castro; Claudineia Lizieri; José João L. L. Souza; Carlos Ernesto G. R. Schaefer; Adriano Nunes-Nesi and Wagner L. Araújo

Accepted at **International Journal of Systematic and Evolutionary Microbiology**

de Alvarenga LV, Vaz MGMV, Genuário DB, Esteves-Ferreira AA, Almeida AVM, de Castro NV, Lizieri C, Souza JJLL, Schaefer CEGR, Nunes-Nesi A, Araújo WL. (2018) Extending the ecological distribution of Desmonostoc genus: proposal of Desmonostoc salinum sp. nov., a novel Cyanobacteria from a saline–alkaline lake. *International Journal of Systematic and Evolutionary Microbiology*; 68:2770–2782 DOI 10.1099/ijsem.0.002878

INTERNATIONAL JOURNAL OF SYSTEMATIC AND EVOLUTIONARY MICROBIOLOGY

TAXONOMIC DESCRIPTION

de Alvarenga *et al.*, *Int J Syst Evol Microbiol*

DOI 10.1099/ijsem.0.002878

MICROBIOLOGY SOCIETY

Extending the ecological distribution of *Desmonostoc* genus: proposal of *Desmonostoc salinum* sp. nov., a novel *Cyanobacteria* from a saline–alkaline lake

Luna Viggiano de Alvarenga,[1,2]† Marcelo Gomes Marçal Vieira Vaz,[1,2]† Diego Bonaldo Genuário,[3] Alberto A. Esteves-Ferreira,[1,2] Allan V. Martins Almeida,[1,2] Naira Valle de Castro,[1,2] Claudineia Lizieri,[1]‡ José João L. L. Souza,[4,5] Carlos Ernesto G. R. Schaefer,[4] Adriano Nunes-Nesi[1,2] and Wagner L. Araújo[1,2,*]

Abstract

Cyanobacteria is an ancient phylum of oxygenic photosynthetic microorganisms found in almost all environments of Earth. In recent years, the taxonomic placement of some cyanobacterial strains, including those belonging to the genus *Nostoc sensu lato*, have been reevaluated by means of a polyphasic approach. Thus, 16S rRNA gene phylogeny and 16S–23S internal transcribed spacer (ITS) secondary structures coupled with morphological, ecological and physiological data are considered powerful tools for a better taxonomic and systematics resolution, leading to the description of novel genera and species. Additionally, underexplored and harsh environments, such as saline–alkaline lakes, have received special attention given they can be a source of novel cyanobacterial taxa. Here, a filamentous heterocytous strain, Nostocaceae CCM-UFV059, isolated from Laguna Amarga, Chile, was characterized applying the polyphasic approach; its fatty acid profile and physiological responses to salt (NaCl) were also determined. Morphologically, this strain was related to morphotypes of the *Nostoc sensu lato* group, being phylogenetically placed into the typical cluster of the genus *Desmonostoc*. CCM-UFV059 showed identity of the 16S rRNA gene as well as 16S–23S secondary structures that did not match those from known described species of the genus *Desmonostoc*, as well as distinct ecological and physiological traits. Taken together, these data allowed the description of the first strain of a member of the genus *Desmonostoc* from a saline–alkaline lake, named *Desmonostoc salinum* sp. nov., under the provisions of the International Code of Nomenclature for algae, fungi and plants. This finding extends the ecological coverage of the genus *Desmonostoc*, contributing to a better understanding of cyanobacterial diversity and systematics.

Cyanobacteria is an ancient phylum of oxygenic photosynthetic microorganisms within the *Bacteria* domain. Members of this phylum present basic nutritional requirements (CO_2, H_2O and light mainly) and display great morphological/metabolic diversity, allowing them to grow and to disperse in a variety of environments, including extreme ones [1, 2]. Saline–alkaline lakes, usually called soda lakes, are an example of such harsh environments. These lakes normally contain amounts of sodium-carbonate/bicarbonate salts up to saturation, forming a buffer system which maintains high pH values (from 9.5 to 11.0) [3]. Saline–alkaline lakes are distributed worldwide, mainly in arid and semi-arid environments, as in the Rift Valley in East Africa [3], but are also found in tropical and sub-tropical regions, as in the Brazilian Pantanal wetlands [4–6] and the Chilean southern region [7]. Laguna Amarga (Torres del Paine National Park, Chile) is a soda lake located in Southern Patagonia [8], a semi-arid area 105 m above sea level, with a windy cold climate (mean annual air temperature of 6.6 °C) and evaporation rates normally greater than precipitation rates [7].

Author affiliations: [1]Departamento de Biologia Vegetal, Universidade Federal de Viçosa, 36570-900, Viçosa, Minas Gerais, Brazil; [2]Max Planck Partner Group at the Departamento de Biologia Vegetal, Universidade Federal de Viçosa, 36570-900, Viçosa, Minas Gerais, Brazil; [3]Laboratório de Microbiologia Ambiental, EMBRAPA Meio Ambiente, 13820-000, Jaguariúna, São Paulo, Brazil; [4]Departamento de Solos, Universidade Federal de Viçosa, 36570-900, Viçosa, Minas Gerais, Brazil; [5]Departamento de Geografia, Universidade Federal do Rio Grande do Norte, 59300-000, Caicó, Rio Grande do Norte, Brazil.

***Correspondence:** Wagner L. Araújo, wlaraujo@ufv.br

Keywords: 16S rRNA gene phylogeny; ITS; *Nostoc sensu lato*; physiology; polyphasic approach; saline environments.

Abbreviations: BI, Bayesian inference; FAMEs, fatty acid methyl esters; GTR+G+I, evolutionary model of substitution with gamma distribution and with an estimate of proportion of invariable sites; ITS, internal transcribed spacer; ML, maximum-likelihood.

†These authors contributed equally to this work.

‡Present address: Instituto de Engenharia e Tecnologia, Centro Universitário de Belo Horizonte, UniBH, 30455-610, Belo Horizonte, Minas Gerais, Brazil.

Three supplementary tables and six supplementary figures are available with the online version of this article.

It seems clear that such extreme environments cause serious limitations to the development of life and it seems reasonable to assume that cyanobacteria strains isolated from such conditions can provide valuable information concerning taxonomy, systematics and ecological distribution.

The taxonomic classification of cyanobacteria was formerly based mainly on morphological characters [9–12]. However, during recent decades, the additional application of molecular data using 16S rRNA gene sequences, has greatly contributed to improving cyanobacterial taxonomy and systematics [13–17]. Ecological and ultrastructural features have also been suggested as fundamental characteristics allowing a more robust characterization [18–20]. Moreover, physiological and metabolic traits can also be powerful tools to enhance our understanding of cyanobacterial evolution, assisting in the systematics of this group [5, 21–24]. The combination of these different methods, known as the 'polyphasic approach', has demonstrated that many morphologically well-defined genera are indeed polyphyletic, resulting in the description of novel genera and species [15, 23, 25–28]. This is notably important for the *Nostoc sensu lato* group, which has been recently split into novel generic entities, *Mojavia* [29], *Desmonostoc* [30], *Halotia* [23] and *Aliinostoc* [28].

In this context, we proposed the hypothesis that saline–alkaline environments harbor novel cyanobacterial strains with unique and unexplored physiological traits. To this end, a filamentous heterocytous cyanobacterial strain isolated from a saline–alkaline lake in Patagonia was characterized applying a polyphasic approach, by using morphological characters, phylogeny of 16S rRNA gene, 16S–23S internal transcribed spacer (ITS) secondary structure, coupled with ecological and physiologic data (growth response to saline conditions and its fatty acid profile determination). Our results allowed the description of the first *Desmonostoc* strain isolated from a saline–alkaline lake, to our knowledge, culminating in the proposal of the novel species, *Desmonostoc salinum* sp. nov. Furthermore, it was demonstrated that this strain is able to thrive at salt concentrations higher than 0.25 M of NaCl.

The cyanobacterial strain analyzed in this study was isolated from periphytic microbial mats collected at Laguna Amarga, Torres del Paine National Park (50° 29′ 00″ S and 72° 45′ 00″ W), Chile, during February 2011 (Fig. 1a, b). Water pH and temperature were measured at the sampling site using a portable Digimed DM-2 meter (Digimed Analítica, Digicrom Analítica) calibrated with buffer solutions of pH 4.0 and 7.0; the temperature was compensated using automatic temperature compensation. Water and periphytic samples were stored in polyethylene bottles and kept on ice for further physical–chemical analysis and isolation procedures. Alkalinity was measured by titrating an aliquot of the solution to pH 8.3 to determine phenolphthalein alkalinity and to a pH near 4.5. Alkalinity is reported as mg $CaCO_3$ l^{-1} equivalent, which can be interpreted as the equivalent amount of calcite needed to consume the amount of acid titrated. A subset of elements was also quantified and are presented in Table S1 (available in the online version of this article). Following these analyses, Laguna Amarga presents high amounts of ions in the water, showing deposits of white sediments in the shoreline (Fig. 1). At sampling, the water temperature was around 6 °C, and the pH was 9.5, presenting a sodium concentration of 28.77 g l^{-1} (equivalent to 1.25 M). The ions SO_4^{2-}, K^+, S^{2-} and Mg^{2+} were also found in high abundance. Carbonate (CO_3^{2-}) and bicarbonate (HCO_3^-) concentrations were 2.67 g l^{-1} (0.044 M) and 0.95 g l^{-1} (0,015 M), respectively (Table S1).

Samples of the periphytic microbial mats (Fig. 1) collected from the shoreline were fragmented and spread on BG-11_0 plates (BG-11 without nitrogen sources) [31]. In the first rounds of the isolation, the plates were maintained at low temperatures, starting at 10±2 °C, which were successively increased, up to 24±2 °C. The plates were maintained under light intensity of 40 µmol m^{-2} s^{-1} and photoperiod of 16/8 h (light/dark). The biomass was constantly analyzed under the microscope and successive streaking was performed until unicyanobacterial colonies were obtained. The strain CCM-UFV059 was the only filamentous heterocyte-forming cyanobacterium isolated from the collected mat. After isolation, the non-axenic unicyanobacterial culture was

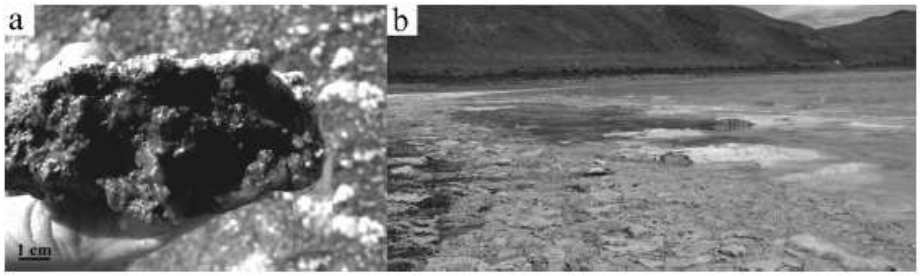

Fig. 1. Samples of periphytic microbial mat adhered to clayey material (a) collected from Laguna Amarga shoreline in January of 2011(b).

maintained in liquid (BG-11_0) medium under the same conditions described above, at the Collection of Cyanobacteria and Microalgae (CCM–UFV), in the Laboratory of Phycology and Molecular Biology, Plant Biology Department at the Universidade Federal de Viçosa.

Morphological characterization was performed as previously described [32, 33], using a Zeiss Axioskop 40 optical light microscope equipped with an AxioVision LE 4.6 digital imaging system (Carl Zeiss) [34]. The morphology of colonies, vegatative filaments and hormogonia were observed; the presence or absence of sheaths was recorded and the size of vegetative cells, heterocytes and akinetes was measured.

For molecular characterization, total genomic DNA was extracted from a 14-day-old culture using the UltraClean Microbial DNA Isolation Kit (MoBio). The 16S and the 16S–23S ITS gene region were PCR-amplified using the primer set 27F1 [35] and 23S30R [36], following steps described previously [12]. The amplicons were, then, cloned into a pGEM-T Easy Vector System (Promega, Madison) according to the manufacturer's manual. Competent *Escherichia coli* DH5α cells were transformed and recombinant plasmids were purified from white colonies using the UltraClean Standard Mini Plasmid Prep Kit (MoBio). Plasmids containing the fragments of interest were sequenced using the M13F/R primer set and the 16S rRNA internal primer sets 341–357F, 357–341R, 685–704F, 704–685R, 1099–1114F, and 1114–1099R [37], exactly as described by Genuário *et al.* [12]. The sequenced fragments were assembled into one contig using the software Phred/Phrap/Consed (Philip Green, University of Washington, Seattle, USA) and only bases with >20 quality were considered.

The 16S rRNA gene sequence obtained in this study and related ones retrieved from GenBank were aligned using CLUSTAL W from MEGA version 5 [38] and trimmed (16S rRNA gene matrix with a 1446 bp length). A total of 108 sequences were considered and used to infer the phylogeny based on the maximum likelihood (ML) method. The general time reversible evolutionary model of substitution with gamma distribution and with an estimate of proportion of invariable sites (GTR+G+I) was selected as the best fitting model, applying the model-testing function in MEGA version 5 [38] and jModelTest 2.1.1 program [39]. The robustness of the phylogenetic trees was estimated by bootstrap analysis using 1000 replications. Bayesian inference was also conducted using MrBayes 3.2 [40], applying two separate runs with four chains each and 50 000 000 Markov chain Monte Carlo generations. Posterior probabilities (PP) were calculated at the conclusion of the Markov Chain Monte Carlo analysis and a traditional burn-in on the first 25 % of the trees was performed. The tree was viewed in FigTree 1.3.1 (http://tree.bio.ed.ac.uk/software/figtree). Given that ML and Bayesian methods resulted in nearly identical topologies, only the ML tree is presented, with indications of ML bootstrap values and Bayesian posterior probabilities.

The 16S–23S ITS gene region obtained was further used for analysis based on secondary structure folding. The selected 16S–23S ITS sequences were aligned with CLUSTAL W from the Mega package [38] (Fig. S1). Their ITS regions (D1–D1′, D2, V2, Box-B, Box-A, D4, V3 and D5) and tRNA genes were found using LocARNA-Alignment and Folding [41, 42] and tRNAscan-SE Search Server (1.21) [43], respectively. The D1–D1′ and V2 secondary structures were folded using the Mfold WebServer with the default conditions except for applying untangle with loop fix as structure draw mode [44]. The sequence of 16S and the 16S–23S ITS gene region obtained from the isolated strain was deposited in the NCBI GenBank database under the accession number KX787933.

To screen microcystin and saxitoxin synthetase genes, three molecular markers were selected from each gene cluster, respectively: *mcyD*, *mcyE* and *mcyG* as well *sxtA*, *sxtB* and *sxtI*. The PCR amplifications of *mcyD* (818 bp) and *mcyE* (809 bp) were conducted using the specific primers designed previously [45] whereas *mcyG* (534 bp) was amplified using the primer set described by Fewer *et al.* [46]. The PCR amplifications were performed as described by Genuário *et al.* [12]. For saxitoxin synthetase genes, the PCR amplification was conducted using the specific primers (*sxtA* – 200 bp; *sxtB* – 400 bp; and *sxtI* – primer set OCT-F/R, 900 bp) and the conditions designed by Hoff-Risseti *et al.* [47].

Given that Laguna Amarga is characterized by a high salt concentration (Table S1), the lethal dose concentration (LD_{50}) of NaCl for CCM-UFV059 was determined. The LD_{50} is the minimum concentration of a specific agent capable of killing 50 % of cells after 72 h of exposure, according to Organization for Economic Co-operation and Development (OECD) Guidelines [48]. Briefly, independent growth curves were performed, in triplicate, using different NaCl concentrations (0, 0.05, 0.075, 0.1, 0.25, 0.5, 0.75, 1, 1.75 M), with CCM-UFV059 being maintained under a photoperiod of 16/8 h (light/dark), 24±2 °C, light intensity of 70 µmol m^2 s^{-1} and constant shaking (30 *g*), for 10 days. Growth evaluation was performed by measuring the number of cells in a Neubauer chamber (Optik Labor), ashes-free dry mass and OD_{750}. Likewise, growth curves using the same salt concentrations were conducted for *Nostoc* sp. PCC7120, which was selected based on its non-NaCl-tolerance (negative control) [34].

The fatty acid profile of this strain was analyzed after cultivation in conditions without salt. Briefly, 10 mg lyophilized cells were independently harvested at four sampling points along the exponential phase of a growth curve (0, start point of exponential phase; 2, 8 and 24 h). The derivatization was conducted according to the Sherlock Microbial Identification MIDI System, using HCl–methanol 6 % (v/v) and hexane (http://www.midi-inc.com/ Technical note #101). A total of 0.05 ml of the non-polar fraction was taken for analysis on model 7890 gas chromatograph (Agilent) equipped with an HP-ultra 2 column (25 m, 0.20 mm ID, 00 : 33 µM film thickness). The MIDI Sherlock version 6.2 (MIDI) software was

used to adjust the operational parameters and for recognition, quantification and comparison with the reference libraries. The results are expressed as percentages in relation to the total response obtained in the chromatogram.

The non-axenic filamentous heterocytous strain, obtained after the isolation procedures, was named as Nostocaceae CCM-UFV059, once its main morphological traits had been matched with those found in members of this family. Under standard conditions (BG-11_0 medium, without NaCl), microscopic inspection revealed that CCM-UFV059 had straight trichomes at the beginning of development, as hormogonia or young trichome, and later was organized in a set of parallel trichomes, enclosed by a diffluent mucilage (Fig. 2a, c). This parallel organization of trichomes, observed in early and middle phases of culture, could be lost later, as a consequence of akinete differentiation. Both intercalary and terminal heterocytes were always present in vegetative trichomes, with the terminal ones being differentiated during the early stages of trichome development. Whilst in the presence of NaCl akinetes were easily found, under standard conditions they were not often observed. Initially, the akinetes were organized in chains, which could be broken, releasing isolated mature akinetes (Fig. 2b, d). Macroscopically, the strain grew as a free-floating gelatinous biomass, which occasionally formed aggregated colonies. Motile hormogonia were frequent and abundant in earlier growth phases, usually containing more than 20 cells, without heterocytes. Vegetative cells presented a dark-green colour, were barrel-shaped, sub-spherical or longer than they were wide (3.7–5.4 µm long and 3.3–4.5 µm wide). Heterocytes were sub-spherical, longer than they were wide (5.8–8.3 µm long and 3.7–4.6 µm wide) with a slight-green or yellowish colour. The akinetes were spherical or sub-spherical (8.3–10.0 µm long and 5.0–8.3 µm wide), with green to yellowish colour and conspicuous granulation (Fig. 2 and Table 1).

The nearly complete 16S rRNA gene (1413 bp) and the 16S–23S ITS gene region (327 bp) were sequenced from the CCM-UFV059 strain. The 16S rRNA gene sequence obtained showed identity higher than 98.5 % to related sequences available in Genbank (Table 2). It is important to mention that among the related sequences, seven were from strains assigned to the genus *Desmonostoc* or belonging to its corresponding phylogenetic clade [30], and seven sequences were related to uncultured bacterium clones harvested from the gut microbial communities of zebrafishes

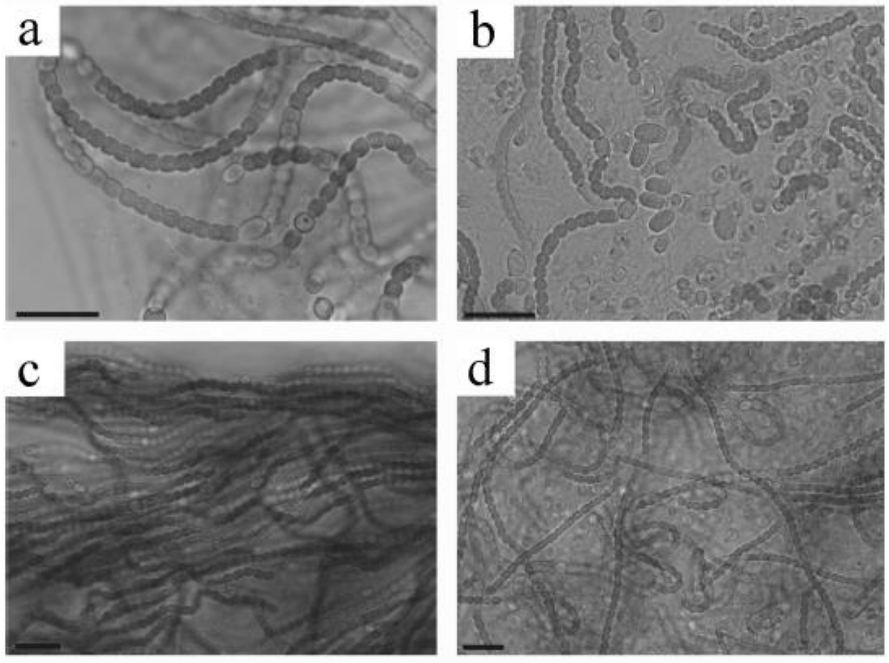

Fig. 2. Photomicrographs of *Desmonostoc salinum* CCM-UFV059. a and c: Vegetative trichomes grown in BG-11_0 without NaCl. b and d: Trichomes grown in BG-11_0 supplemented with 890 mM NaCl. b Presence of akinetes after 96 h of cultivation in BG-11_0 with 890 mM NaCl. Bars, 20 µm.

Table 1. Morphometric characteristics of *Desmonostoc salinum* CCM-UFV059

All measurements [mean, (range)] are given in µm.

Cyanobacterial strain	Vegetative cells		Heterocytes		Akinetes		
	Length	Width	Length	Width	Length	Width	Shape
Desmonostoc salinum CCM-UFV059	4.5 (3.7–5.4)	4.2 (3.3–4.5)	7.0 (5.8–8.3)	4.2 (3.7–4.6)	9.0 (8.3–10.0)	7.0 (5.0–8.3)	Oval

[49] (Table 2). In the phylogenetic reconstruction based on 16S rRNA gene sequences, the sequence of CCM-UFV059, grouped in a robust clade (94 % bootstrap value, ML; and posterior probability of 1, BI) with other sequences of *Desmonostoc* (Cluster *Desmonostoc sensu stricto* – *Desmonostoc* spp., Figs 3 and S4). The sequences assigned to the genus *Desmonostoc* characterized by Hrouzek *et al.* [30] and the recently described *D. geniculatum* [50] were all included in this cluster (Figs 3 and S4). Additionally, the comparison of the 16S rRNA gene sequence of CCM-UFV059 with a subset of selected sequences used for phylogenetic reconstruction, including those from members of the genera *Nostoc sensu stricto*, *Mojavia* and *Halotia* (Table S2) showed identities ranging from 97.5 to 99.8 % against sequences of members of the genus *Desmonostoc* and from 94.6 to 96.6 % against those of members of the other selected genera (Table S2). Furthermore, the 16S rRNA gene sequence of CCM-UFV059 has an identity of 97.9 % against the sequence of *Desmonostoc muscorum* Lukesova 1/87 (AM711523), the type-species of the genus *Desmonostoc* [30], and 97.5 % against the sequence from *Desmonostoc geniculatum* HA4340-LM1 (KU161660), which have been previously described [50] (Table S2).

The novel 16S–23S ITS spanned the D1–D1′, D2, V2 and D5 regions and the secondary structures of D1–D1′ and V2 regions were folded. The length and secondary structures of the novel 16S–23S were compared against sequences from those strains of the genus *Desmonostoc* available and the type strains of the type species of the genera *Nostoc*, *Mojavia* and *Halotia* (Table S3; Figs 4, 5, S2 and S3). Within *Desmonostoc* 16S–23S ITS sequences, the length of D1–D1′, V2 and D5 regions were 65–69, 29–62 and 16–21 bp, respectively (Table S3). For the remaining analysed genera, these regions presented a wider variation 60–67, 27–76 and 14–21 bp for D1–D1′, V2 and D5 regions, respectively. Considering the sequence length, all the regions from CCM-UFV059 coincided with those of *Demonostoc* sp. 111_CR4_BG11B and *Desmonostoc* sp. 111_CR4_BG11N, indicating that they might represent the same species (Table S3). Similarly, their D1–D1′ and V2 secondary structures precisely matched (Figs 4, 5). Eight D1–D1′ helical patterns were recognized among the 16S–

Table 2. Sequence identity (%) of 16S rRNA gene fragments among *Desmonostoc salinum* CCM-UFV059 and other cyanobacterial strains available in GenBank

Strain	Length (bp)	Closest match (Accession number)	C* (%)	I† (%)
Desmonostoc salinum CCM-UFV059	1413	*Desmonostoc* sp. 8964:3 (AM711541)‡	100	99.8
		Desmonostoc endophytum IAM M-267 (AB093490)‡	100	99.7
		Uncultured bacterium JFR0702_jaa51e01 (HM780037)‡	100	99.7
		Desmonostoc sp. PCC9231 (AY742452)‡	99	99.7
		Desmonostoc sp. PCC8306 (HG004584)‡	100	99.6
		Uncultured bacterium JFR0702_jaa37g03 (HM780016)‡	100	99.4
		Uncultured bacterium JFR0702_jaa50a03 (HM780005)‡	100	99.3
		Uncultured bacterium JFR0702_jaa38d08 (HM780003)‡	100	99.2
		Uncultured bacterium JFR0702_jaa37c06 (HM780249)‡	100	99.1
		Uncultured bacterium JFR0702_jaa37g03 (HM780016)‡	100	99.4
		Uncultured bacterium JFR0702_jaa50a03 (HM780005)‡	100	99.3
		Uncultured bacterium JFR0702_jaa37d05 (HM780163)‡	100	99.0
		Uncultured bacterium JFR0702_jaa40g08 (HM780211)‡	99	99.0
		Desmonostoc sp. PCC8107 (HG004583)‡	100	98.5
		Nostoc linckia var. *arvense* IAM M-30 (AB325907)‡	100	98.5
		Desmonostoc sp. Cr4 (AM711533)‡	100	98.5

*Coverage.

†Identity.

‡Published sequence.

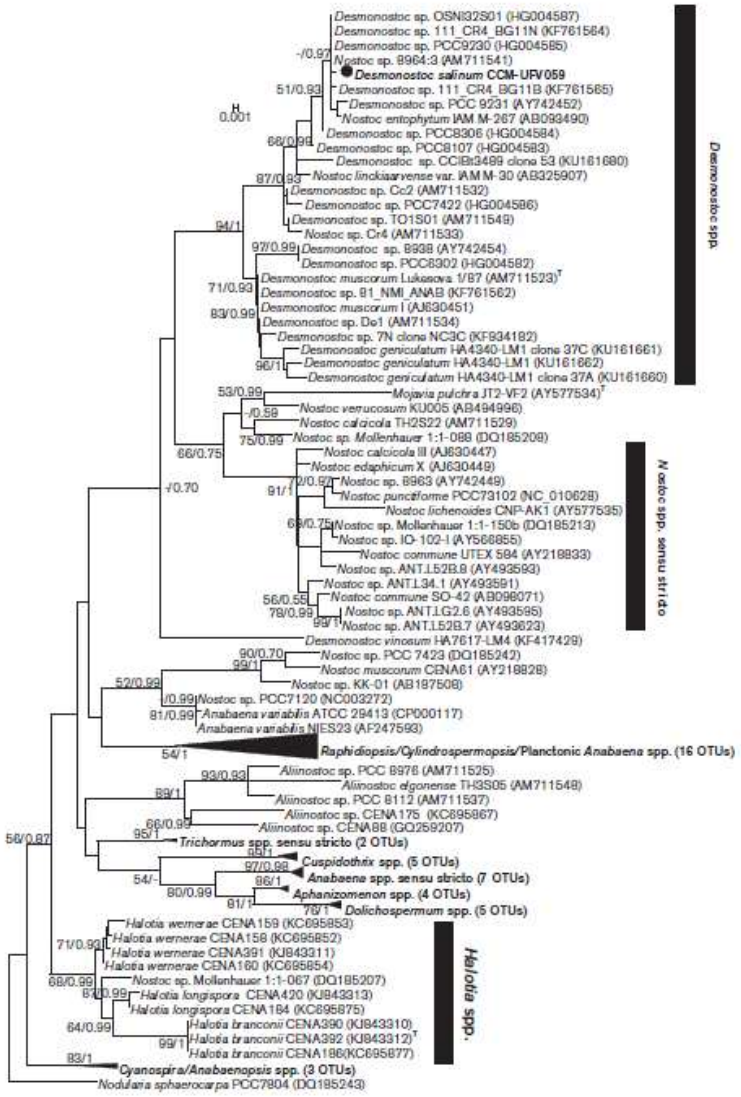

Fig. 3. Maximum likelihood phylogenetic tree based on the 16S rRNA gene sequences of nostocacean cyanobacteria. The sequence of *Desmonostoc salinum* CCM-UFV059 is shown in bold type with a black circle. Bootstrap (greater than 50%) and probability values, obtained from ML and Bayesian inference, respectively, are displayed in front of the relevant nodes.

23S sequences analyzed and all of them shared the same basal stem structure (GACCU–AGGUC) (Figs 4 and S2). Interestingly, the secondary structure from CCM-UFV059 coincided only with those from *Desmonostoc* sp. 111_CR4_BG11B and *Desmonostoc* sp. 111_CR4_BG11N helixes (Fig. 4). Altogether, one single unpaired nucleotide located in first internal loop after the basal stem and two unpaired nucleotides in the lateral bulge are the main differences when compared with the remaining helical patterns (Fig. 4). The number of V2 helical patterns was slightly higher among the 16S–23S sequences analyzed and they did not share the same sequence in their basal stems

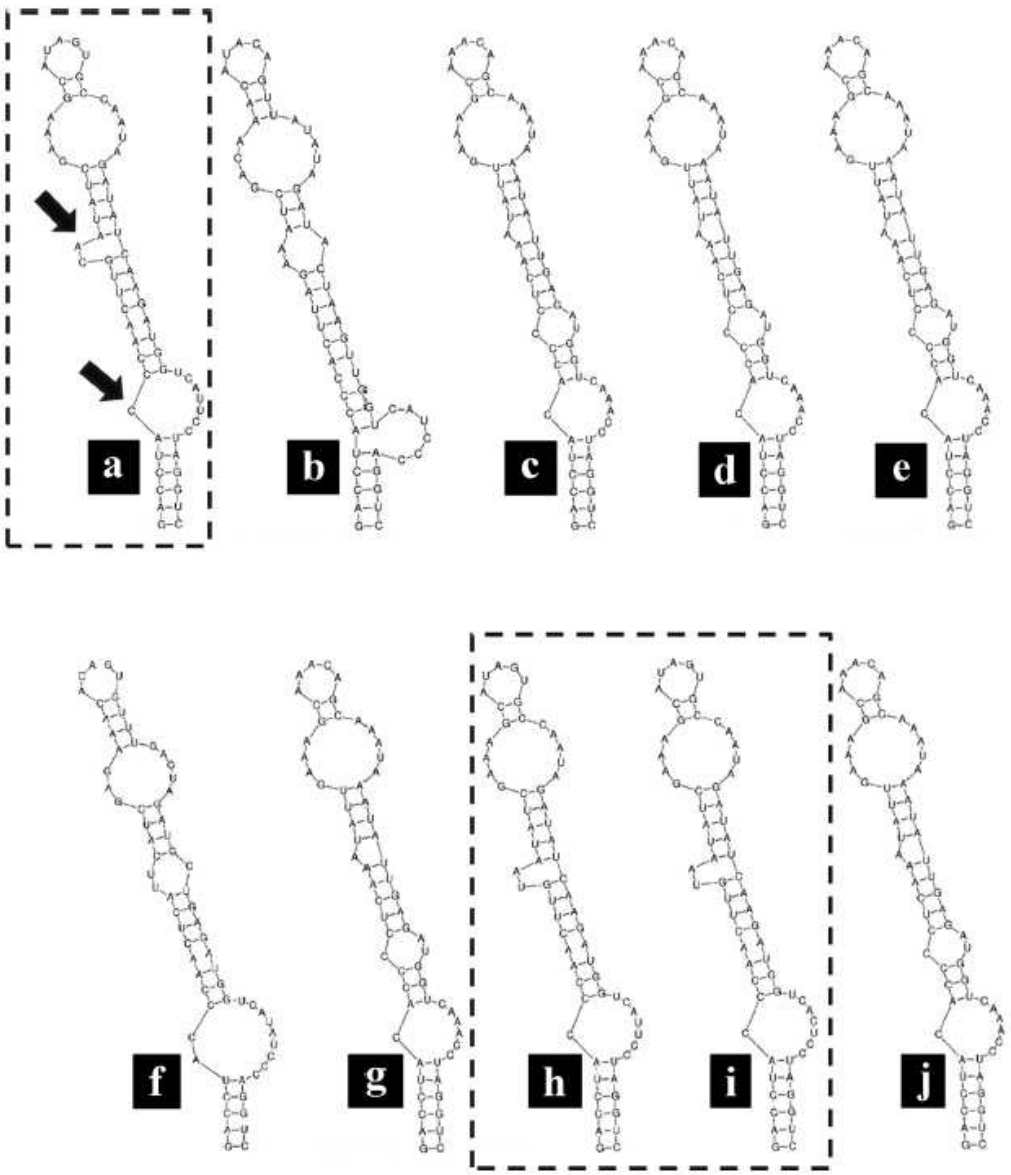

Fig. 4. D1–D1′ secondary structures of the 16S–23S ITS sequences from selected strains of members of the genus *Desmonostoc*. a - *Desmonostoc salinum* CCM-UFV059; b - *Desmonostoc vinosum* HA7617-LM4 (KF417429); c - *Desmonostoc geniculatum* HA4340-LM1 (KU161662); d - *Desmonostoc geniculatum* HA4340-LM1 (KU161661); e - *Desmonostoc geniculatum* HA4340-LM1 (KU161660); f - *Desmonostoc* sp. CCIBt3489 (KU161680); g - *Desmonostoc* sp. 7N (KF934182); h - *Desmonostoc* sp. 111_CR4_BG11B (KF761565); i - *Desmonostoc* sp. 111_CR4_BG11N (KF761564) and j - *Desmonostoc* sp. 81_NMI_ANAB (KF761562). The structures presented in a, h and i are the most similar. The arrows indicate common specific traits in these secondary structures.

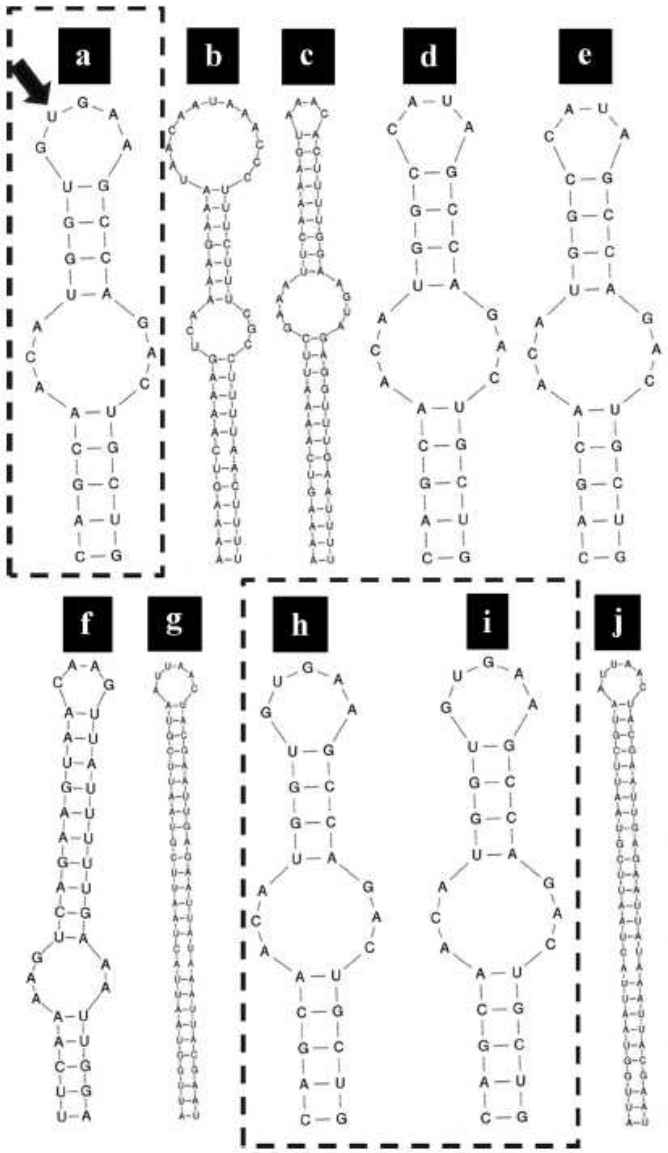

Fig. 5. V2 secondary structures of the 16S–23S ITS sequences from selected strains of members of the genus *Desmonostoc*. a - *Desmonostoc salinum* CCM-UFV059; b - *Desmonostoc vinosum* HA7617-LM4 (KF417429); c - *Desmonostoc geniculatum* HA4340-LM1 (KU161662); d - *Desmonostoc geniculatum* HA4340-LM1 (KU161661); e - *Desmonostoc geniculatum* HA4340-LM1 (KU161660); f - *Desmonostoc* sp. CCIBt3489 (KU161680); g - *Desmonostoc* sp. 7N (KF934182); h - *Desmonostoc* sp. 111_CR4_BG11B (KF761565); i *Desmonostoc* sp. 111_CR4_BG11N (KF761564) and j - *Desmonostoc* sp. 81_NMI_ANAB (KF761562). The structures presented in a, h and i are the most similar. The arrow indicates common specific trait in these secondary structures.

even when compared only among the sequences from members of the genus *Desmonostoc* (Figs 5 and S3). Again, the V2 secondary structure from CCM-UFV059 agreed only with those from *Desmonostoc* sp. 111_CR4_BG11B and *Desmonostoc* sp. 111_CR4_BG11N helixes mainly by their six unpaired nucleotide located at the terminal loop (Fig. 5). All this information interpreted altogether indicates that the novel CCM-UFV059, *Desmonostoc* sp. 111_CR4_BG11B and *Desmonostoc* sp. 111_CR4_BG11N represent a single species.

The molecular screening for genes involved in the biosynthesis of microcystin and saxitoxin did not produce any positive reaction, indicating that CCM-UFV059 does not have the genetic potential to produce these toxins. Moreover, the chemical analysis conducted using its biomass aiming to access these toxins did not detect their presence (data not shown). It should be mentioned that, to date, there is no register of strains of members of the genus *Desmonostoc* capable of producing such cyanotoxins.

The LD_{50} observed for CCM-UFV059 was 0.89 M whereas it was only 0.1 M for PCC7120 (Fig. S5), indicating that this novel strain can tolerate high NaCl concentrations. Next, the growth of CCM-UFV059 was evaluated in culture media applying NaCl concentrations below the LD_{50} dose. By increasing the salt concentration, clear reductions in the growth of CCM-UFV059 were observed, measured both by OD_{750} and ashes-free dry mass (Fig. S6). In the absence of NaCl (standard conditions), CCM-UFV059 showed a six-day exponential phase (from the second to the eighth days) (Fig. S6a) and the maximum dry mass was achieved after 8 days of cultivation (Fig. S6). A longer lag phase and a shorter exponential phase were observed in the presence of 0.25 M NaCl, leading to a reduction of 31 % in biomass production. Although treatments with 0.5 and 0.75 M NaCl did not show any expressive growth (Fig. S6), it was possible to observe, through microscopic analysis, the differentiation of vegetative cells into akinetes. The differentiation started at the second day of exposure to 0.75 M NaCl, similarly to the cultures growing at the LD_{50} (Fig. 2b, d).

The fatty acid methyl esters (FAMEs) profile showed a major abundance of palmitic acid (16 : 0) (28 %), palmitoleic acid (16 : 1ω7*c*) (18 %) and oleic acid (18 : 1ω7*c*) (33 %). Myristic acid (14 : 0 anteiso) (3 %), linoleic acid (18 : 2ω6,9*c*) (7 %) and other FAMEs were also found in minor amounts. The FAMEs profile did not present significant variation among the four sampling points, which encompassed a complete day into the exponential phase, indicating that the FAMEs profile must be seen as an important taxonomic marker (Fig. 6) [51]. The FAMEs profile of CCM-UFV059 presented clear differences from those described by Temina *et al.* [52] in a study analyzing a subset of *Nostoc*-like strains. However, a deeper comparison was hampered since no other strain belonging to a member of the genus *Desmonostoc* has been analyzed to date by means of fatty acid profile. Nevertheless, this result serves as a foundation for comparison in further studies aiming to characterize the intra- and inter-generic diversity of strains belonging to *Nostoc sensu lato*.

Laguna Amarga, from which the novel species *Desmonostoc salinum* CCM-UFV059 was isolated, showed high pH (>9.0), high dissolved content of Na^+, K^+, Mg^+ and SO_4^{2-} and high content of carbonates, as sodium carbonate/bicarbonate precipitates (Table S1). Such harsh environmental conditions can be a limiting factor for many organisms, including cyanobacteria. In fact, only a few organisms can grow in saline–alkaline lakes, like Laguna Amarga [4, 53]. Taking into account morphological results, CCM-UFV059 resembles the morphotypes of the related genera, *Nostoc sensu stricto*, *Desmonostoc* and *Halotia*. That being said, the identification of diacritical morphological features among these genera and species is apparently highly complicated [23]. However, it is important to mention that akinete differentiation observed under both standard culture conditions and high salt concentrations, the dark green of vegetative cells, the production of large amounts of exopolysaccharides during the whole life cycle and the parallel organization of trichomes can be assumed to be important morphological traits distiguishing members of the genus *Desmonostoc*.

The phylogenetic analyses presented here (Tables 2 and S2; Figs 3 and S4) coupled with the cut off values for genus and species delimitation (95 and 97.5 %, respectively) [54, 55], clearly indicates that CCM-UFV059 represents a member of the genus *Desmonostoc* (identity $\geq$95 %). More importantly, our results are suggestive of a novel specific entity. Although these last identity values are slightly higher than the ones proposed for species delimitation, this numeric percentage value cannot be used as a robust diacritical trait for species separation, especially for nostocacean taxa, for which broader limits are accepted [23, 56, 57]. In addition, on the basis of phylogenetic reconstruction, the *Desmonostoc* cluster presented two major subclusters in which the first subcluster harbored the 16S rRNA gene sequence retrieved from the type species (*Desmonostoc muscorum* Lukesova 1/87) and other sequences from other members of the genus (*D. muscorum* I, *Desmonostoc* sp. PCC6302 and *Desmonostoc* sp. 8938). Notably, this cluster corresponds to the *Desmonostoc* cluster D2 presented by Hrouzek *et al.* [30], and represents the 'type' cluster of *D. muscorum*. In addition, from this subcluster emerged a subdivision containing three sequences of *Desmonostoc geniculatum* HA4340-LM1, a recently described species from Hawaiian cave walls [50]. The second subcluster accommodated the novel 16S rRNA gene sequence retrieved from the CCM-UFV059 and other sequences assigned to the *Desmonostoc* and also corresponded to the cluster D1 revealed by Hrouzek *et al.* [30]. Internally, the 16S rRNA gene sequence from CCM-UFV059 clustered together with eight other sequences and these sequences shared more than 99.5 % identity among

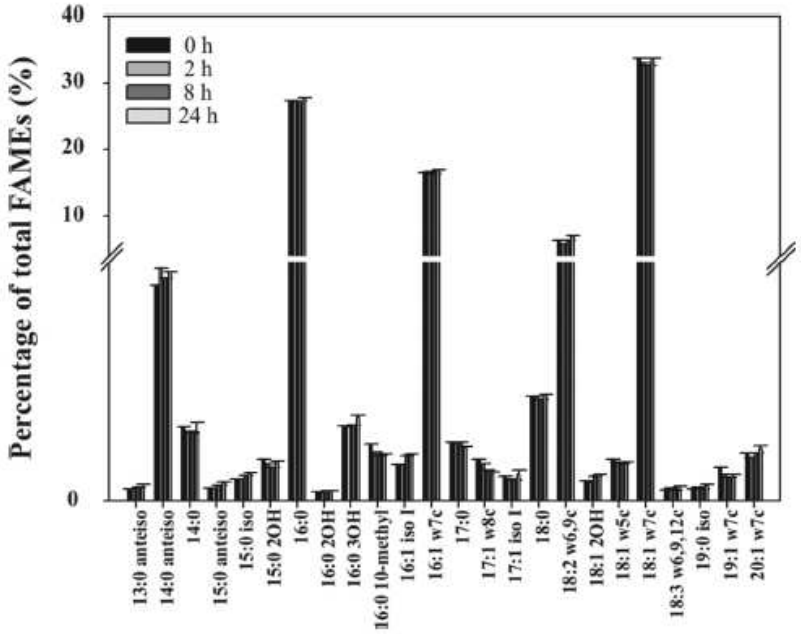

Fig. 6. Fatty acid profile, as percentage of each fatty acid with respect to total fatty acid fraction, for *Desmonostoc salinum* CCM-UFV059. Values are expressed as means of three replicates.

themselves, indicating that they must represent the same species.

Analysis of 16S–23S ITS secondary structures has been considered to be a powerful tool for delimitation of cyanobacterial species [58], among which V2 helix is the most variable and D1–D1′ more important for separation of strains in different species [23, 27]. Length comparison among the regions within the 16S–23S sequences showed that the D1–D1′, V2 and D5 regions from CCM-UFV059 and those of *Desmonostoc* sp. 111_CR4_BG11B and *Desmonostoc* sp. 111_Cr4_BG_11N coincided and that their D1–D1′ and V2 secondary structures matched precisely (Figs 4, 5). These similarities indicate that CCM-UFV059 and two strains (*Desmonostoc* sp. 111_CR4_BG11B and *Desmonostoc* sp. 111_CR4 _BG11N), which had been isolated from the walls of caves on Kauai, Hawaii, for which detailed information about their sampling sites are lacking [50], represent a single species. Likewise, ecological information from the remaining strains in the *D. salinum* sub cluster (Fig. 3) is not precise. More importantly, these sequences do not have their 16S–23 ITS available, impairing a better comparison about their relatedness at species level.

Strains assigned to the genus *Desmonostoc* are normally found in non-extreme environments, characterized by moist or wet meadow, field and forest soils [30] and more recently, strains of species of the genus *Desmonostoc* have also been recovered from caves on Kauai, Hawaii [50]. It is worthy of mention that these strains are rarely found in periphyton, biofilms as well as in deserts; however, some strains are symbiotic to *Cycas* and *Gunnera* [30, 59]. To our knowledge, CCM-UFV059 is the first strain of a member of the genus *Desmonostoc* isolated from a saline–alkaline lake, an extreme environment considering both the high pH and salinity of the sampled site. When considered together, the ecological features of this novel strain, which is highly distinct from previously described species, coupled with molecular and phylogenetic data obtained here, make it seem reasonable to propose the description of *Desmonostoc salinum* sp. nov.

The strain *Desmonostoc salinum* CCM-UFV059 was able to grow in presence of different NaCl concentrations, showing a LD_{50} of 0.89 M, a value eight times higher than found in others filamentous heterocytous species [34]. Given that Na^+ is the most abundant ion in Laguna Amarga (Table S1), it was used for simulating the natural conditions faced by this strain. It is well known that cyanobacterial strains can grow in marine waters (salinity approximately 3.5%) and other saline environments such as saline–alkaline lakes, soda lakes or saltworks [4, 6, 53, 60]. This fact apart, the

classification of these cyanobacteria as halotolerant and halophilic has been widely discussed [61–64] and despite being able to grow in presence of high salt concentrations (up to 0.25M NaCl), *Desmonostoc salinum* CCM-UFV059 may be classified as halotolerant, as it does not require specific salts or higher salt concentrations to survive. Accordingly, at concentrations exceeding 0.25 M NaCl CCM-UFV059 decreased or even ceased its growth by differentiating akinetes, which are again viable when inoculated in fresh medium. Recently, a novel nostocacean genus, *Halotia*, has been described based not only on the ecological origin of the isolated strains (intertidal zones, mangroves and seashores from Brazilian mangroves and Antarctica), but also on their physiological responses of its members to saline conditions and its phylogenetic placement apart from the *Nostoc* cluster *sensu stricto*, as well as the novel 16S–23S ITS sequences and secondary structures of its members [23]. Given the combination of ecological (sampling sites) and physiological information (capability of growth in saline culture media) for cyanobacterial taxonomy, the genus *Halotia* was therefore described as halotolerant. In contrast, *Oxynema thaianum* [60] and *Acaryochloris marina* [65] were described as halophilic, requiring NaCl concentrations of up to 15% (2.58 M) and from 1–5 % (0.17–0.85 M), respectively, for their growth. In general, physiological investigations have been left out of taxonomic studies conducted with cyanobacterial strains; however, ecological data seems to be of pivotal importance as a feature to be considered, providing a wider resolution of cyanobacteria's diversity.

By applying a polyphasic approach, based on morphological, molecular, ecological, and physiological data, we present here compelling evidence for the description of *Desmonostoc salinum* sp. nov. In summary, the work presented here is, to our knowledge, the first description of a halotolerant species belonging to the genus *Desmonostoc*. Remarkably, our molecular results (16S rRNA gene phylogeny and 16S–23S ITS secondary structure) coupled with ecological data demonstrated the potential of a polyphasic approach as a tool for the precise recognition of the novel specific entity. Although complete genome sequencing was not performed for *Desmonostoc salinum* CCM-UFV059, it seems clear that further investigation in order to obtain a better understanding about the molecular mechanisms behind its halotolerance is required. It is also worth pointing out that more genomic data will certainly improve the public genome database for taxonomic and physiological purposes. Accordingly, a deeper investigation of the intriguing aspects associated with the ecophysiology of this novel strain should be targeted for future research aiming to enhance our understanding of salt tolerance in cyanobacteria.

Taken together, the results presented in this study allowed the proposal of the novel species *Desmonostoc salinum* sp. nov., with *Desmonostoc salinum* CCM-UFV059 as reference strain. This proposal is given under the provisions of the International Code of Nomenclature for algae, fungi and plants.

DIAGNOSIS FOR *DESMONOSTOC SALINUM* SP. NOV.

Desmonostoc salinum sp. nov. is described under the provisions of the International Code of Nomenclature for algae, fungi and plants [66].

DESMONOSTOC SALINUM (ALVARENGA *ET AL.*) SP. NOV.

Phylum: Cyanobacteria

Order: Nostocales

Family: Nostocaceae according to Hoffmann *et al.* [18]

Description: The sampled periphytic microbial mat used for cyanobacterial isolation presented a thickness of 4.0 cm, without laminated structure, with a gray layer on the surface and greenish inside, occurring at the edge of Laguna Amarga. The trichomes are straight at the beginning of development, as hormogonia or young trichomes, and later organized in parallel, enclosed by a diffluent mucilage. This parallel organization of trichomes observed in later phases of cultures can be lost as a consequence of akinete differentiation. Both intercalary and terminal heterocytes were always present in vegetative trichomes, with the terminal ones having been differentiated in the early stages of trichome development. Initially, the akinetes were organized in chains, which can be broken, releasing isolated mature akinetes. Macroscopically, the strain grows as a gelatinous free-floating biomass, which occasionally forms aggregated colonies. Motile hormogonia are frequent and abundant in earlier growth phases, usually containing more than 20 cells. Vegetative cells present a dark-green colour and are barrel shaped, sub-spherical, longer than they are wide (3.7–5.4 µm long and 3.3–4.5 µm wide). Heterocytes are subspherical, longer than they are wide (5.8–8.3 µm long and 3.7–4.6 µm wide) with a light green or yellowish colour. The akinetes are spherical or subspherical (8.3–10.0 µm long and 5.0–8.3 µm wide), with green to yellowish colouration and conspicuous granulation. Reproduction occurs via hormogonia differentiation. This species is typical from saline–alkaline environments.

Diagnosis: This novel species was defined according to molecular (16S rRNA gene identity, 16S–23S ITS secondary structure folding), phylogenetic position (based on 16S rRNA gene) and physiological/ecological traits.

Etymology: (sa.li'num. N.L. neut. adj. *sal, salinum*, salty, salted, saline) The specific epithet '*salinum*' (N. L. neut. adj.) refers to the salinity of the sampling site, Laguna Amarga.

Type locality: Periphytic mats in Laguna Amarga, Torres del Paine National Park, Chile (50° 29′ 00″ S and 72° 45′ 00″ W).

Holotype: Freeze-dried sample of strain CCM-UFV059 deposited at Herbarium VIC ('Herbário VIC': Universidade Federal de Viçosa, Viçosa, Minas Gerais State, Brazil) – voucher 47.756.

Reference strain: *Desmonostoc salinum* CCM-UFV059.

Living culture: Living cultures of the type strain (*Desmonostoc salinum* CCM-UFV059), from which the holotype was derived, are available at Collection of Cyanobacteria and Microalgae at Universidade Federal de Viçosa (CCM-UFV), under the internal code CCM-UFV059.

DNA sequence available: 16S rRNA gene and 16–23S ITS region: NCBI accession number KX787933.

Funding information
This work was supported by funding from the Max Planck Society, the National Council for Scientific and Technological Development (CNPq-Brazil) and the Foundation for Research Assistance of the Minas Gerais State, Brazil (FAPEMIG, Grants APQ-01106-13 and APQ-01357-14) to W.L.A. L.V.A. was supported by scholarships from the Brazilian Federal Agency for Support and Evaluation of Graduate Education (CAPES). A.A.E-F was supported by scholarships from CNPq. N.V.C. and A.V.A. were supported by student fellowships from FAPEMIG and FUNARBE, respectively. M.G.M.V.V. was supported by scholarships from CAPES/FAPEMIG (BPD-00514-14) and CAPES (PNPD-1638006). D.B.G. was supported by a post-doctoral scholarship (2014/26131-7), from Fundação de Amparo à Pesquisa do Estado de São Paulo (FAPESP, São Paulo State, Brazil). Research fellowships granted by CNPq-Brazil to W.L.A. are also gratefully acknowledged. This work is a contribution of TERRANTAR Centre, INCT-Cryosphere (INCT Criosfera).

Conflicts of interest
The authors declare that there are no conflicts of interest.

References

1. **Kopp RE, Kirschvink JL, Hilburn IA, Nash CZ.** The Paleoproterozoic snowball Earth: a climate disaster triggered by the evolution of oxygenic photosynthesis. *Proc Natl Acad Sci USA* 2005;102:11131–11136.
2. **Tomitani A, Knoll AH, Cavanaugh CM, Ohno T.** The evolutionary diversification of cyanobacteria: molecular-phylogenetic and paleontological perspectives. *Proc Natl Acad Sci USA* 2006;103:5442–5447.
3. **Sorokin DY, Berben T, Melton ED, Overmars L, Vavourakis CD *et al.*** Microbial diversity and biogeochemical cycling in soda lakes. *Extremophiles* 2014;18:791–809.
4. **Andreote AP, Vaz MG, Genuário DB, Barbiero L, Rezende-Filho AT *et al.*** Nonheterocytous cyanobacteria from Brazilian saline–alkaline lakes. *J Phycol* 2014;50:675–684.
5. **Vieira Vaz MG, Genuário DB, Andreote AP, Malone CF, Sant'anna CL *et al.*** *Pantanalinema* gen. nov. and *Alkalinema* gen. nov.: novel pseudanabaenacean genera (Cyanobacteria) isolated from saline–alkaline lakes. *Int J Syst Evol Microbiol* 2015;65:298–308.
6. **Genuário DB, Andreote APD, Vaz M, Fiore MF.** Heterocyte-forming cyanobacteria from Brazilian saline–alkaline lakes. *Mol Phylogenet Evol* 2017;109:105–112.
7. **Saijo Y, Mitamura O, Tanaka M.** A note on the chemical composition of lake water in the Laguna Amarga, a saline lake in Patagonia, Chile. *Int J Salt Lake Research* 1995;4:165–167.
8. **Zuñiga O, Wilson R, Amat F, Hontoria F.** Distribution and characterization of Chilean populations of the brine shrimp *Artemia* (Crustacea, Branchiopoda, Anostraca). *Int J Salt Lake Res* 1999;8:23–40.
9. **Anagnostidis K, Komárek J.** Modern approach to the classification system of cyanophytes. 1-Introduction. *Arch Hydrobiol Suppl Algol Stud* 1985;38-39:291–302.
10. **Taton A, Grubisic S, Ertz D, Hodgson DA, Piccardi R *et al.*** Polyphasic study of Antarctic cyanobacterial strains. *J Phycol* 2006;42:1257–1270.
11. **Turicchia S, Ventura S, Komárková J, Komárek J.** Taxonomic evaluation of cyanobacterial microflora from alkaline marshes of northern Belize. 2. Diversity of oscillatorialean genera. *Nova Hedwigia* 2009;89:165–200.
12. **Genuário DB, Corrêa DM, Komárek J, Fiore MF.** Characterization of freshwater benthic biofilm-forming *Hydrocoryne* (Cyanobacteria) isolates from Antarctica. *J Phycol* 2013;49:1142–1153.
13. **Robertson BR, Tezuka N, Watanabe MM.** Phylogenetic analyses of *Synechococcus* strains (Cyanobacteria) using sequences of 16S rDNA and part of the phycocyanin operon reveal multiple evolutionary lines and reflect phycobilin content. *Int J Syst Evol Microbiol* 2001;51:861–871.
14. **Komarek J.** Cyanobacterial taxonomy: current problems and prospects for the integration of traditional and molecular approaches. *Algae* 2006;21:349–375.
15. **Fiore MF, Sant'anna CL, Azevedo M, Komárek J, Kaštovský J *et al.*** The cyanobacterial genus *Brasilonema* , gen. nov., a molecular and phenotypic evaluation. *J Phycol* 2007;43:789–798.
16. **Silva CS, Genuário DB, Vaz MG, Fiore MF.** Phylogeny of culturable cyanobacteria from Brazilian mangroves. *Syst Appl Microbiol* 2014;37:100–112.
17. **Bravakos P, Kotoulas G, Skaraki K, Pantazidou A, Economou-Amilli A.** A polyphasic taxonomic approach in isolated strains of Cyanobacteria from thermal springs of Greece. *Mol Phylogenet Evol* 2016;98:147–160.
18. **Hoffmann L, Komárek J, Kaštovský J.** System of cyanoprokaryotes (cyanobacteria) – state in 2004. *Arch Hydrobiol Suppl Algol Stud* 2005;117:95–115.
19. **Korelusová J, Kas˘tovský J, Komárek J.** Heterogeneity of the cyanobacterial genus *Synechocystis* and description of a new genus, *Geminocystis*. *J Phycol* 2009;45:928–937.
20. **Moreira D, Tavera R, Benzerara K, Skouri-Panet F, Couradeau E *et al.*** Description of *Gloeomargarita lithophora* gen. nov., sp. nov., a thylakoid-bearing, basal-branching cyanobacterium with intracellular carbonates, and proposal for *Gloeomargaritales* ord. nov. *Int J Syst Evol Microbiol* 2017;67:653–658.
21. **Nübel U, Garcia-Pichel F, Muyzer G.** The halotolerance and phylogeny of cyanobacteria with tightly coiled trichomes (*Spirulina* Turpin) and the description of *Halospirulina tapeticola* gen. nov., sp. nov. *Int J Syst Evol Microbiol* 2000;50:1265–1277.
22. **Choi DH, Noh JH, Lee CM, Rho S.** *Rubidibacter lacunae* gen. nov., sp. nov., a unicellular, phycoerythrin-containing cyanobacterium isolated from seawater of Chuuk lagoon, Micronesia. *Int J Syst Evol Microbiol* 2008;58:2807–2811.
23. **Genuário DB, Vaz MG, Hentschke GS, Sant'anna CL, Fiore MF.** *Halotia* gen. nov., a phylogenetically and physiologically coherent cyanobacterial genus isolated from marine coastal environments. *Int J Syst Evol Microbiol* 2015;65:663–675.
24. **Genuário DB, Vaz M, Melo IS.** Phylogenetic insights into the diversity of homocytous cyanobacteria from Amazonian rivers. *Mol Phylogenet Evol* 2017;116:120–135.
25. **Rajaniemi P, Hrouzek P, Kastovská K, Willame R, Rantala A *et al.*** Phylogenetic and morphological evaluation of the genera *Anabaena*, *Aphanizomenon*, *Trichormus and Nostoc* (Nostocales, Cyanobacteria). *Int J Syst Evol Microbiol* 2005;55:11–26.
26. **Papaefthimiou D, Hrouzek P, Mugnai MA, Lukesova A, Turicchia S *et al.*** Differential patterns of evolution and distribution of the symbiotic behaviour in nostocacean cyanobacteria. *Int J Syst Evol Microbiol* 2008;58:553–564.
27. **Sciuto K, Moro I.** Detection of the new cosmopolitan genus *Thermoleptolyngbya* (Cyanobacteria, Leptolyngbyaceae) using the 16S

rRNA gene and 16S-23S ITS region. *Mol Phylogenet Evol* 2016;105:15–35.

28. **Bagchi SN, Dubey N, Singh P.** Phylogenetically distant clade of *Nostoc*-like taxa with the description of *Aliinostoc* gen. nov. and *Aliinostoc morphoplasticum* sp. nov. *Int J Syst Evol Microbiol* 2017;67:3329–3338.
29. **Řeháková K, Johansen JR, Casamatta DA, Xuesong L, Vincent J.** Morphological and molecular characterization of selected desert soil cyanobacteria: three species new to science including *Mojavia pulchra* gen. et sp. Nov. *Phycologia* 2007;46:481–502.
30. **Hrouzek P, Lukesova A, Mares J, Ventura S.** Description of the cyanobacterial genus *Desmonostoc* gen. nov. including *D. muscorum* comb. nov. as a distinct, phylogenetically coherent taxon related to the genus *Nostoc*. *Fottea* 2013;13:201–213.
31. **Rippka R, Stanier RY, Deruelles J, Herdman M, Waterbury JB.** Generic assignments, strain histories and properties of pure cultures of cyanobacteria. *Microbiology* 1979;111:1–61.
32. **Komárek J, Anagnostidis K.** Modern approach to the classification system of Cyanophytes 4-Nostocales. *Arch Hydrobiol Suppl Algol Stud* 1989.
33. **Komárek J.** Cyanoprokaryota. In: Budel B, Gartner G, Krientz L and Schagerl M (editors). *Part 3: Heterocytous Genera (Süßwasserflora von Mitteleuropa, vol. 19/3)*. Munich: Springer; 2013.
34. **Rai S, Agrawal C, Shrivastava AK, Singh PK, Rai LC.** Comparative proteomics unveils cross species variations in *Anabaena* under salt stress. *J Proteomics* 2014;98:254–270.
35. **Neilan BA, Jacobs D, del Dot T, Blackall LL, Hawkins PR *et al.*** rRNA sequences and evolutionary relationships among toxic and nontoxic cyanobacteria of the genus *Microcystis*. *Int J Syst Bacteriol* 1997;47:693–697.
36. **Taton A, Grubisic S, Brambilla E, de Wit R, Wilmotte A.** Cyanobacterial diversity in natural and artificial microbial mats of Lake Fryxell (McMurdo Dry Valleys, Antarctica): a morphological and molecular approach. *Appl Environ Microbiol* 2003;69:5157–5169.
37. **Lane D.** 16S/23S rRNA sequencing. In: *Nucleic Acid Techniques in Bacterial Systematics*; 1991. pp. 125–175.
38. **Tamura K, Peterson D, Peterson N, Stecher G, Nei M *et al.*** MEGA5: molecular evolutionary genetics analysis using maximum likelihood, evolutionary distance, and maximum parsimony methods. *Mol Biol Evol* 2011;28:2731–2739.
39. **Darriba D, Taboada GL, Doallo R, Posada D.** jModelTest 2: more models, new heuristics and parallel computing. *Nat Methods* 2012;9:772.
40. **Ronquist F, Huelsenbeck JP.** MrBayes 3: Bayesian phylogenetic inference under mixed models. *Bioinformatics* 2003;19:1572–1574.
41. **Smith C, Heyne S, Richter AS, Will S, Backofen R.** Freiburg RNA Tools: a web server integrating INTARNA, EXPARNA and LOCARNA. *Nucleic Acids Res* 2010;38:W373–W377.
42. **Will S, Joshi T, Hofacker IL, Stadler PF, Backofen R.** LocARNA-P: accurate boundary prediction and improved detection of structural RNAs. *RNA* 2012;18:900–914.
43. **Schattner P, Brooks AN, Lowe TM.** The tRNAscan-SE, snoscan and snoGPS web servers for the detection of tRNAs and snoRNAs. *Nucleic Acids Res* 2005;33:W686–W689.
44. **Zuker M.** Mfold web server for nucleic acid folding and hybridization prediction. *Nucleic Acids Res* 2003;31:3406–3415.
45. **Rantala A, Fewer DP, Hisbergues M, Rouhiainen L, Vaitomaa J *et al.*** Phylogenetic evidence for the early evolution of microcystin synthesis. *Proc Natl Acad Sci USA* 2004;101:568–573.
46. **Fewer DP, Rouhiainen L, Jokela J, Wahlsten M, Laakso K *et al.*** Recurrent adenylation domain replacement in the microcystin synthetase gene cluster. *BMC Evol Biol* 2007;7:183.
47. **Hoff-Risseti C, Dörr FA, Schaker PD, Pinto E, Werner VR *et al.*** Cylindrospermopsin and saxitoxin synthetase genes in *Cylindrospermopsis raciborskii* strains from Brazilian freshwater. *PLoS One* 2013;8:e74238.
48. **OECD.** OECD Guidelines for the Testing of Chemicals. Organization for Economic Co-operation and Development.. 1994.
49. **Roeselers G, Mittge EK, Stephens WZ, Parichy DM, Cavanaugh CM *et al.*** Evidence for a core gut microbiota in the zebrafish. *ISME J* 2011;5:1595–1608.
50. **Miscoe LH, Johansen JR, Vaccarino MA, Pietrasiak N, Sherwood AR.** Novel cyanobacteria from caves on Kauai, Hawaii. *Gebr Bibliotheca Phycologica* 2016;120:75–152.
51. **Sahu A, Pancha I, Jain D, Paliwal C, Ghosh T *et al.*** Fatty acids as biomarkers of microalgae. *Phytochemistry* 2013;89:53–58.
52. **Temina M, Rezankova H, Rezanka T, Dembitsky VM.** Diversity of the fatty acids of the *Nostoc* species and their statistical analysis. *Microbiol Res* 2007;162:308–321.
53. **Dadheech PK, Glöckner G, Casper P, Kotut K, Mazzoni CJ *et al.*** Cyanobacterial diversity in the hot spring, pelagic and benthic habitats of a tropical soda lake. *FEMS Microbiol Ecol* 2013;85:389–401.
54. **Stackebrandt E, Goebel BM.** Taxonomic Note: a place for DNA–DNA reassociation and 16S rRNA sequence analysis in the present species definition in bacteriology. *Int J Syst Evol Microbiol* 1994;44:846–849.
55. **Ludwig W, Strunk O, Klugbauer S, Klugbauer N, Weizenegger M *et al.*** Bacterial phylogeny based on comparative sequence analysis. *Electrophoresis* 1998;19:554–568.
56. **Flechtner VR, Boyer SL, Johansen JR, Denoble ML.** *Spirirestis rafaelensis* gen. et sp. nov. (Cyanophyceae), a new cyanobacterial genus from arid soils. *Nova Hedwigia* 2002;74:1–24.
57. **Berrendero E, Perona E, Mateo P.** Phenotypic variability and phylogenetic relationships of the genera *Tolypothrix* and *Calothrix* (Nostocales, Cyanobacteria) from running water. *Int J Syst Evol Microbiol* 2011;61:3039–3051.
58. **Iteman I, Rippka R, Tandeau de Marsac N, Herdman M.** Comparison of conserved structural and regulatory domains within divergent 16S rRNA–23S rRNA spacer sequences of cyanobacteria. *Microbiology* 2000;146:1275–1286.
59. **Svenning MM, Eriksson T, Rasmussen U.** Phylogeny of symbiotic cyanobacteria within the genus *Nostoc* based on 16S rDNA sequence analyses. *Arch Microbiol* 2005;183:19–26.
60. **Chatchawan T, Komárek J, Strunecký O, Šmarda J, Peerapornpisal Y.** *Oxynema* , a new genus separated from the genus *Phormidium* (Cyanophyta). *Cryptogamie, Algologie* 2012;33:41–59.
61. **Thajuddin N, Subramanian G.** Survey of cyanobacterial flora of the southern east coast of India. *Botanica Marina* 1992;35:305–314.
62. **Apte SK, Thomas J.** Possible amelioration of coastal soil salinity using halotolerant nitrogen-fixing cyanobacteria. *Plant Soil* 1997;189:205–211.
63. **Moisander PH, McClinton E, Paerl HW.** Salinity effects on growth, photosynthetic parameters, and nitrogenase activity in estuarine planktonic cyanobacteria. *Microb Ecol* 2002;43:432–442.
64. **Oren A.** Diversity of halophilic microorganisms: environments, phylogeny, physiology, and applications. *J Ind Microbiol Biotechnol* 2002;28:56–63.
65. **Miyashita H, Ikemoto H, Kurano N, Miyachi S, Chihara M.** *Acaryochloris marina* gen. et sp. nov. (cyanobacteria), an oxygenic photosynthetic prokaryote containing chl *d* as a major pigment1. *J Phycol* 2003;39:1247–1253.
66. **McNeill J, Barrie FR, Buck WR, Demoulin V, Greuter W *et al.*** International code of nomenclature for algae, fungi, and plants (Melbourne Code). *Regnum Vegetabile* 2012;154:208.

Extending the ecological distribution of *Desmonostoc* genus: Proposal of *Desmonostoc salinum* sp. nov., a novel *Cyanobacteria* from a saline-alkaline lake

Luna Viggiano de Alvarenga[1,2], Marcelo Gomes Marçal Vieira Vaz[1,2], Diego Bonaldo Genuário[3], Alberto A. Esteves-Ferreira[1,2], Allan V. Martins Almeida [1,2], Naira Valle de Castro[1,2], Claudineia Lizieri[1,#], José João L.L. Souza[4,5], Carlos Ernesto G.R. Schaefer[4], Adriano Nunes-Nesi[1,2], and Wagner L. Araújo[1,2*]

INTERNATIONAL JOURNAL OF SYSTEMATIC AND EVOLUTIONARY MICROBIOLOGY

[*]**Corresponding author:** Wagner L. Araújo; Departamento de Biologia Vegetal, Universidade Federal de Viçosa, 36570-900 Viçosa, Minas Gerais, Brazil; Tel: +55 31 3899.2169; Fax: +55 31 3899.2580; Email: wlaraujo@ufv.br

Supplementary data

Figure S1. Alignment of nucleotide sequences of ITS regions from *Desmonostoc* and other selected strains.

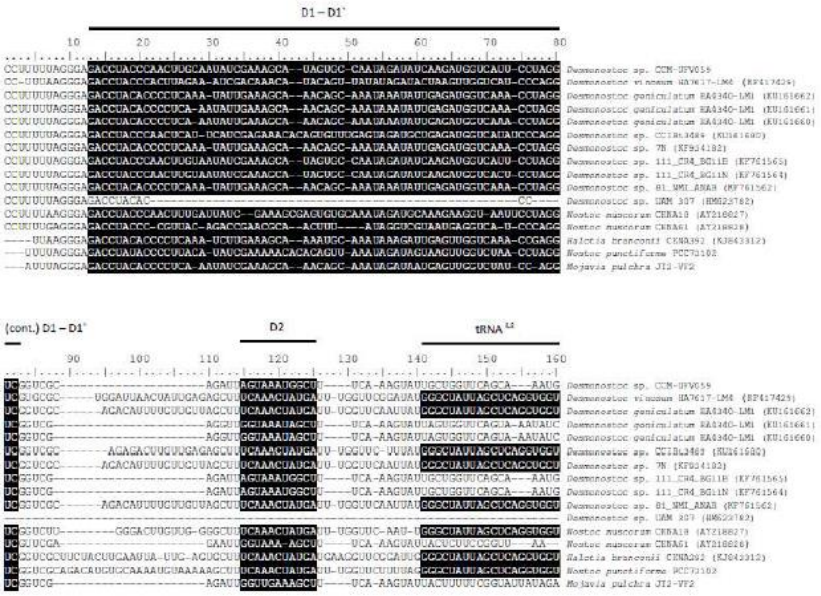

Figure S1. Cont.

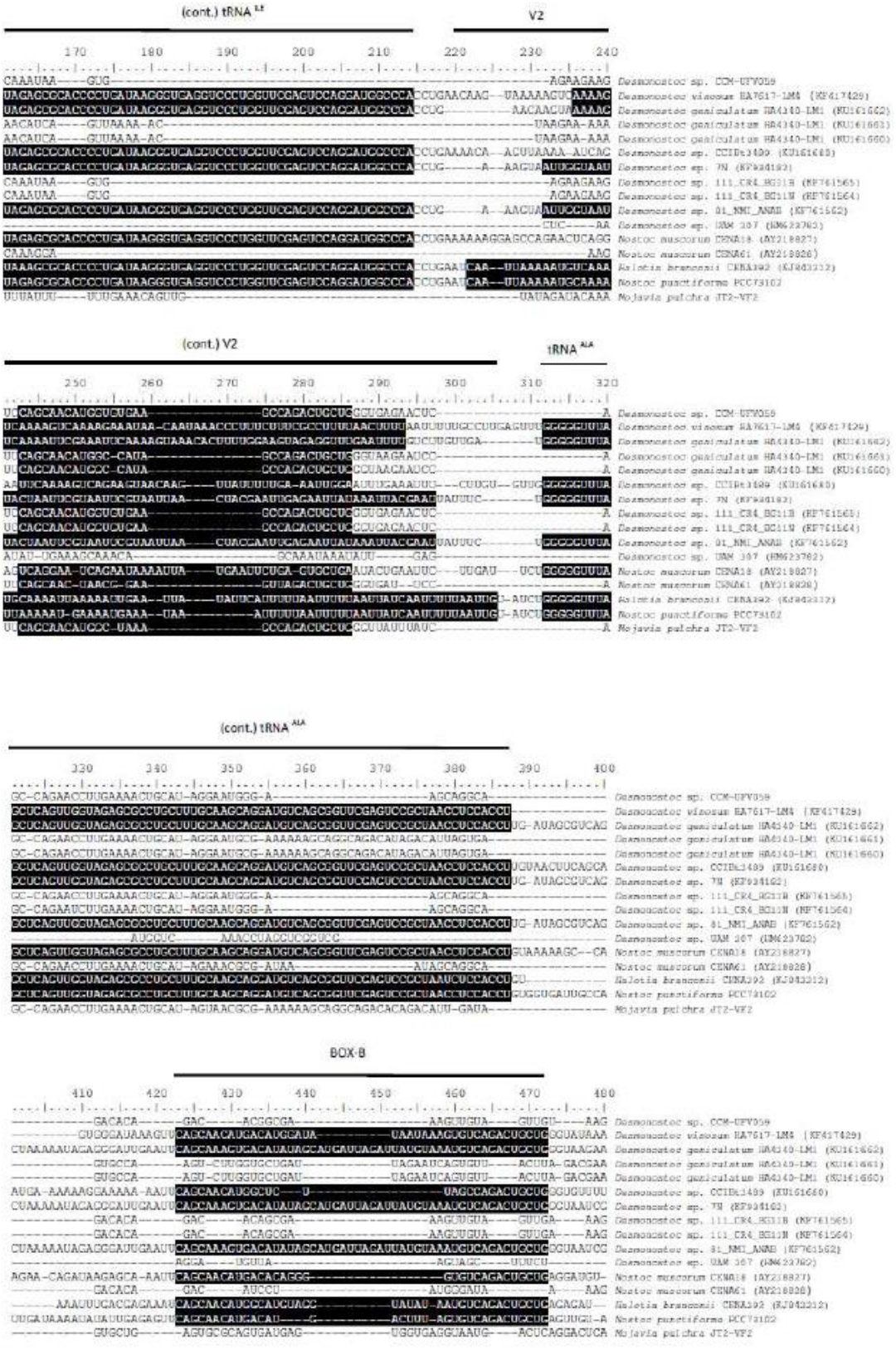

Figure S1. Cont.

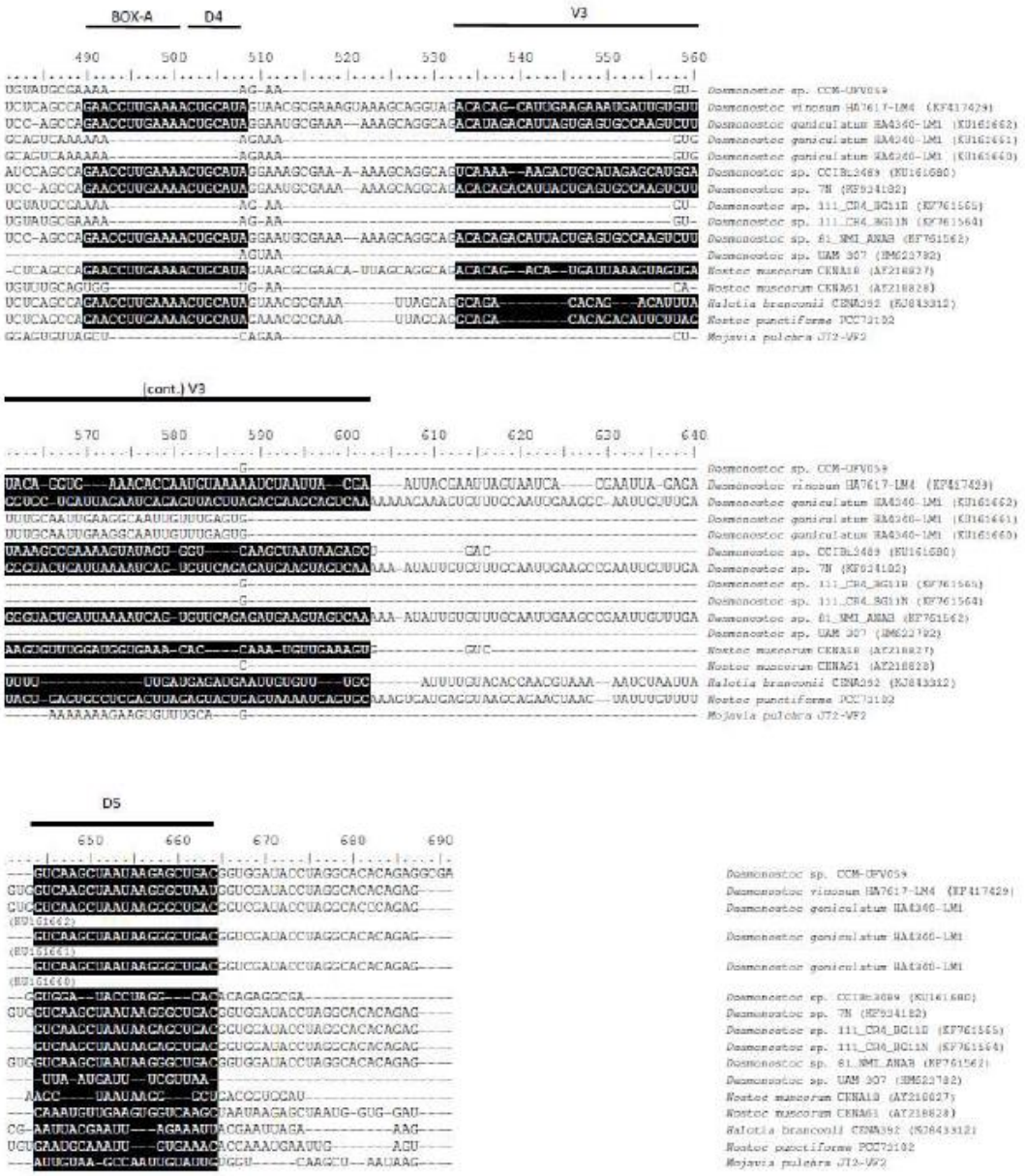

Figure S2. D1-D1' secondary structures of the 16-23S ITS sequences from selected *Desmonostoc* spp. and other morphologically-related genera. **A** - *Desmonostoc salinum* CCM-UFV059; **B** - *Desmonostoc vinosum* HA7617-LM4 (KF417429); **C** - *Desmonostoc geniculatum* HA4340-LM1 (KU161662); **D** - *Desmonostoc geniculatum* HA4340-LM1 (KU161661);**E** - *Desmonostoc geniculatum* HA4340-LM1 (KU161660); **F** - *Desmonostoc* sp. CCIBt3489 (KU161680); **G** - *Desmonostoc* sp. 7N (KF934182); **H** - *Desmonostoc* sp. 111_CR4_BG11B (KF761565); **I** - *Desmonostoc* sp. 111_CR4_BG11N (KF761564); **J** - *Desmonostoc* sp. 81_NMI_ANAB (KF761562); **K** - *Nostoc muscorum* CENA18 (AY218827); **L** - *Nostoc muscorum* CENA61 (AY218828); **M** - *Halotia branconii* CENA392 (KJ843312); **N** - *Nostoc punctiforme* PCC73102 (NC_010628); **O** - *Mojavia pulchra* JT2-VF2 (AY577534).

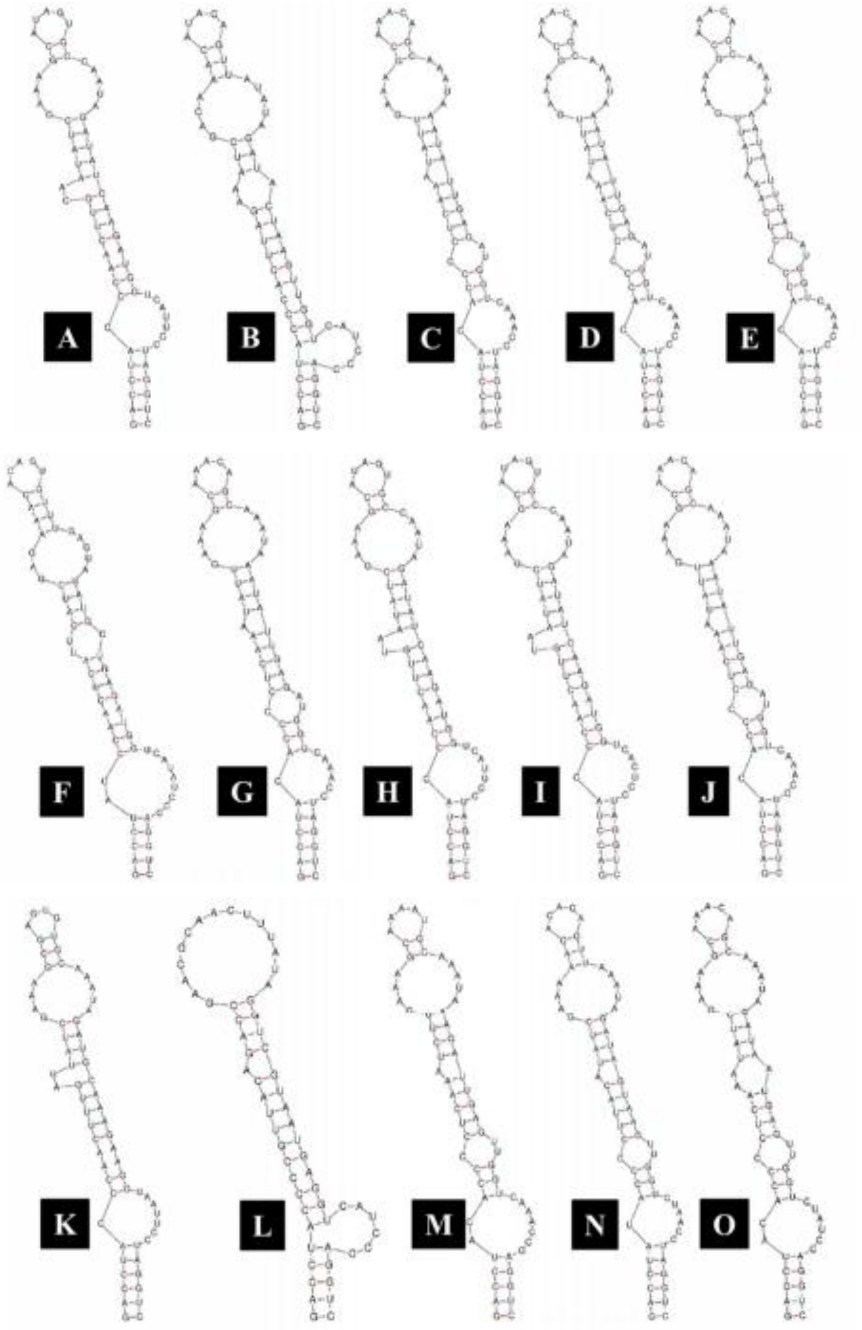

Figure S3. V2 secondary structures of the 16-23S ITS sequences from selected *Desmonostoc* spp. and other morphologically-related genera **A** - *Desmonostoc salinum* CCM-UFV059; **B** - *Desmonostoc vinosum* HA7617-LM4 (KF417429); **C** - *Desmonostoc geniculatum* HA4340-LM1 (KU161662); **D** - *Desmonostoc geniculatum* HA4340-LM1 (KU161661);**E** - *Desmonostoc geniculatum* HA4340-LM1 (KU161660); **F** - *Desmonostoc* sp. CCIBt3489 (KU161680); **G** - *Desmonostoc* sp. 7N (KF934182); **H** - *Desmonostoc* sp. 111_CR4_BG11B (KF761565); **I** - *Desmonostoc* sp. 111_CR4_BG11N (KF761564); **J** - *Desmonostoc* sp. 81_NMI_ANAB (KF761562); **K** - *Nostoc muscorum* CENA18 (AY218827); **L** - *Nostoc muscorum* CENA61 (AY218828); **M** - *Halotia branconii* CENA392 (KJ843312); **N** - *Nostoc punctiforme* PCC73102 (NC_010628); **O** - *Mojavia pulchra* JT2-VF2 (AY577534).

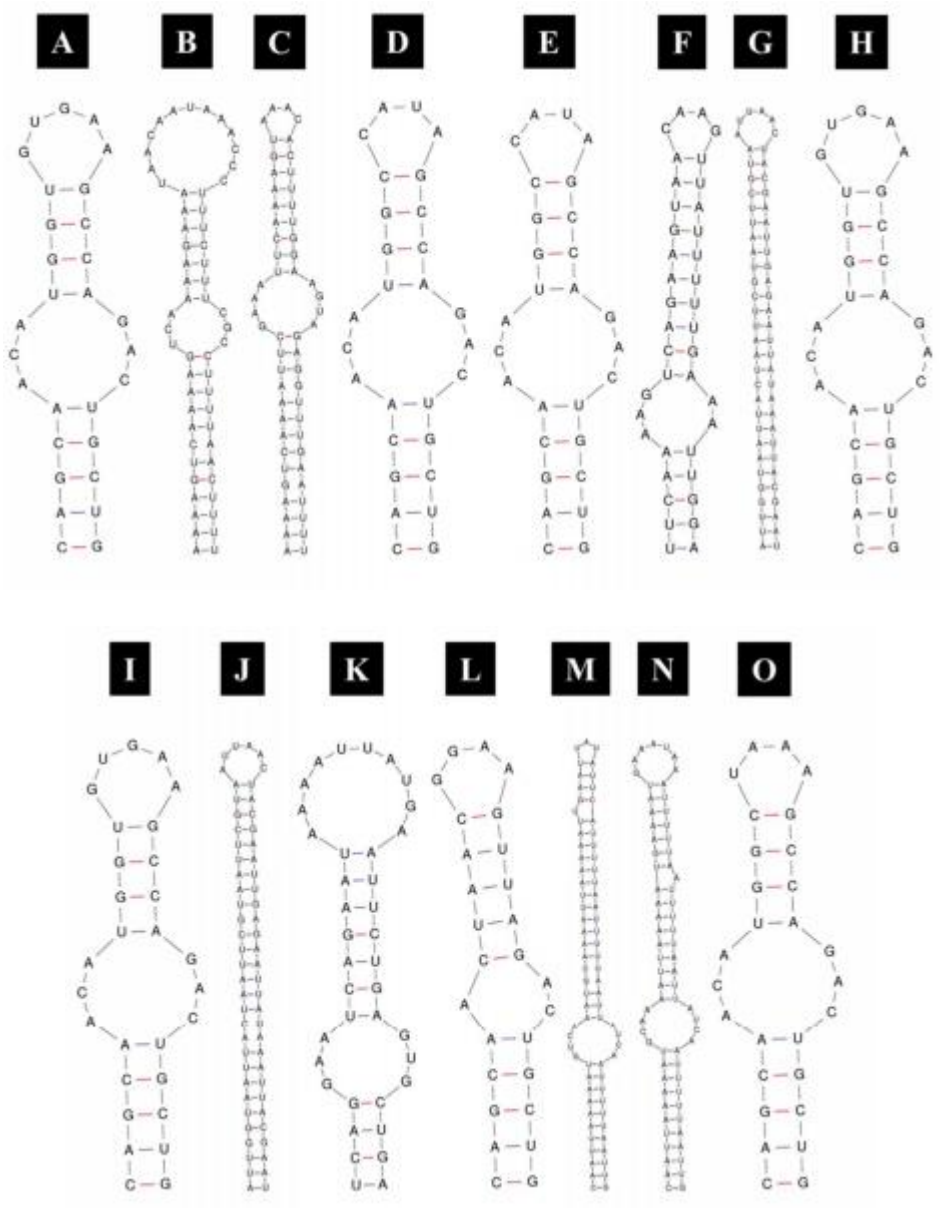

Figure S4. Maximum likelihood phylogenetic tree based on the 16S rRNA gene sequences of nostocacean cyanobacteria. The sequence of *Desmonostoc salinum* CCM-UFV059 is shown in bold with a black circle. Bootstrap values (greater than 50 %) are displayed in front of the relevant nodes.

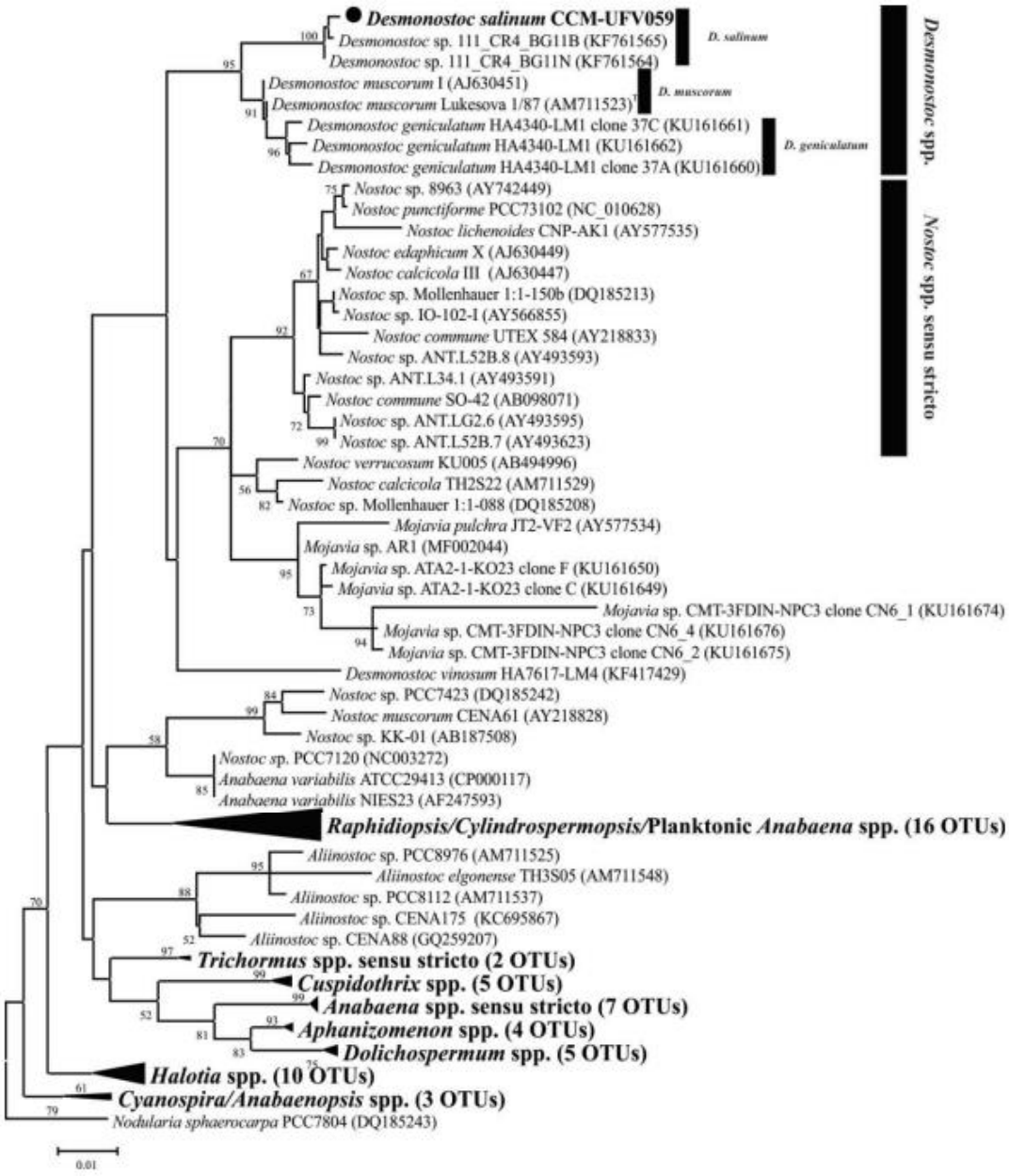

Figure S5. Lethal dose (LD_{50}) determination for *Desmonostoc salinum* CCM-UFV059 and *Nostoc* sp. PCC7120 after 72 hours of exposure to variable NaCl concentrations. The line indicates the threshold of 50 % of cellular death.

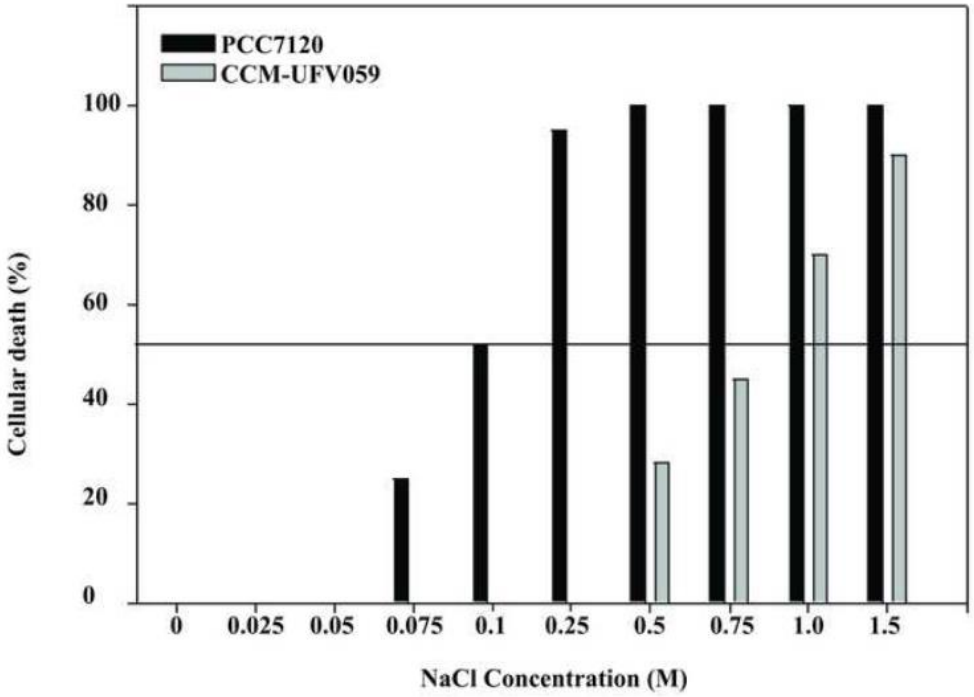

Figure S6. Growth curves of *Desmonostoc salinum* CCM-UFV059 strain under different NaCl concentrations (below LD_{50} dose). The growth was monitored every day, during 10 days by optical density (**A**) and dry weight (**B**). Values represent trend curves made from the average ± standard error (n = 3). Black filled circles (●): BG-11_0 without salt (0 M); Empty circles (○): BG-11_0 plus 0.25 M (NaCl); Black filled triangles (▼): BG-11_0 plus 0.50 M (NaCl); Empty triangles (Δ): BG-11_0 plus 0.75 M (NaCl).

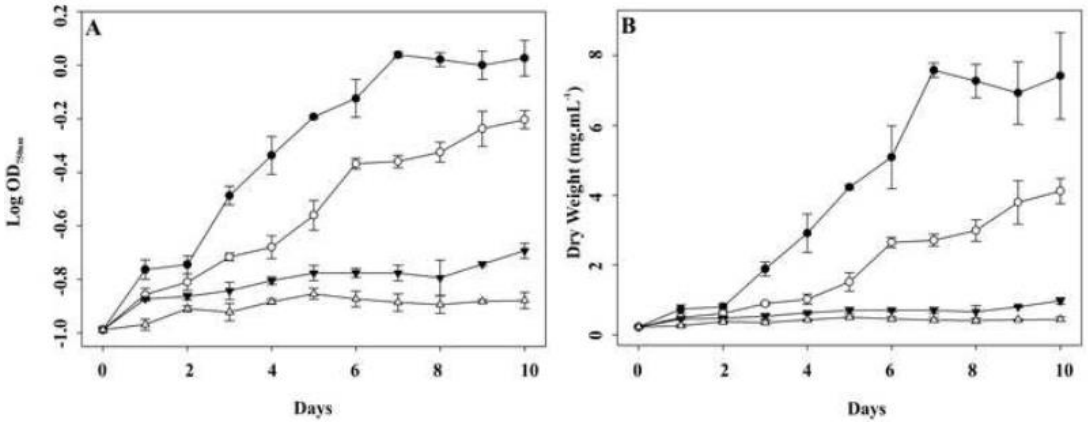

Table S1. General abiotic characteristics of Laguna Amarga[a].

Characteristics	Laguna Amarga
pH[#]	9.5
Alkalinity	3.622 g·L^{-1} (sum of HCO_3^-/CO_3^{2-})
HCO_3^-[§]	0.954 g·L^{-1} (15.6446 mmol·L^{-1} ± 0.4669)
CO_3^{2-}[§]	2.668 g·L^{-1} (44.4639 mmol·L^{-1} ± 0.3734)
OH^-[§]	0.000 g·L^{-1}

Ionic composition[§]		
Na	1251.299 mM	28.78 ± 3.27*
SO_4^{2-}	358.0725 mM	34.37 ± 3.55*
K	166.3975 mM	6.49* ± 0.107*
Mg	65.1216 mM	1,56* ± 0.024 *
Sr	0.0016 mM ± 0.0003	-
Si	0.1505 mM ± 0.02	-
Al	0.0219 mM ± 0.0016	-
Ba	0.001 mM ± 0.0002	-
Bi	0.005 mM ± 0.0002	-
Ca	0.535 mM ± 0.031	-
Cr	0.0143 mM ± 0.0028	-
Fe	0.0001 mM ± 0.00002	-
Mn	0.0006 mM ± 0.00003	-
Mo	0.0002 mM ± 0.00002	-
Ni	0.0004 mM ± 0.00005	-
Pb	0.0015 mM 0.0002	-

Ag and Cu was not detect. Cd and Co was in concentration lower than 0.0001 mM.

[a]Briefly, the elements Ag (silver), Al (aluminum), Ba (barium), Bi (bismuth), Ca (calcium), Cd (cadmium), Co (cobalt), Cr (chromium), Cu (copper), Fe (iron), K (potassium), Mg (magnesium), Mn (manganese), Mo (molybdenum), Na (sodium), Ni (nickel), Pb (lead) and Sr (strontium) were analyzed from filtered (0.45 µm pore size membrane) and acidified water samples (double-distilled HNO3), using a Perkin Elmer Optimum-3300 DV ICP-OES connected to a Perkin Elmer AutoSampler AS-90 plus. Additionally, Si (silicon) was analyzed in non-acidified samples. Analysis were carried out under the following conditions: 1,300 W RF Power, 15 L·min-1 plasma gas flow, 0.6 L·min-1 auxiliary gas flow, 0.8 L min-1 nebulizer gas flow, 1 s (minimum) to 5 s (maximum) integration time, 40 s delay time, 60 s rinse time, with 3 replicates. Triton X-100 0.5 % and HNO3 1 % were used as rinse solution. Manganese (Mn) solutions were used to optimize and calibrate the ICP-OES previously. Borate (Br), nitrate (NO3-), sulfate (SO42-), fluoride (F2-) and chloride (Cl-) were analyzed in non-acidified samples using a Dionex DX-600 Ionic exchanger chromatographer. The IonPac S11, IonPac AG11, IonPac ATC-3 analytical columns were used and ultrapure water, NaOH (10 mmol), NaOH (100 mmol) and metanolmethanol (100 %) were used as eluents. The analytical quality was checked according to Dunnivant (2004).

[#]Measurement of pH was conducted once during the sampling.

[§]Measurements of HCO_3^-, CO_3^{2-} and other ions were taken in triplicates and the results are the mean value, followed by standard deviation.

*Dissolved ionic concentration: g·L^{-1}.

Table S2. Identity matrix among *Desmonostoc salimum* CCM-UFV059 sequence and a subset of 16S rRNA gene sequences selected from the phylogenetic tree.

Strains	1	2	3	4	5	6	7	8	9	10	11	12	13	14	15	16	17	18
1. *Desmonostoc salimum* CCM-UFV059	-																	
2. *Desmonostoc* sp. PCC9231 (AY742452)	99.7	-																
3. *Desmonostoc* sp. 111_CR4_BG11B (KF761565)	99.7	99.5	-															
4. *Desmonostoc* sp. 111_CR4_BG11N (KF761564)	99.8	99.6	99.7	-														
5. *Desmonostoc* sp. PCC8306 (HG004584)	99.6	99.5	99.6	99.7	-													
6. *Desmonostoc* sp. PCC8107 (HG004583)	98.5	98.4	99.2	99.3	98.9	-												
7. *Desmonostoc* sp. CCIBt3489 (KU161680)	98.3	98.2	97.2	98.8	98.4	98.0	-											
8. *Desmonostoc* sp. Cc2 (AM711532)	98.2	98.1	98.9	99.0	98.2	98.3	98.4	-										
9. *Desmonostoc* sp. PCC7422 (HG004586)	98.5	98.4	98.8	98.9	98.8	98.3	98.3	98.9	-									
10. *Desmonostoc* sp. PCC6302 (HG004582)	97.8	97.8	98.1	98.2	97.9	97.3	97.8	98.2	98.0	-								
11. *Desmonostoc geniculatum* HA4340-LM1 (KU161660)	97.5	97.5	94.5	94.5	97.8	97.5	97.8	98.2	98.3	98.7	-							
12. *Desmonostoc* sp. 7N (KF934182)	97.8	97.7	96.7	96.8	98.0	97.7	92.2	98.7	98.0	99.2	99.0	-						
13. *Desmonostoc muscorum* Lukesova 1/87 (AM711523)^{T}	97.9	97.8	98.1	98.2	98.0	97.4	97.9	98.2	98.0	99.4	99.1	99.6	-					
14. *Desmonostoc* sp. 81_NMI_ANAB (KF761562)	98.0	97.9	96.9	97.0	98.1	97.9	92.4	98.8	98.1	99.3	99.1	99.7	99.8	-				
15. *Mojavia pulchra* JT2-VF2 (AY577534)^{T}	94.9	94.9	95.0	95.1	94.9	95.2	94.8	95.5	95.2	95.4	94.6	95.1	95.1	95.1	-			
16. *Nostoc calcicola* TH2S22 (AM711529)	96.6	96.6	96.6	96.7	96.8	96.6	97.1	97.1	96.7	96.9	96.3	96.7	96.8	96.7	96.0	-		
17. *Nostoc punctiforme* PCC73102 (NC_010628)^{R}	94.9	94.9	95.7	95.7	95.1	94.8	95.6	95.4	95.4	96.1	96.0	96.3	95.6	96.3	95.8	96.2	-	
18. *Halotia branconii* CENA392 (KJ843312)^{T}	94.6	94.5	94.9	95.0	94.9	95.1	94.3	94.4	94.5	94.3	94.4	94.7	94.4	94.8	95.1	95.2	94.2	-

^{T}Type-species and ^{R} reference sequence

Table S3. Lengths of the 16-23S ITS regions from sequences of *Desmonostoc salimum* CCM-UFV059, *Desmonostoc* spp. and other morphologically-related genera.

Strain	Complete ITS length (nt)	Lenght of 16-23S ITS regions (nt)								
		D1-D1`	D2	tRNA^{Ile}	V2	tRNA^{Ala}	BOX-B	BOX-A	D4	V3	D5
Desmonostoc salimum CCM-UFV059	327	66	11	n.f.	29	n.f.	n.f.	n.f.	n.f.	n.f.	21
Desmonostoc vinosum HA7617-LM4 (KF417429)	624	65	11	74	57	76	40	12	7	63	21
Desmonostoc geniculatum HA4340-LM1 (KU161662)	653	65	11	74	58	76	50	12	7	69	21
Desmonostoc geniculatum HA4340-LM1 (KU161661)	392	65	11	n.f.	28	n.f.	n.f.	n.f.	n.f.	n.f.	21
Desmonostoc geniculatum HA4340-LM1 (KU161660)	392	65	11	n.f.	28	n.f.	n.f.	n.f.	n.f.	n.f.	21
Desmonostoc sp. CCIBt3489 (KU161680)	578	69	11	74	39	76	29	12	7	63	16
Desmonostoc sp. 7N (KF934182)	651	65	11	74	62	76	50	12	7	69	21
Desmonostoc sp. 111_CR4_BG11B (KF761565)	322	66	11	n.f.	29	n.f.	n.f.	n.f.	n.f.	n.f.	21
Desmonostoc sp. 111_CR4_BG11N (KF761564)	322	66	11	n.f.	29	n.f.	n.f.	n.f.	n.f.	n.f.	21
Desmonostoc sp. 81_NMI_ANAB (KF761562)	651	65	11	74	62	76	50	12	7	69	21
Desmonostoc sp. UAM 307 (HM623782)	123	n.f.	n.f.	n.f.	n.f.	n.f.	n.f.	n.f.	n.f.	n.f.	16
Nostoc muscorum CENA18 (AY218827)[a]	569	67	11	n.f.	38	n.f.	32	12	7	60	14
Nostoc muscorum CENA61 (AY218828)[a]	299	60	10	n.f.	27	n.f.	n.f.	n.f.	n.f.	n.f.	21
Halotia branconii CENA392 (KJ843312)[a]	583	65	11	74	76	76	39	12	7	44	18
Nostoc punctiforme PCC73102 (NC_010628)[a]	622	67	11	74	70	76	35	12	7	61	18
Mojavia pulchra JT2-VF2 (AY577534)[a]	380	64	11	n.f.	28	n.f.	n.f.	n.f.	n.f.	n.f.	20

[a]morphologically-related genera; n.f.: not found

THE NOVEL STRAIN *Desmonostoc salinum* CCM-UFV059 SHOWS HIGHER SALT AND DESICCATION RESISTANCE COMPARED TO THE MODEL STRAIN *NOSTOC* sp. PCC7120

Luna Viggiano de Alvarenga, Wagner L. Araújo and Martin Hagemann

To be submitted at **Environmental Microbiology**

THE NOVEL STRAIN *Desmonostoc salinum* CCM-UFV059 SHOWS HIGHER SALT AND DESICCATION RESISTANCE COMPARED TO THE MODEL STRAIN *Nostoc* sp. PCC7120

Luna Viggiano de Alvarenga[1,2,3], Wagner L. Araújo[1,2] and Martin Hagemann[3*]

[1]Departamento de Biologia Vegetal, Universidade Federal de Viçosa, 36570-900, Viçosa, Minas Gerais, Brazil

[2]Max-Planck Partner Group at the Departamento de Biologia Vegetal, Universidade Federal de Viçosa, 36570-900, Viçosa, Minas Gerais, Brazil

[3]Institut für Biowissenschaften, Abteilung Pflanzenphysiologie, Universität Rostock, A.-Einstein-Str. 3, Rostock D-18059, Germany.

[*]**Corresponding author:** Prof. Dr. Martin Hagemann. Institut für Biowissenschaften, Abteilung Pflanzenphysiologie, Universität Rostock, A.-Einstein-Str. 3, Rostock D-18059, Germany. Tel: +49(0)3814986113; Fax: +49(0)3814986112; Email: martin.hagemann@uni-rostock.de

Running title: Physiological responses of *D. salinum* to salt and desiccation

Keywords: compatible solutes, sucrose, stress and trehalose.

ABSTRACT

Desmonostoc salinum is a new cyanobacterial (order *Nostocales*/ Fam. *Nostocaceae*) previously isolated from a saline-alkaline lake. The acclimation towards salt and desiccation stress of *D. salinum* CCM-UFV059 was compared to the related and well-characterized, *Nostoc* sp. PCC7120. Salt-stressed cells of *D. salinum* CCM-UFV059 maintained low cellular Na^+ concentrations and accumulated high amounts of sucrose and to a lower extent trehalose. These features permitted *D. salinum* CCM-UFV059 to grow and maintain photosynthesis at twofold higher salinities than *Nostoc* sp. PCC7120. Moreover, *D. salinum* CCM-UFV059 also induced sucrose over-accumulation under desiccation stress conditions, which allowed this strain to overcome this stress in contrast to *Nostoc* sp. PCC7120. Furthermore, additional mechanisms such as the presence of highly unsaturated lipids in the membrane and an efficient ion transport system could also explain, at least partially, how *D. salinum* CCM-UFV059 is able to acclimate to high salinities and to resist to longer desiccation periods. Collectively, our results provide the first insights into the physiological and metabolic adaptations explaining the remarkable high salt and desiccation tolerance which qualify *D. salinum* CCM-UFV059 as attractive model for further analysis of stress acclimation among heterocytes N_2-fixing cyanobacteria.

1. INTRODUCTION

Cyanobacteria are widespread photosynthetic prokaryotes and are among the oldest organisms on Earth. During their long evolution, cyanobacteria developed an enormous diversity in terms of morphology, metabolic plasticity and molecular properties, which seems to be important to cope with limiting environmental conditions and allowed their ecological success in almost all known photic ecosystems (Steinhauser et al., 2012). One of the most emblematic examples of extreme environments on Earth are soda lakes, highly alkaline lagoons enriched with carbonate salts (Foti et al., 2008). This habitat presents reduced species diversity and only highly specialized organisms, including members of the phylum *Cyanobacteria* (Andreote et al., 2014; Genuário et al., 2017). However, until 2008, no nitrogen-fixing cyanobacteria had been detected in this environment (Foti et al., 2008), and since the beginning of this decade, few cyanobacteria able to perform N_2-fixation have been reported from saline and alkaline lakes around the world (Tsyrenova et al., 2011; Dadheech et al., 2013; Genuário et al., 2017; de Alvarenga et al., 2018). The situation is similar in full marine systems, where heterocytous cyanobacteria are rarely found, e.g. *Richelia* spp. (Foster et al. 2011).

The nitrogenase, an O_2-sensitive enzyme complex, is responsible for catalyzing cyanobacterial nitrogen fixation. To cope with the production of O_2 inside their own cells by photosynthesis, cyanobacteria have evolved strategies to protect the nitrogenase complex, through spatial or temporal separation of these two incompatible metabolic processes (Esteves-Ferreira et al., 2017). In heterocytous cyanobacteria, photosynthesis is performed in vegetative cells, whereas the N_2-fixation takes place inside specialized cells called heterocyte. This differentiation process is evolutionarily advantageous because it enables the filaments to perform nitrogen fixation without any

time restrictions. Studies from the last century showed the high sensitivity of nitrogenase towards high salt contents, especially Na^+ (Vitousek et al., 1991, Fernandes et al., 1993), which could explain partially the restricted presence of nitrogen-fixing organisms in saline and particularly hypersaline environments.

Cyanobacteria from extreme environments are potential sources of novel genes, products and important targets for biotechnological application. Once isolated, these strains could be screened for useful metabolites and the mechanisms that enable them to inhabit and/or tolerate such conditions could be investigated (Genuário et al., 2019). Moreover, compared with land plants, cyanobacteria are also useful organisms for a number of industrial applications due to their high photosynthetic efficiency, rapid cell growth, basic nutritional requirements (sunlight, water, and CO_2 mainly) and the possibility of genetic manipulation (Heidorn et al., 2011; Ruffing, 2011). Given their natural diversity and ability to grow in a variety of habitats, such as areas not usable for agriculture, there is a growing interest in characterizing cyanobacteria for their potential in the production of biomass and biofuels (Parmar et al., 2011; Pade and Hagemann, 2014). Considering the high demand for potable water, the future mass cultivation of cyanobacteria for biotechnological purposes should be done in saline/brackish waters avoiding competition with agriculture. However, cyanobacterial growth in saline media may impact the cellular metabolism and yield of the product of interest (Florian et al., 2013; Pade et al., 2016).

The vast majority of organisms, including cyanobacteria and all eukaryotes, use the "salt-out" strategy for acclimation to saline environments. This strategy maintains a low level of toxic inorganic ions, such as Na^+ and Cl^- within the cytoplasm, by active export of toxic inorganic ions to avoid damages to the metabolism (Fulda et al., 2006; Hagemann, 2011). To maintain internal turgor and to drive water uptake,

these organisms accumulate organic osmoprotective compounds, which do not interfere with the basal cellular metabolism (Brown, 1974; Marin et al. 2002; Hagemann, 2011). These osmoprotective compounds, commonly referred to as compatible solutes, help to maintain membrane integrity and stability of the cellular protein apparatus. According to the preferred compatible solutes produced, cyanobacteria can be distinguished in three groups: strains with low salt tolerance usually accumulate sucrose and/or trehalose, moderate halotolerant strains use glucosylglycerol (GG), and halophilic strains, which have an absolute requirement for a minimal salt concentration, synthesize glycine betaine or glutamate betaine as their main compatible solute (Hagemann, 2011 b; Oren, 2015). Recently, homoserine betaine has been also identified as compatible solute in the marine N_2-fixing cyanobacterium *Trichodesmium erythraeum* (Pade et al., 2016).

The ability of cyanobacteria to synthesize sucrose, however, appears to be widespread among cyanobacteria because the majority of cyanobacterial genomes encodes for enzymes capable of synthesizing this compound (Klähn and Hagemann, 2011; Kolman & Salerno, 2016). Unlike other compatible solutes, sucrose and trehalose can interact directly with macromolecules. The hydroxyl group of these soluble carbohydrates allows them to contact polar clusters of glycerolipids, allowing sucrose and trehalose to partially replenish lost water from the membrane hydration layer (Potts, 2005). In addition to this, sucrose is the only compatible solute to be associated with a taxonomic unit, being the main compound found in strains of the genera *Nostoc* and *Anabaena* in response to saline stress. In cyanobacteria which differentiate heterocytes, sucrose also plays an important role as transport sugar, since it is translocated from the vegetative cells performing photosynthesis into the heterocytes where fixed nitrogen is converted into glutamate and other amino acids

using carbon skeletons and energy produced from imported sucrose (Culmino et al., 2007; Nürnberg et al., 2015). The participation of sucrose in primary cell metabolism may be the reason why its accumulation occurs in response to low salt concentrations and usually is not sufficient to generate resistance at higher concentrations (Klähn & Hagemann, 2011; Kolman et al., 2015). Compared to sucrose, trehalose is a less-studied compatible solute, being commonly associated with filamentous mat-forming cyanobacteria, isolated from terrestrial or freshwater habitats and accumulating in response to desiccation stress (Klähn & Hagemann, 2011; Ranaan et al., 2016). Moreover, the accumulation of trehalose in response to saline stress was detected in 44 strains including 20 strains where it represents the main compatible solute (Hagemann, 2013).

The acclimation to saline environments involves a coordinated mechanism among cyanobacteria, which is relatively well understood for the model strain *Synechocystis* sp. PCC 6803 (Marin et al., 2004; Hagemann, 2011). During the first two hours after salt exposure occurs the initial synthesis of compatible solutes and uptake of K^+, leading to the immediate extrusion of Na^+ (Hagemann, 2011). Subsequently, about 12 hours after salt exposure, the extrusion of K^+ and Cl^- occurs. In *Synechocystis* sp. PCC 6803, Na^+ transporters are pre-existing and activated following the exposure to concentrations of 300 mM NaCl (Marin et al., 2004). Moreover, the instauration status of the membranes seems to be another important feature to salt tolerance in cyanobacteria. It has been demonstrated that polyunsaturated fatty acids are involved in the protection of the photosynthetic machinery against salt stress (Sakamoto & Murata, 2002). Accordingly, the unsaturation of fatty acids has two effects: alleviating of NaCl-induced damages and

enhancing the PSI and PSII damages repair (Allakhverdiev et al., 2001; Allakhverdiev & Murata, 2008).

The strain *Desmonostoc salinum* CCM-UFV059 is a filamentous heterocytous cyanobacterium, which was isolated from a benthic microbial mat occurring at the shore of a hypersaline lake (Laguna Amarga) and represents the first member of the genus *Desmonostoc* in the order Nostocales found in a saline-alkaline environment (de Alvarenga et al., 2018). Briefly, we previously observed that the LD_{50}, value that represents the salt concentration capable of killing 50 % of cells after 72 h of exposure, was 890 mM NaCl (de Alvarenga et al, 2018), a concentration nine times higher than found in the model filamentous strain *Nostoc* sp. PCC7120 (Agrawal et al., 2014).

Most studies on cyanobacterial salt acclimation have been carried out on unicellular strains, which cannot fix N_2. To close this gap, this study aimed at to decipher the main salt acclimation mechanisms employed by *D. salinum* CCM-UFV059 to thrive in a saline environment. Moreover, an improved understanding of salt acclimation processes in cyanobacteria might allow biotechnological applications of these organisms as feedstock and biofuel production, through cultivation in brackish or wastewater (Pade & Hagemann, 2015).

2. MATERIAL AND METHODS

2.1 Cyanobacterial strains

The strain *Desmonostoc salinum* CCM-UFV059 (hereafter *D. salinum* CCM-UFV059) used in this study was isolated from a saline-alkaline lake (de Alvarenga et al., 2018), and is currently available at the Collection of Cyanobacteria and Microalgae at the Universidade Federal de Viçosa (CCM-UFV). The model strain *Nostoc* sp. PCC7120 (hereafter *Nostoc* PCC7120), available at the Pasteur Culture Collection

(PCC), was used as control during the experiments. The cultures were maintained in glass Erlenmeyer flasks (125 mL) filled with 40 mL of liquid nitrate-containing BG-11 medium without sodium carbonate (modified Rippka et al., 1979) under the following conditions: 24 ± 2 °C, continuous light of 100 μmol photons m^{-2} s^{-1}.

2.2 Experimental setup

All the experiments were grown in glass Erlenmeyer flasks (50 mL) filled with 20 mL of BG-11 medium, under 24 ± 2 °C, continuous light of 100 μmol photons m^{-2} s^{-1}. The salt stress experiment was performed with *D. salinum* CCM-UFV059 and *Nostoc* PCC7120 cells pre-inoculated during three days in BG-11. The cells were then kept for 24 h in BG-11 supplemented with 0 M; 0.25 M and 0.5 M NaCl, and harvest by filtration for biochemical analysis.

The desiccation experiments were conducted with cells of *D. salinum* CCM-UFV059 and *Nostoc* PCC7120 previous inoculated in BG-11 supplemented with 0 M and 0.1 M NaCl for three days, posteriorly this cells were placed on glass fiber filters and subjected to the dehydration chamber system described by Karsten et al. (2014). The system allows to follow the kinetics of effective quantum yield of photosystem II (Y(II)) using noninvasive pulse amplitude modulation (PAM) fluorometry (PAM 2500; Heinz Walz GmbH, Effeltrich, Germany) during the dehydration and rehydration phases. The Y(II) of cells was measured every 20 min until the cells were completely desiccated (Y(II) = 0) in the chamber filled with silica gel to create a low humidity of approximately 5%. After the dehydration period, the dried glass fiber filters were transferred to a new chamber filled with 100 mL tap water instead of silica gel to create a high humidity atmosphere (>95 %). The filters were rehydrated by

adding 200 µL of the standard growth medium to each filter and recovery of Y(II) was followed with the same methodology as described above.

2.3 Photosynthetic activity measurements

Measurements of photosynthesis and dark respiration were carried out with cells of *D. salinum* CCM-UFV059 or *Nostoc* PCC7120 that were exposed toward three different salt concentrations (0 M; 0.25 M and 0.5 M NaCl) for 24 h using a Clark-type electrode connected to a biological oxygen monitor (Chlorolab 2 System, Hansatech, Norfolk, UK) as previously described (Jeon et al., 2005). The instrument was calibrated using a solution of sodium hydrosulfite and BG-11 medium to set 0% saturation. Then, 2 mL of culture containing approximately 2 µg Chl a mL^{-1} was inoculated in the electrode chamber and the net photosynthetic rates (*A*) were measured at the saturating light intensity of 100 µmol photons m^{-2} s^{-1} and 25 °C for 5 min.

2.4 Analysis of sodium (Na^+) and potassium (K^+) ion contents

The concentrations of Na^+ and K^+ were determined according to Mikkat et al. (2000) using a flame photometer (PFP7; Jenway). Briefly, cells from 5 mL of *D. salinum* CCM-UFV059 or *Nostoc* PCC7120 culture were harvested after exposure to three different salt concentrations (0 M; 0.25 M and 0.5 M NaCl) for 24 h on polycarbonate filters (diameter 47 mm, pore size 0.2 µm, Millipore) and washed twice with 5 mL of ice-cold isotonic $Ca(NO_3)_2$ solution. The filters were placed into 15 mL vials containing 10 mL deionized water and the ions were extracted by boiling. The filters were removed from the hot solution, after cooling the cells were pelleted by centrifugation. The ion extracts were used with 1:50 dilution for flame photometry.

The filters and all other materials used for ion determination were extensively rinsed with hot deionized water before use.

2.5 Analysis of sucrose and trehalose contents

The cells were harvested by filtration from 5 mL of *D. salinum* CCM-UFV059 or *Nostoc* PCC7120 culture after exposure to three different salt concentrations (0 M; 0.25 M and 0.5 M NaCl) for 24 h and before, during and after the desiccation stress.. The quantification of compatible solutes sucrose and trehalose was conducted according to Kirsch et al. (2017).. The low molecular weight compounds were extracted off the cells with ethanol (80 %, HPLC grade, Roth, Germany) at 68 ºC for 2 h. Fifty micrograms of sorbitol were added to the samples as an internal standard. After centrifugation, the supernatants were collected and freeze-dried. The dry extracts were washed with 500 µL of pure ethanol (HPLC grade, Roth, Germany) and freeze-dried again. Organic compounds were then analyzed by gas chromatography.

2.6 Quantification of other metabolites

Cells subjected to salt and/or desiccation stress were harvested and extracted for LC-MS analysis as described above (item 2.4). The cells from the desiccation stress experiment were harvested during the beginning of the experiment after the effective quantum yield of photosystem II (Y(II)) reached zero, and after rehydration, marked by the recovery of Y(II). The dried extracts were dissolved in 400 µL water and filtrated through 0.2 µm filters (Omnifix®-F, Braun, Germany). The cleared supernatants were analyzed using the high-performance liquid chromatograph mass spectrometer LCMS-8050 system (Shimadzu, Japan) and the incorporated LC-MS/MS method package for primary metabolites (version 2, Shimadzu, Japan). In brief, 1 µL

of each extract was separated on a pentafluorophenylpropyl (PFPP) column (Supelco Discovery HS FS, 3 µm, 150 x 2.1 mm) with a mobile phase containing 0.1% formic acid. The compounds were eluted at 0.25 mL min^{-1} using the following gradient: 1 min 0.1% formic acid, 95% distilled water, 5% acetonitrile, within 15 min linear gradient to 0.1% formic acid, 5% distilled water, 95% acetonitrile, 10 min 0.1% formic acid, 5% distilled water, 95% acetonitrile. Aliquots were continuously injected in the MS/MS part and ionized via electrospray ionization (ESI). The compounds were identified and quantified using the multiple reaction monitoring (MRM) values given in the LC-MS/MS method package and the LabSolutions software package (Shimadzu, Japan). The metabolites were determined as relative metabolite abundances, which were calculated by normalization of signal intensity to that of the internal standard carnitine and cell dry mass.

2.7 Gene expression analysis

To determine if the compatible solute synthesis is stimulated at transcriptional levels, we aimed to analyze the salt-dependent expression of related genes. The genome sequence of *D. salinum* CCM-UFV059 is unknown, therefore, we started to obtain partial genes for sucrose (*sps* and *spp*) or trehalose (*treY* and *treZ*) biosynthesis. To obtain these genes via PCR we used degenerated primers (Primers are listed in Supplementary Table 1), which were deduced from annotated gene sequences of Nostocales such as *Nostoc* PCC7120, *Nostoc calcicola* and *Nostoc linckia*. After the PCR, bands corresponding to the expected sizes were only obtained for the maltooligosyl trehalose trehalohydrolase (*treZ*) and sucrose-phosphate phosphatase (*spp*) genes, which act as the first enzyme of the synthesis pathway of trehalose and the second enzyme of the synthesis pathway of sucrose, respectively. Sequencing of

the obtained fragments supported the nature of these partial sequences since they showed significant similarities to annotated *treZ* and *spp* genes. These partial gene sequences of *D. salinum* CCM-UFV059 were used to design specific primers for qRT-PCR (Primers are listed in Supplementary Table 1).

Total RNA from *D. salinum* CCM-UFV059 was isolated using the TRIzol® protocol with an additional step during the extraction to ensure complete cell lysis (10 min at 65 ºC). The RNA was reverse transcribed into cDNA using Transcriptor First Strand cDNA Synthesis Kit (Roche 0489686600). The qPCR expression analysis of *treZ* and *spp* were performed on a LightCycler 1.5 system (Roche) using SYBR Green fluorescence (Roche) for detection and oligonucleotides described in the supplemental material (Supplementary Table 2). Gene expression was normalized to the constitutively expressed rRNA 16S reference gene and the average cycle threshold (n = 3) used to calculate relative expression values via the comparative Ct ($^{\Delta\Delta}$Ct)-method.

2.8 FAMEs profiling

The fatty acid methyl esters (FAMEs) profile of *D. salinum* CCM-UFV059 was analyzed using cells after cultivation in nitrate-containing BG-11 with and without 0.1 M NaCl. Briefly, 10 mg lyophilized cells were harvested during the exponential phase of a growth curve in three replicates. Fatty acid derivatization was conducted according to the Sherlock Microbial Identification MIDI System, using HCl–methanol 6 % (v/v) and hexane (http://www.midi-inc.com/ Technical note #101). A total of 0.05 mL of the non-polar fraction was taken for analysis on model 7890 gas chromatograph (Agilent) equipped with an HP-ultra 2 column (25 m, 0.20 mm ID, 00: 33 μM film thickness). The MIDI Sherlock version 6.2 (MIDI) software was used to adjust the operational parameters and for recognition, quantification, and comparison with the

reference libraries. The results are expressed as percentages of the total FAME content obtained in the chromatogram.

2.9 Statistical analysis

The Student's *t* test was used to compare values between *D. salinum* CCM-UFV059 and *Nostoc* PCC7120 at 5% of significance level ($P < 0.05$) using the algorithm embedded into Microsoft Excel 10.0 (Microsoft). Metabolomics data from *D. salinum* CCM-UFV059 and *Nostoc* PCC7120 cells were analyzed in comparison with the control treatment of each strain namely 0 M NaCl and before desiccation for salt and desiccation stress, respectively.

3. RESULTS

3.1 Acclimation of cells to salt stress

We have previously demonstrated that *D. salinum* CCM-UFV059 display remarkable salt tolerance among strains of the order Nostocales, which corresponds to its isolation from an alkaline soda lake (Alvarenga et al. 2018). To obtain further insight into the physiological basis of this high salt tolerance, we here compared *D. salinum* CCM-UFV059 with the strain *Nostoc* PCC7120, which represents the best studied cyanobacterium model of the order Nostocales. Under the conditions used here, *D. salinum* CCM-UFV059 was able to sustain photosynthesis and growth when exposed to 500 mM NaCl, while *Nostoc* PCC7120 only showed growth and photosynthetic activity up to the maximum concentration of 200 mM NaCl (Fig. 1). However, under control conditions of NaCl-free BG-11 *Nostoc* PCC7120 showed much higher growth rates and photosynthetic activity than *D. salinum* CCM-UFV059 (Fig. 1).

Our analyses of low molecular sugars supported the notion that *Nostoc* PCC7120 used sucrose as the main compatible solute, which accumulated high levels of sucrose (~ 22 nmol per mg dry weight) and trehalose as minor compatible solute at 0.2 M NaCl (Fig. 2). Trehalose and sucrose contents were lower in *Nostoc* PCC7120 cells exposed to 0.5 M NaCl in agreement with the strong photosynthetic inhibition under this condition. *D. salinum* CCM-UFV059 also accumulated sucrose as main compatible solute and trehalose as second compound (Fig. 2). Notably, sucrose reached about four times higher levels at 0.25 M NaCl. Moreover, trehalose and especially sucrose showed increased levels in cells of *D. salinum* CCM-UFV059 at 0.5 M NaCl. Interestingly, *D. salinum* CCM-UFV059 cells already contained relatively high sucrose amounts when cultivated in NaCl-free BG-11, whereas *Nostoc* PCC7120 cells only accumulated traces of sucrose. Despite the increase of sucrose and trehalose amounts after 24 h of cell exposure to salt stress, the expression of *spp* and *treZ* was not stimulated in salt stressed cells of *D. salinum* CCM-UFV059 (Fig. 3).

We further compared Na^+ and K^+ levels in *D. salinum* CCM-UFV059 and *Nostoc* PCC7120 showing that the intracellular Na^+ content was lower in *D. salinum* CCM-UFV059 cells (~75%) compared to *Nostoc* PCC7120 after exposure to 0.25 M NaCl for 24 h, while the content of K^+ was two times higher (Fig. 4). Lower amounts of the toxic Na^+ and higher amounts of the compatible ion K^+, correlate well with the observed salt tolerance levels of these strains. This finding indicates that an efficient Na^+ export and a better K^+ uptake could be a key reason for the higher salt tolerance of the species *D. salinum* CCM-UFV059.

Although salt tolerance between *D. salinum* CCM-UFV059 and *Nostoc* PCC7120 is markedly different, both strains displayed a similar metabolic profile after 24 h exposure to 0.25 M and 0.5 M NaCl. Thus, only few metabolites showed

significant differences under high salt concentration, which was mostly conserved between both strains with the exception of citrate and methionine. For instance, GABA and several amino acids (e.g. glutamine, glutamate and lysine) significantly increased, while aspartate decreased (Fig. 5). GABA, an intermediate for amino acids metabolism, is known to often enhance in response to stress due to an increase in the glutamate decarboxylase activity (Boonburapong et al., 2016, Zhang et al., 2016). The reduced amount of aspartate could thus suggest an increased flux towards glutamate and then GABA.

3.2 Desiccation stress

Due to both its ability to produce trehalose in response to salt stress and the environment where *D. salinum* CCM-UFV059 was isolated, we here hypothesized that this species is also able to deal with desiccation stress. Because our preliminary results revealed that trehalose accumulation is salt induced, we included cells pre-grown at 0.1 M NaCl-containing BG-11 medium. Desiccated cells of the model strain *Nostoc* PCC7120 showed a continuous decrease of the Y(II) reaching only 50 % of the initial values already after 60 min and dropped to zero after 3 h. In contrast to our expectations, salt-acclimated cells of *Nostoc* PCC7120 showed even faster inhibition of the Y(II) than cells from freshwater medium (Fig. 6). Notably, *D. salinum* CCM-UFV059 displayed a remarkable desiccation tolerance. Cells of *D. salinum* CCM-UFV059 were able to sustain normal Y(II) for a long time, presenting an abrupt and rapid decay after 210 min of exposure to the stress (Fig. 6). Remarkably, Y(II) values started to increase immediately after hydration and it was observed that 170 min after the hydration the Y(II) % of *D. salinum* CCM-UFV059 cells pre-grown without salt and cells exposed to 0.1 M NaCl was 80 % and 55 %, respectively. Moreover, 24 h

after hydration *D. salinum* CCM-UFV059 cells were fully recovered and cells exposed to 0.1 M NaCl presented Y(II) equal to 85 % of the initial value, whereas desiccated cells of *Nostoc* PCC7120 could not recover Y(II) at all after rehydration (data not shown). It seems therefore reasonable to assume that *D. salinum* CCM-UFV059 is much higher desiccation tolerant than the model cyanobacterium *Nostoc* PCC7120.

The difference in desiccation tolerance is also seen in terms of compatible solute levels in both strains. Accordingly, changes in the amount of sucrose in cells of *Nostoc* PCC7120 were not observed neither during the desiccation stress nor after rehydration in not acclimated cells. However, cells of *Nostoc* PCC7120 pre-grown in 0.1 M NaCl displayed a slight increase of sucrose during the desiccation stress (Fig. 7A). By contrast, cells of *D. salinum* CCM-UFV059 accumulated large amounts of sucrose in response to desiccation stress. The ratio of sucrose in *D. salinum* CCM-UFV059 cells growing in BG-11 was 1: 2.5: 1.5 (before desiccation: during desiccation: after rehydration) and in cells growing in BG-11 with 0.1 M NaCl, 1: 2.5 : 1. Moreover, the initial levels of sucrose in *D. salinum* CCM-UFV059 cells grown in BG-11 with 0.1 M NaCl were 5 times higher compared to cells grown without salt. The maximum content of sucrose (~250 nmol.mg dry weight^{-1}) was observed in *D. salinum* CCM-UFV059 grown in BG-11 with 0.1 M NaCl, during the desiccation stress. Trehalose content increased in *Nostoc* PCC7120 cells grown without salt during the desiccation stress (Fig. 7B) as previously reported (Higo et al., 2006). During desiccation stress the amount of trehalose in cells of *Nostoc* PCC7120 and *D. salinum* CCM-UFV059 pre-cultivated in BG-11 without salt was 10 and 40 nmol mg^{-1} dry weight, respectively. The ratio of trehalose in *D. salinum* CCM-UFV059 before desiccation, during desiccation and after rehydration was 1: 10: 5 in cells growing in BG-11 and 1: 6: 2 in cells growing in BG-11 with 0.1 M NaCl. The initial levels of trehalose in *D. salinum*

CCM-UFV059 cells grown in BG-11 with 0.1 M NaCl were 2.5 times higher compared to cells grown without salt. Despite the higher amount of trehalose and sucrose produced, *D. salinum* CCM-UFV059 presented enhanced sensibility to the combination of desiccation and salt stress, which is probably related to the higher internal ionic content of these cells compared to cells from NaCl-free BG-11 medium. The metabolite profile of *Nostoc* PCC7120 cells shows a strong reduction of the metabolism when the cells are exposed to desiccation stress, as observed by the absence of changes in comparison to cell before desiccation (Fig. 8), which explain, at least partially, the incapacity of such cells to fully recover after stress. This fact apart, cells of *Nostoc* PCC7120 cultivated in BG-11 with 0.1 M NaCl, displayed an accentuated increase of GABA and proline; moreover, the content of leucine, isoleucine, phenylalanine, and histidine slightly increase during the stress. GABA is frequently associated with abiotic stress responses as an alternative respiratory substrate (Sweetlove et al., 2010) and proline can act as an oxidative protector molecule and contributes to the osmotic adjustment in response to salt stress (Rezayian et al., 2018). Therefore, the production of GABA and proline is likely part of salt acclimation strategy, yet it did not support desiccation tolerance as depicted by the faster decline of Y(II) in salt-acclimated cells and the inability to recover from the stress. Moreover, after rehydration *Nostoc* PCC7120 cells significantly reduced all metabolites (Fig. 8). *D. salinum* CCM-UFV059 cells cultivated in BG-11 showed increased contents of GABA and succinate during the stress (Fig. 8). After rehydration, a decrease of arginine, glutamate, glycine, aspartate, and proline, with no changes of others metabolite was observed for those cells. During the desiccation and after the hydration cells of *D. salinum* CCM-UFV059 grown in BG-11 with 0.1 M NaCl were characterized by increased levels of glutamine and lysine, with further reductions in

the levels of aspartate and glutamate after rehydration. Moreover, methionine was the only metabolite reduced in all strains during the desiccation (Fig. 8).

3.3 FAMEs analysis

To gain further insights into the differential salt tolerance between *D. salinum* CCM-UFV059 and *Nostoc* PCC7120 we further analysed the changes in the fatty acid composition during the desiccation treatment in *D. salinum* CCM-UFV059 cells. Fifteen unsaturated (UFA) and saturated (SFA) fatty acid were unequivocally identified. Cells of *D. salinum* CCM-UFV059 growing in BG-11 contained 57 % of UFA and 43 % of SFA whereas cells of *D. salinum* CCM-UFV059 cultivated in BG-11 supplemented with 0.1 M NaCl increased the percentage of UFA to 62 % (Fig. 9). Overall, palmitic acid (16:0) and palmitoleic acid (16:1) and oleic acid (18:1) and linoleic acid (18:2) were found as major fatty acids in cells of *D. salinum* CCM-UFV059. Although only a 5 % increase of UFA concentration was observed in cells exposed to saline conditions, it seems reasonable to assume this as an acclimation towards salt stress. Interestingly, cells of *D. salinum* CCM-UFV059 displayed a higher percentage of UFA than *Nostoc* PCC7120 under conditions without salt (Shukla et al., 2012), which could be an indicative of cell adaptation to saline and drought conditions, allowing this species to thrive in a harsh environment such as Laguna Amarga.

4. DISCUSSION

D. salinum CCM-UFV059 presented a remarkable salt tolerance among Nostocales, especially when compared to the strain *Nostoc* PCC7120. Although both strains accumulate sucrose as the main compatible solute, *D. salinum* CCM-UFV059 was able to produce three times the amount of sucrose after 24 h of exposure to 0.25

M NaCl, reaching relatively high values (~100 nmol mg^{-1} dry weight) (Fig. 2A). Similar values have been reported for cells of *Nostoc muscorum* after eight days of exposure to 0.2 M NaCl (Blumwald et al., 1982), while *Synechocystis* sp. PCC 6803 exposed to 0.2 M NaCl for 24 h contained only one-fifth of such levels of sucrose but high amounts of glucosylglycerol (Kirsch et al., 2018). These findings indicate that the production of compatible solute is likely not the main responsible for the differential halotolerance between the strains *D. salinum* CCM-UFV059 and *Nostoc* PCC7120. Differences were also found regarding the ion relations in these two strains and, as such, whereas *D. salinum* CCM-UFV059 contained less of the toxic Na^+ it has enhanced amounts of the compatible K^+ (Fig. 4). This is consistent with early studies which point out that the inorganic ion export capability was most likely the main mechanism involved in salt tolerance in cyanobacteria (Apte et al., 1987). This idea was further strengthened by the discovery of sucrose as the main compatible solute in the marine genus *Prochlorococcus* (Klähn et al., 2010). The operon Mrp (*multiple resistance and pH adaptation*) is the only experimentally verified carrier involved in the Na^+ extrusion in *Nostoc* PCC7120 (Blanco-Rivero et al., 2005). The same system seems to be important for the uptake of HCO_3^-, because this operon is usually found downstream to the *bicA* and / or *sbtA* in cyanobacteria, both encoding Na^+ / HCO_3^- symporters. Accordingly, it is possible that the principal role of the Mrp system is to maintain the Na^+ gradient used by these and other transporters to capture inorganic carbon, especially in alkaline environments (Fukaya et al., 2009). This operon was also later identified in the halophilic species *A. halophytica* (Fukaya et al., 2009) and appears to be found in almost all cyanobacteria (Hagemann, 2011). The lower content of Na^+ found in cells of *D. salinum* CCM-UFV059 exposed to salt stress might indicated the presence of additional ion export system, which could act preventing the

accumulation of Na^+ ions in the metabolism. For example, different Na^+/H^+ antiporters were discussed to play crucial roles for Na^+ in the cyanobacterial model *Synechocystis* sp. PCC 6803 (Elanskaya et al., 2002; Inaba et al., 2001; Wang et al., 2002). Although by using genomic tools available at the moment we could not experimentally identify this transporter in *D. salinum* CCM-UFV059, further studies including the full genome sequencing of this strain are clearly required to fully elucidate the importance of this mechanism.

The higher unsaturation of membrane lipids is often directly related to stress including salt tolerance among cyanobacteria, most likely via the protection of the photosynthetic machinery and its possible role in the activity of the Na^+ / H^+ antiporters (Los et al., 2013). Thus, the greater fatty acid unsaturation presented by *D. salinum* CCM-UFV059 cultured in medium supplemented with 0.1 M NaCl may possibly activate Na^+ / H^+ antiporters via enhanced fluidity of the membrane. Consequently, the protection of the metabolism against Na^+ allows the maintenance of photosynthesis and thus culminating in more available energy for the production of compatible solutes and global acclimation process (Allakhverdiev et al., 2001). Taken together, the high production of compatible solutes (Fig. 2), the efficient ion transport system (Fig. 4), and the unsaturated fatty acids profile (Fig. 9), displayed by *D. salinum* CCM-UFV059 represent conspicuous features selected in the harsh environment of Laguna Amarga, which allow the cells to thrive in a high saline habitat.

D. salinum CCM-UFV059 was also able to produce high amounts of sucrose and trehalose in response to desiccation (Fig. 7), and promptly recover the Y(II) (Fig. 6) after desiccation stress, even when pre-grown under saline conditions. Notably, our knowledge regarding desiccation in cyanobacteria remains fragmentary; however, the presence of a dense exopolysaccharide (EPS) (Liu et al., 2017) and trehalose synthesis

(Higo et al., 2006), both features apparently shown by *D. salinum* CCM-UFV059 (de Alvarenga et al., 2018) seems to be essential to cope with this stress. To date, most of the desiccation experiments with the strain *Nostoc* PCC7120 were performed through a slow dehydration process, allowing a metabolic readjustment and the cellular reactivation after hydration (Katoh et al., 2004; Higo et al., 2006; Yoshimura et al., 2007). Nevertheless, to reproduce environmental conditions similar to those in which the *D. salinum* CCM-UFV059 was collected, our experiments were performed with dehydration through silica gel and not by exposure to warm temperatures (~ 30°C) in petri dishes. It is highly possible, therefore, that because of this quick desiccation, the cells of *Nostoc* PCC7120 were neither able to recover nor to produce large amounts of sucrose or especially trehalose as previously observed (Higo et al., 2006). Conversely, *D. salinum* CCM-UFV059 cells adapted to the imposed stress, responding to the combination of salt and desiccation stress and producing high amounts of sucrose. It seems reasonable to anticipate that *D. salinum* CCM-UFV059 most likely experienced desiccation periods during its lifetime and thus display adaptation mechanisms to quickly respond to the dehydration process. Further analysis including the full genomic sequencing and transcriptomics approaches are still required to better understand both physiological and molecular plasticity as well as the adaptive strategies of *D. salinum* CCM-UFV059. Notwithstanding, due to both the remarkable salt and desiccation tolerance displayed by *D. salinum* CCM-UFV059 and the knowledge of its ecological background, our results allows us to propose this strain as a new model for heterocytous cyanobacteria in the field of environmental stress physiology.

ACKNOWLEDGEMENTS

We want to express our gratitude to Prof. Ulf Karsten and Dr. Karin Glaser (Department of Applied Ecology and Phycology of the University of Rostock) for helping with the desiccation experiments. The working stay of LVA at University of Rostock was supported by funding from Deutsche Akademische Austauschdienst (DAAD) and National Council for Scientific and Technological Development (CNPq-Brazil, Grant 290078/2017-2). The LC-MS equipment at University of Rostock was financed through the HBFG program (GZ: INST 264/125-1 FUGG). Research fellowship granted by CNPq-Brazil to W.L.A. is gratefully acknowledged.

CONFLICTS OF INTEREST

The authors declare no conflicts of interest.

REFERENCES

Agrawal C., Sen S., Singh S., Rai S., Singh P.K., Singh V.K., Rai L.C. (2014) Comparative proteomics reveals association of early accumulated proteins in conferring butachlor tolerance in three N_2-fixing *Anabaena* spp. J Proteomics 96: 271–290.

Allakhverdiev, S. I., & Murata, N. (2008) Salt stress inhibits photosystems II and I in cyanobacteria. Photosynthesis Research, 98(1-3), 529-539

Allakhverdiev, S. I., Kinoshita, M., Inaba, M., Suzuki, I., & Murata, N. (2001) Unsaturated Fatty Acids in Membrane Lipids Protect the Photosynthetic Machinery against Salt-Induced Damage inSynechococcus. Plant Physiology, 125(4), 1842-1853.

Andreote, A. P. D., Vaz, M. G. M. V., Genuário, D. B., Barbiero, L., Rezende-Filho, A. T., & Fiore, M. F. (2014) Nonheterocytous cyanobacteria from Brazilian saline-alkaline lakes. Journal of Phycology, 50(4), 675-684.

Apte, S. K., Reddy, B. R., & Thomas, J. (1987) Relationship between sodium influx and salt tolerance of nitrogen-fixing cyanobacteria. Applied and Environmental Microbiology, 53(8), 1934-1939.

Blanco-Rivero, A., Leganes, F., Fernandez-Valiente, E., Calle, P., & Fernandez-Pinas, F. (2005) MrpA, a gene with roles in resistance to Na^+ and adaptation to alkaline pH in the cyanobacterium Anabaena sp. PCC7120. Microbiology, 151(5), 1671-1682.

Boonburapong, B., Laloknam, S., & Incharoensakdi, A. (2016) Accumulation of gamma-aminobutyric acid in the halotolerant cyanobacterium Aphanothece halophytica under salt and acid stress. Journal of Applied Phycology, 28(1), 141-148.

Brown, A. D. (1974) Microbial water relations: features of the intracellular composition of sugar-tolerant yeasts. Journal of bacteriology, 118(3), 769-777.

Cumino, A. C., Marcozzi, C., Barreiro, R., & Salerno, G. L. (2007) Carbon cycling in Anabaena sp. PCC7120. Sucrose synthesis in the heterocytes and possible role in nitrogen fixation. Plant Physiology, 143(3), 1385-1397.

Dadheech, P.K., Glockner, G., Casper, P., Kotut, K., Mazzoni, C.J., Mbedi, S. (2013) Cyanobacterial diversity in the hot spring, pelagic and benthic habitats of a tropical soda lake. FEMS Microbiol. Ecol. 85 (2), 389_401.

de Alvarenga, L. V., Vaz, M. G. M. V., Genuário, D. B., Esteves-Ferreira, A. A., Almeida, A. V. M., de Castro, N. V., ... & Araújo, W. L. (2018) Extending the ecological distribution of Desmonostoc genus: proposal of Desmonostoc salinum sp. nov., a novel Cyanobacteria from a saline-alkaline lake. International journal of systematic and Evolutionary Microbiology, 68(9), 2770-2782.

Elanskaya IV, Karandashova IV, Bogachev AV & Hagemann M (2002) Functional analysis of the Na+/H+ antiporter encoding genes of the cyanobacterium Synechocystis PCC 6803. Biochem (Mosc) 67: 432-440.

Esteves-Ferreira, A. A., Cavalcanti, J. H. F., Vaz, M. G. M. V., Alvarenga, L. V., Nunes-Nesi, A., & Araújo, W. L. (2017) Cyanobacterial nitrogenases: phylogenetic diversity, regulation and functional predictions. Genetics and Molecular Biology, 40(1), 261-275

Fernandes, T. A., Iyer, V., & Apte, S. K. (1993) Differential responses of nitrogen-fixing cyanobacteria to salinity and osmotic stresses. Applied and Environmental Microbiology, 59(3), 899-904.

Flores, E., López-Lozano, A., & Herrero, A. (2015) Nitrogen fixation in the oxygenic phototrophic prokaryotes (cyanobacteria): the fight against oxygen. Biological Nitrogen Fixation, 879-890.

Florian A., Araújo W.L., Fernie A.R. (2013) New insights into photorespiration obtained from metabolomics. Plant Biol 15: 656–666.

Foster, R. A., Kuypers, M. M., Vagner, T., Paerl, R. W., Musat, N., & Zehr, J. P. (2011) Nitrogen fixation and transfer in open ocean diatom–cyanobacterial symbioses. The ISME journal, 5(9), 1484.

Foti, M. J., Sorokin, D. Y., Zacharova, E. E., Pimenov, N. V., Kuenen, J. G., & Muyzer, G. (2008) Bacterial diversity and activity along a salinity gradient in soda lakes of the Kulunda Steppe (Altai, Russia). Extremophiles, 12(1), 133-145

Fukaya, F., Promden, W., Hibino, T., Tanaka, Y., Nakamura, T., & Takabe, T. (2009) An Mrp-like cluster in the halotolerant cyanobacterium *Aphanothece halophytica* functions as a Na^+/H^+ antiporter. Applied and Environmental Microbiology, 75(20), 6626-6629.

Fulda, S., Mikkat, S., Huang, F., Huckauf, J., Marin, K., Norling, B., & Hagemann, M. (2006) Proteome analysis of salt stress response in the cyanobacterium *Synechocystis* sp. strain PCC 6803. Proteomics, 6(9), 2733-2745.

Genuário, D. B., Andreote, A. P. D., Vaz, M. G. M. V., & Fiore, M. F. (2017) Heterocyte-forming cyanobacteria from Brazilian saline-alkaline lakes. Molecular Phylogenetics and Evolution, 109, 105-112.

Genuário, D. B., Vaz, M. G., Santos, S. N., Kavamura, V. N., & Melo, I. S. (2019) Cyanobacteria from Brazilian extreme environments: toward functional exploitation. in microbial diversity in the genomic era (pp. 265-284). Academic Press.

Hagemann M. (2011) Molecular biology of cyanobacterial salt acclimation. FEMS Microbiology Reviews, 35(1), 87-123.

Hagemann M. (2013) Genomics of salt acclimation: synthesis of compatible solutes among cyanobacteria. In: Chauvat F, Cassier Chauvat C (eds) Book series: advances in botanical research, vol 65. Elsevier, San Diego, pp 27–55

Hagemann M., Fulda S. & Schubert H. (1994) DNA, RNA, and protein synthesis in the cyanobacterium Synechocystis sp. PCC 6803 adapted to different salt concentrations. Curr Microbiol 28: 201–207.

Hagemann M., Ribbeck-Busch K., Klähn S., Hasse D., Steinbruch R., Berg G. (2008) The Plant-Associated bacterium *Stenotrophomonas rhizophila* expresses a new enzyme for the synthesis of the compatible solute glucosylglycerol. J Bacteriol 190: 5898–5906

Hagemann M., Schoor A. & Erdmann N. (1996) NaCl acts as a direct modulator in the salt adaptive response: salt-dependent activation of glucosylglycerol synthesis in vivo and in vitro. J Plant Physiol 149: 746–752.

Heidorn T., Camsund D., Huang H-H., Lindberg P., Oliveira P., Stensjo K., Lindblad P. (2011) Synthetic biology in cyanobacteria: Engineering and analyzing novel functions. In C Voigt, ed, Methods in Enzymology, vol 497: Synthetic Biology, methods for part/device characterization and chassis engineering, pp 539-579

Higo, A., Katoh, H., Ohmori, K., Ikeuchi, M., & Ohmori, M. (2006). The role of a gene cluster for trehalose metabolism in dehydration tolerance of the filamentous cyanobacterium *Anabaena* sp. PCC7120. Microbiology, 152(4), 979-987.

Inaba M., Sakamoto A. & Murata N. (2001) Functional expression in *Escherichia coli* of low-affinity and high-affinity $Na(^+)(Li(^+))/H(^+)$ antiporters of *Synechocystis*. J Bacteriol 183: 1376-1384.

Jeon, Y. C., Cho, C. W. & Yun, Y. S. (2005) Measurement of microalgal photosynthetic activity depending on light intensity and quality. Biochem Eng J, 27, 127-131.

Karsten, U., Herburger, K., & Holzinger, A. (2014) Dehydration, temperature, and light tolerance in members of the aeroterrestrial green algal genus *Interfilum (Streptophyta*) from biogeographically different temperate soils. Journal of Phycology, 50(5), 804-816.

Katoh, H., Asthana, R. K., & Ohmori, M. (2004) Gene expression in the cyanobacterium *Anabaena* sp. PCC7120 under desiccation. Microbial Ecology, 47(2), 164-174.

Kirsch, F., Pade, N., Klähn, S., Hess, W. R., & Hagemann, M. (2017) The glucosylglycerol-degrading enzyme GghA is involved in acclimation to fluctuating salinities by the cyanobacterium *Synechocystis* sp. strain PCC6803. Microbiology, 163(9), 1319-1328.

Klähn, S., & Hagemann, M. (2011) Compatible solute biosynthesis in cyanobacteria. Environmental Microbiology, 13(3), 551-562.

Kolman M., Salerno G. (2016) Sucrose in bloom-forming cyanobacteria: loss and gain of genes involved in its biosynthesis. Environmental Microbiology. 18 (2):439-49.

Kolman, M., Nishi, C., Perez-Cenci, M., & Salerno, G. (2015) Sucrose in cyanobacteria: from a salt-response molecule to play a key role in nitrogen fixation. Life, 5(1), 102-126.

Lane, D.J. (1991) 16S/23S rRNA sequencing. In: STACKEBRANDT, E. & GOODFELLWON, M. (eds.). Nucleic acid techniques in bacterial systematics. Chichester: John Wiley & Sons, pp. 115-175.

Liu, W., Cui, L., Xu, H., Zhu, Z., & Gao, X. (2017) The Flexibility-Rigidity Coordination of Dense exopolysaccharide matrix in terrestrial cyanobacteria acclimated to periodic desiccation. Applied and environmental microbiology, AEM-01619.

Los, D. A., Mironov, K. S., & Allakhverdiev, S. I. (2013) Regulatory role of membrane fluidity in gene expression and physiological functions. Photosynthesis Research, 116(2-3), 489-509.

Marin K., Huckauf J., Fulda S., Hagemann M. (2002) Salt-dependent expression of glucosylglycerol-phosphate synthase, involved in osmolyte synthesis in the cyanobacterium *Synechocystis* sp. Strain PCC6803. J Bacteriol 184: 2870–2877.

Marin K., Kanesaki Y., Los D.A., Murata N., Suzuki I., Hagemann M. (2004) gene expression profiling reflects physiological processes in salt acclimation of *Synechocystis* sp. strain PCC 6803. Plant Physiol 136: 3290–3300.

Mikkat, S., Milkowski, C., & Hagemann, M. (2000) The gene sll0273 of the cyanobacterium *Synechocystis* sp. strain PCC6803 encodes a protein essential for growth at low Na+/K+ ratios. Plant, Cell & Environment, 23(6), 549-559.

Nürnberg D.J., Mariscal V., Bornikoel J., Nieves-Morión M., Krauß N., Herrero A., Maldener I., Flores E., Mullineaux C.W. (2015) Intercellular diffusion of a fluorescent sucrose

analog via the septal junctions in a filamentous cyanobacterium. MBio.Mar 17;6(2):e02109.

Oren, A. (2007) Diversity of organic osmotic compounds and osmotic adaptation in cyanobacteria and algae. In Algae and Cyanobacteria in Extreme Environments (pp. 639-655). Springer, Dordrecht.

Oren, A. (2015) Cyanobacteria in hypersaline environments: biodiversity and physiological properties. Biodiversity and Conservation, 24(4), 781-798.

Pade N., Erdmann S., Enke H., Dethloff F., Dühring U., Georg J., Wambutt J., Kopka J., Hess W.R., Zimmermann R. (2016) Insights into isoprene production using the cyanobacterium Synechocystis sp. PCC 6803. Biotechnol Biofuels 9: 89.

Pade, N., & Hagemann, M. (2014) Salt acclimation of cyanobacteria and their application in biotechnology. Life, 5(1), 25-49.

Pade, N., Michalik, D., Ruth, W., Belkin, N., Hess, W. R., Berman-Frank, I., & Hagemann, M. (2016) Trimethylated homoserine functions as the major compatible solute in the globally significant oceanic cyanobacterium Trichodesmium. Proceedings of the National Academy of Sciences, 113(46), 13191-13196.

Parmar A., Singh N.K., Pandey A., Gnansounou E., Madamwar D. (2011) Cyanobacteria and microalgae: A positive prospect for biofuels. Bioresour Technol 102: 10163–10172.

Potts, M., Slaughter, S. M., Hunneke, F. U., Garst, J. F., & Helm, R. F. (2005) Desiccation tolerance of prokaryotes: application of principles to human cells. Integrative and Comparative Biology, 45(5), 800-809.

Raanan H., Oren N., Treves H., Berkowicz S.M., Hagemann M., Pade N., Keren N., Kaplan A. Simulated soil crust conditions in a chamber system provide new insights on cyanobacterial acclimation to desiccation. Environmental Microbiology, 18(2), 414-426.

Rezayian, M., Niknam, V., & Faramarzi, M. A. (2018) Antioxidative responses *of Nostoc ellipsosporum* and *Nostoc piscinale* to salt stress. Journal of Applied Phycology, 1-13.

Ruffing A.M. (2011) Engineered cyanobacteria: Teaching an old bug new tricks. Bioengineered Bugs 2: 136-149

Sakamoto, T., & Murata, N. (2002) Regulation of the desaturation of fatty acids and its role in tolerance to cold and salt stress. Current Opinion in Microbiology, 5(2), 206-210.

Shukla, E., Singh, S. S., Singh, P., & Mishra, A. K. (2012) Chemotaxonomy of heterocytous cyanobacteria using FAME profiling as species markers. Protoplasma, 249(3), 651-661.

Steinhauser, D., Fernie, A.R., & Araújo, W. L. (2012) Unusual cyanobacterial TCA cycles: not broken just different. Trends in Plant Science, 17(9), 503-509.

Sweetlove, L.J. Katherine F.M. Beard, Adriano Nunes-Nesi, Alisdair R. Fernie and R. George Ratcliffe (2010). Not just a circle: flux modes in the plant TCA cycle. Trends Plant Sci. 15, 462–470

Vitousek, P. M., & Howarth, R. W. (1991) Nitrogen limitation on land and in the sea: how can it occur? Biogeochemistry, 13(2), 87-115.

Wang H.L., Postier B.L. & Burnap R.L. (2002) Polymerase chain reaction-based mutageneses identify key transporters belonging to multigene families involved in Na^+ and pH homeostasis of *Synechocystis* sp. PCC6803. Mol Microbiol 44: 1493-1506.

Xiong W., Brune D., Vermaas W.F. (2014) The γ-aminobutyric acid shunt contributes to closing the tricarboxylic acid cycle in *Synechocystis* sp. PCC6803. Mol Microbiol. 93(4):786-96.

Yoshimura, H., Okamoto, S., Tsumuraya, Y., & Ohmori, M. (2007) Group 3 sigma factor gene, sigJ, a key regulator of desiccation tolerance, regulates the synthesis of extracellular polysaccharide in cyanobacterium *Anabaena* sp. strain PCC7120. DNA Research, 14(1), 13-24.

Zhang, C. C., Zhou, C. Z., Burnap, R. L., & Peng, L. (2018) Carbon/Nitrogen Metabolic Balance: Lessons from Cyanobacteria. Trends in Plant Science. 23(12), 1116-1130.

Zhang, S., Qian, X., Chang, S., Dismukes, G. C., & Bryant, D. A. (2016) Natural and synthetic variants of the tricarboxylic acid cycle in cyanobacteria: introduction of the GABA shunt into *Synechococcus* sp. PCC7002. Frontiers in Microbiology, 7, 1972.

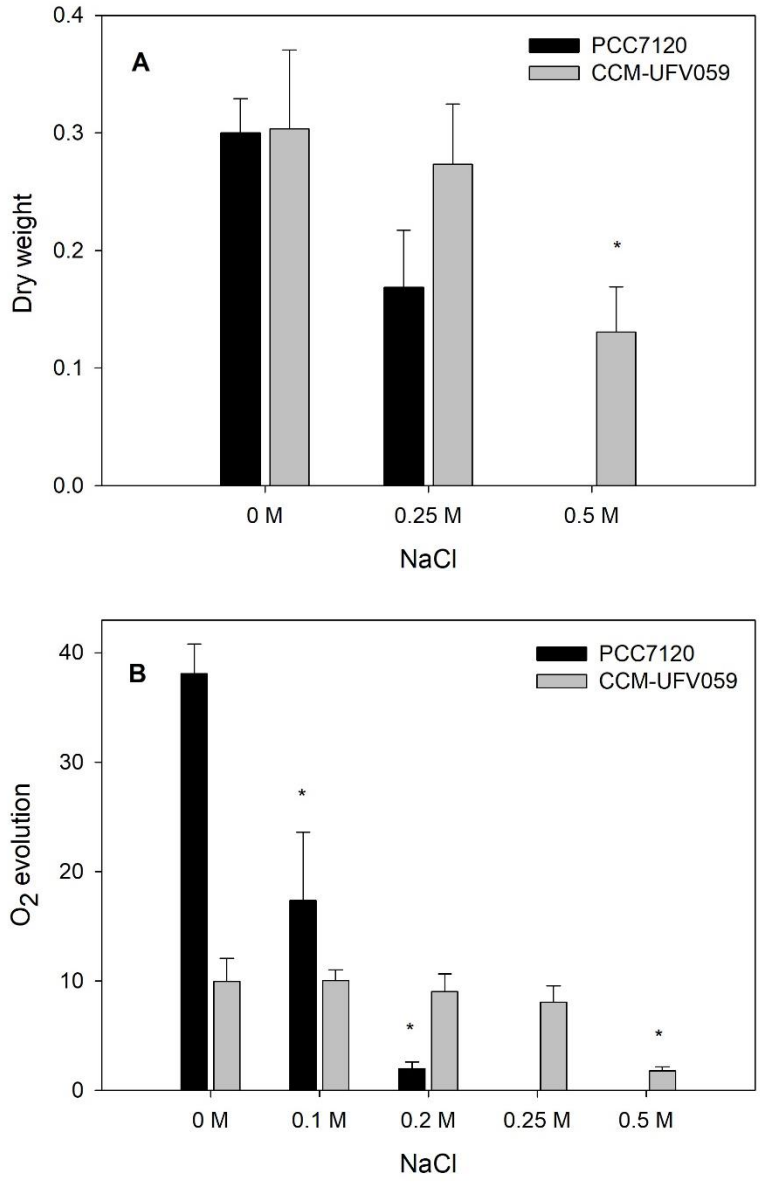

Figure 1: Differential responses of *D. salinum* CCM-UFV059 and *Nostoc* sp. PCC7120 after exposure to salt stress for 24 h. Cells were grown in nitrate-containing BG-11 medium supplemented with different concentrations of NaCl. (A) Growth expressed in dry weight (mg mL^{-1}) and (B) O_2 evolution (O_2 nmol.min^{-1}.mg dry $weight^{-1}$). Values represent mean ± SE from four biological replicates.

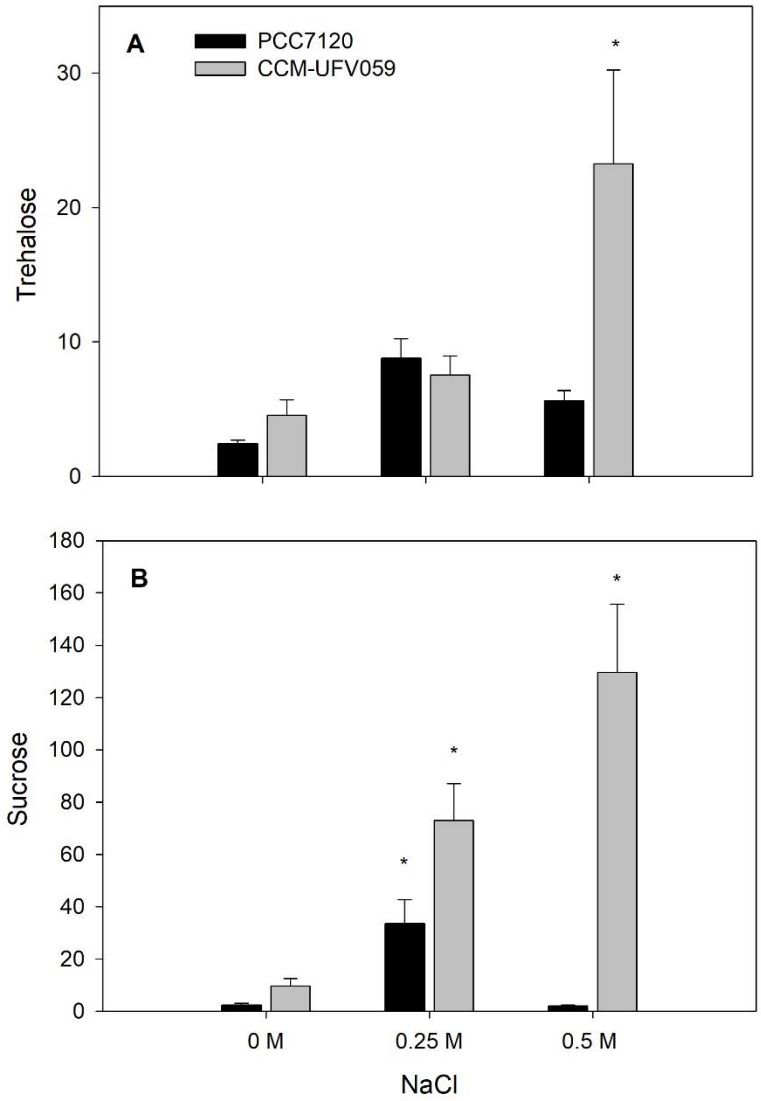

Figure 2: Differential accumulation of compatible solutes in *D. salinum* CCM-UFV059 or *Nostoc* sp. PCC7120 after exposure to salt stress for 24 h. (A) Trehalose and (B) sucrose, expressed in nmol.mg dry weight^{-1}. Cells were grown in nitrate-containing BG-11 medium supplemented with different concentrations of NaCl. Values represent mean ± SE from four biological replicates. Asterisks designate values that were significantly different from each respective 0 M NaCl treatment (P<0.05) by Student's *t*-test.

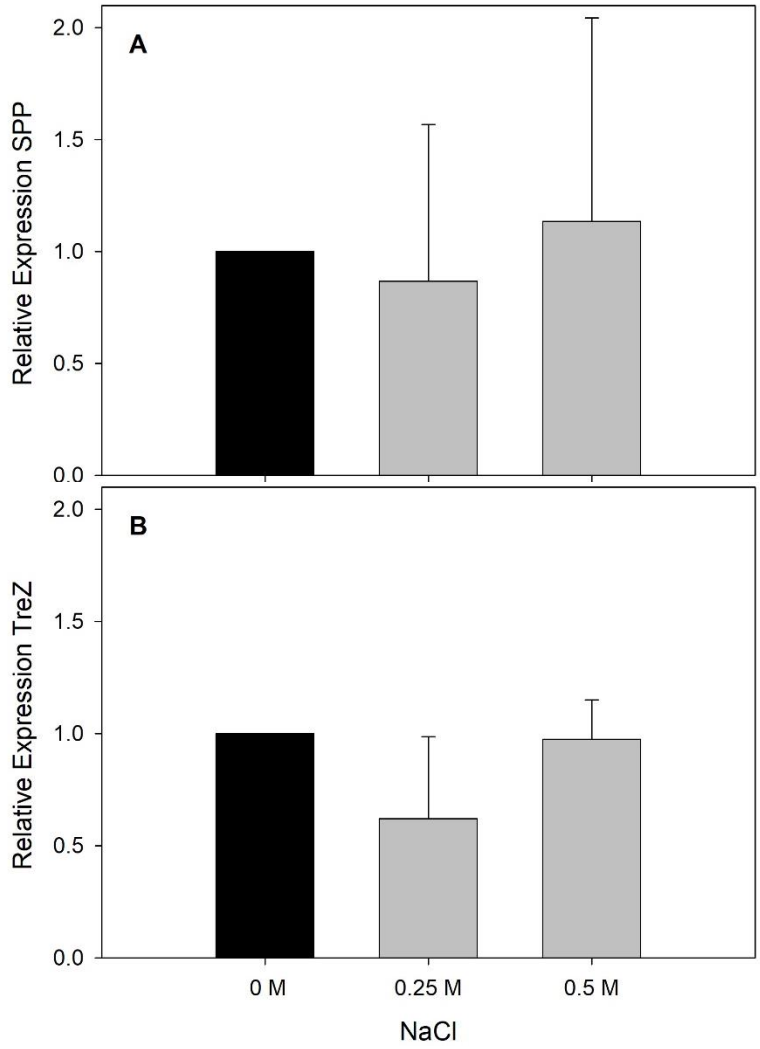

Figure 3: Relative expression of genes from the synthesis pathway of the compatible solutes sucrose and trehalose in *D. salinum* CCM-UFV059. (A) Sucrose phosphate phosphatase (SPP) and (B) Maltooligosyl trehalose trehalohydrolase (TreZ). Cells were grown in nitrate-containing BG-11 medium supplemented with different concentrations of NaCl. RNA was isolated from cells acclimated to different NaCl-levels, reverse-transcribed into cDNA, and then used for real-time qPCR. The cDNA amounts were calibrated using the constitutively expressed 16s rDNA (16s MV). Values represent mean ± SE from three biological replicates.

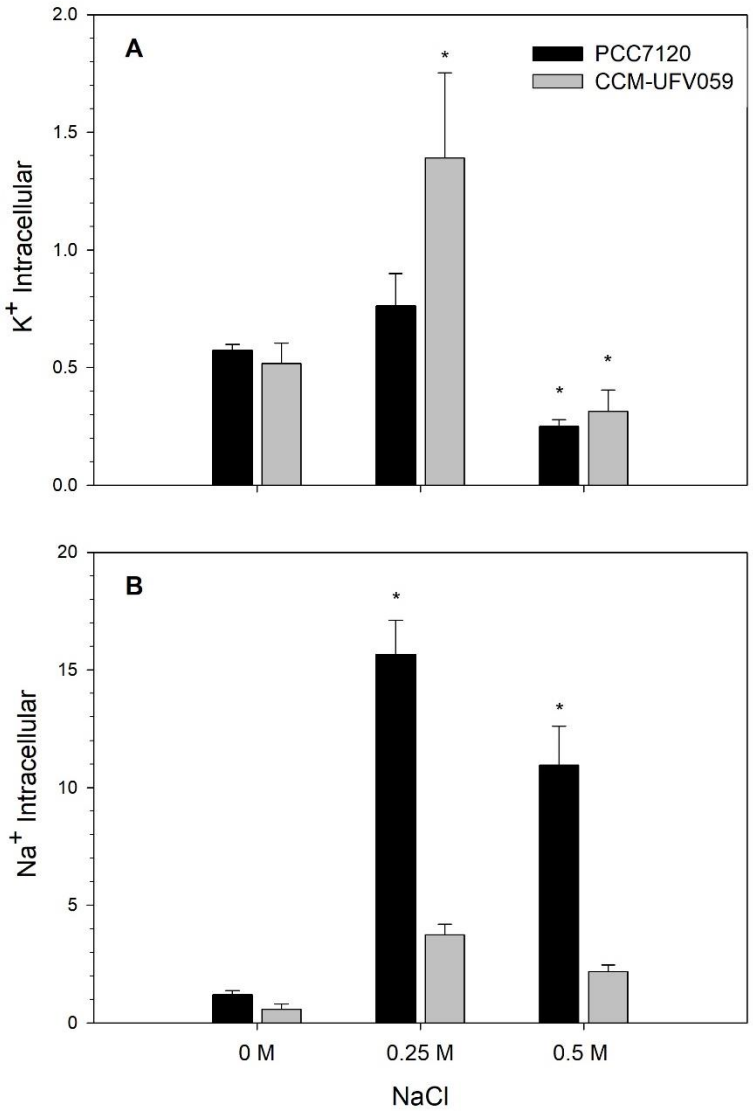

Figure 4: Accumulation of ions inside the cells of *D. salinum* CCM-UFV059 or *Nostoc* sp. PCC7120 after exposure to salt stress for 24 h. Cells were grown in nitrate-containing BG-11 medium supplemented with different concentrations of NaCl. (A) Sodium and (B) potassium are expressed as μmol.mg of dry weight^{-1}. Values represent mean ± SE from four biological replicates. Asterisks designate values that were significantly different from each respective 0 M NaCl treatment (P<0.05) by Student's *t*-test.

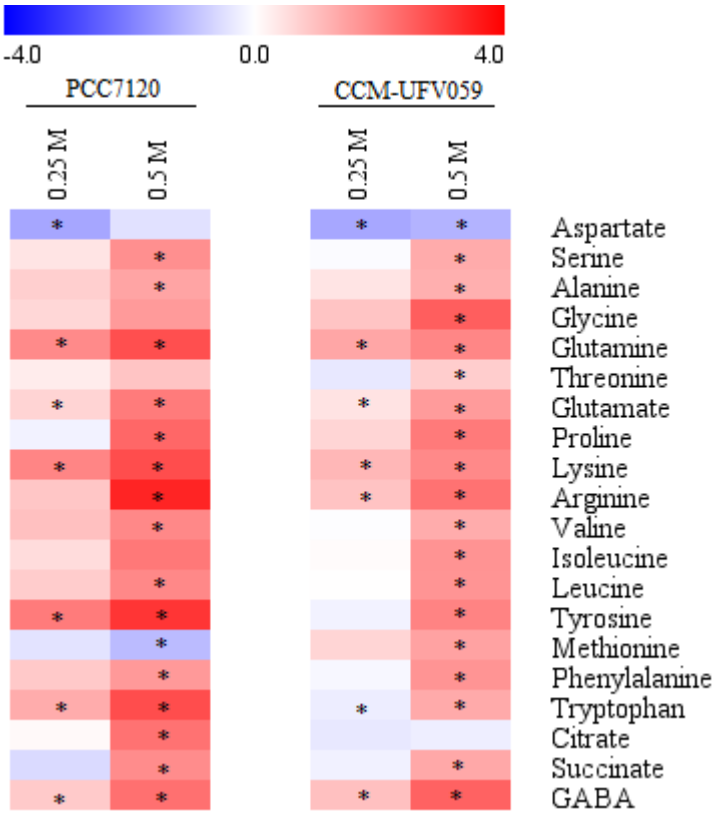

Figure 5: Relative levels of identified metabolites of *D. salinum* CCM-UFV059 or *Nostoc* sp. PCC7120 after exposure to salt stress for 24 h. Cells were grown in nitrate-containing BG-11 medium supplemented with different concentrations of NaCl. Selected metabolites were determined by LC-MS as described in 'Materials and methods'. The full datasets from these metabolic profiling studies are additionally available in Supplementary Table 3. The colour code of the heat map is given as the X-fold changes. Data are normalized with respect to the mean response calculated for the control (0 M NaCl) of each strain (to allow statistical assessment, individual replicates from this set were normalized in the same way). Values represent mean ± SE from four biological replicates. Asterisks designate values that were significantly different from control (P<0.05) by Student's t-test.

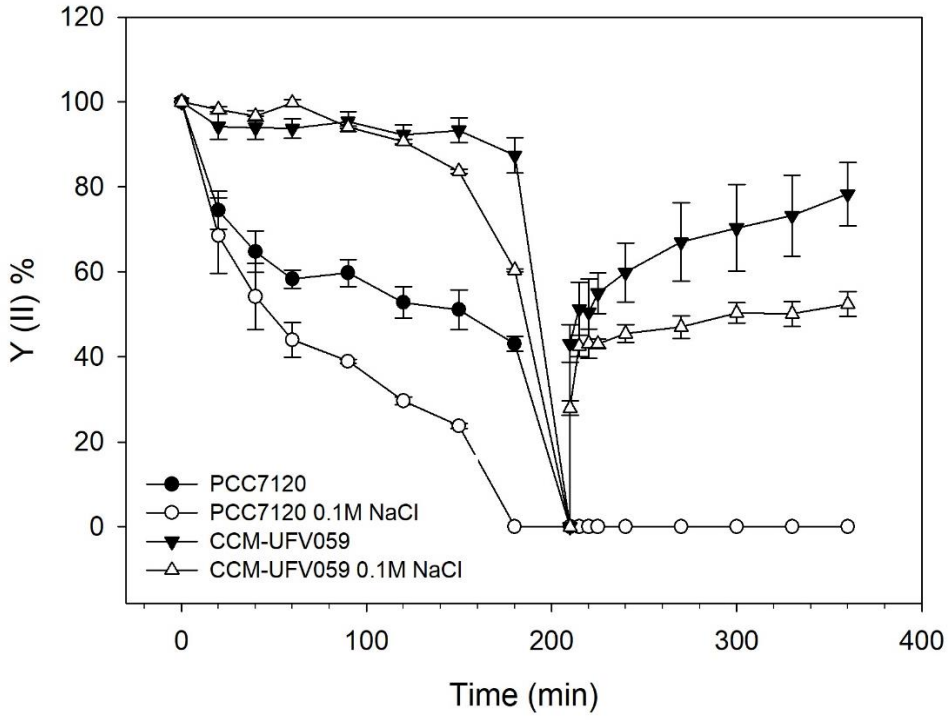

Figure 6: Photochemical efficiency of photosystem II (Y(II)) in cells of *D. salinum* CCM-UFV059 or *Nostoc* sp. PCC7120. Cells were pre-cultivated in nitrate-containing BG-11 medium with and without 0.1 M NaCl for three days. The cells were exposed to drought stress for 3.5 h until Y(II) reached zero. Then they were rehydrated for 3 h. Values represent mean ± SE from four biological replicates.

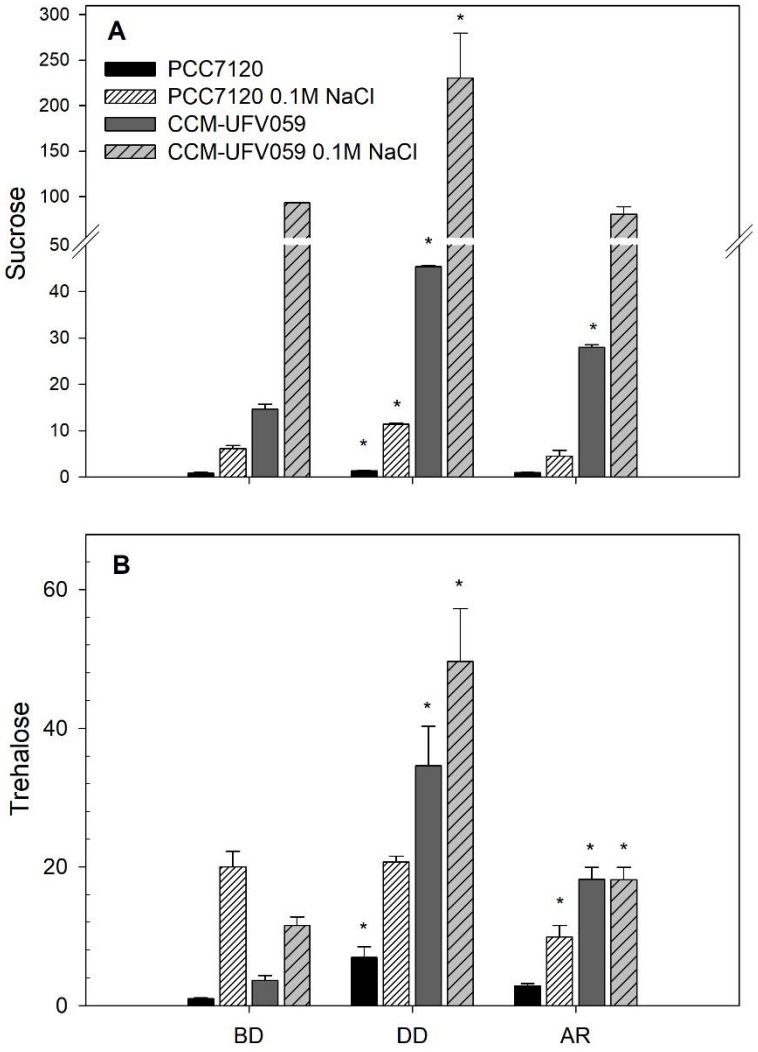

Figure 7: Accumulation of compatible solutes inside the cells of *D. salinum* CCM-UFV059 or *Nostoc* sp. PCC7120 after exposure to desiccation stress. Cells were grown in nitrate-containing BG-11 medium supplemented with or without 0.1 M NaCl. Samples were harvested before (BD) and during (DD) desiccation stress as well as after rehydration (AR). (A) Sucrose and (B) Trehalose are expressed as nmol mg^{-1} of dry weight. Values represent mean ± SE from four biological replicates. Asterisks designate values that were significantly different from each respective BD treatment (P<0.05) by Student's *t*-test.

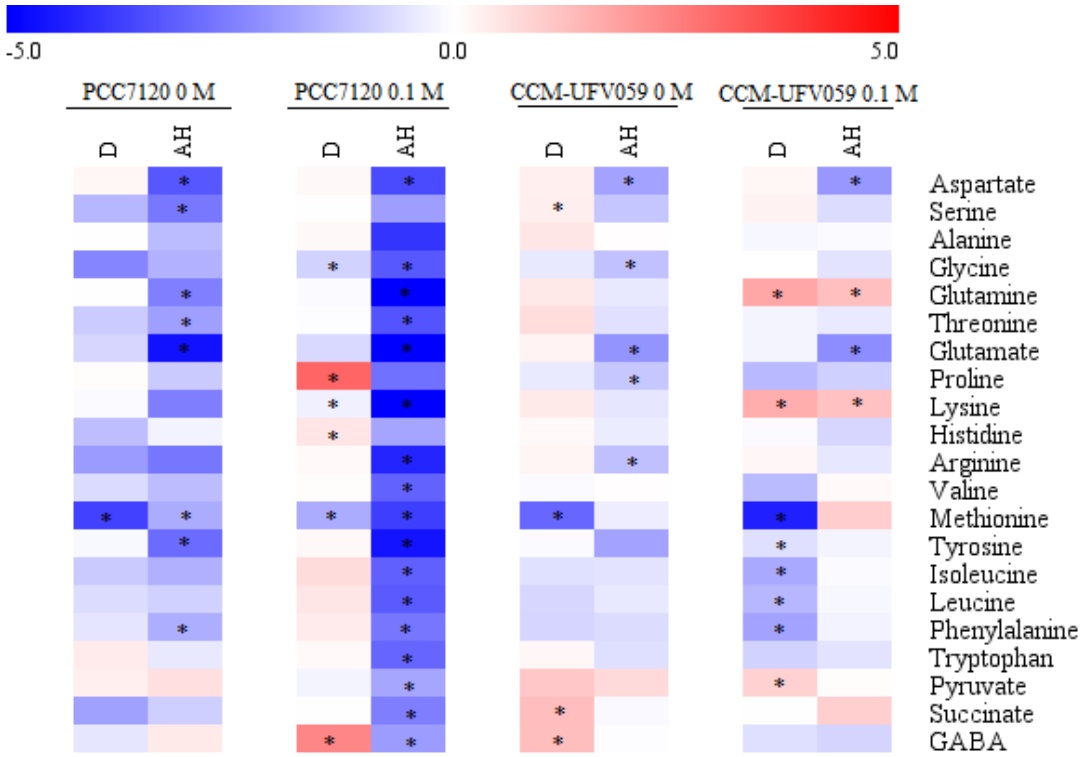

Figure 8: Relative levels of identified metabolites of *D. salinum* CCM-UFV059 or *Nostoc* sp. PCC7120 after exposure to desiccation stress. Cells were grown in nitrate-containing BG-11 medium supplemented with and without 0.1 M NaCl. Samples were harvested before (BD) and during (DD) desiccation stress as well as after rehydration (AR). Selected metabolites were determined by LC-MS as described in 'Materials and methods'. The full datasets from these metabolic profiling studies are additionally available in Supplementary Table 4. The colour code of the heat map is given as the X-fold changes. Data are normalized with respect to the mean response calculated for the control (BD) of each strain (to allow statistical assessment, individual replicates from this set were normalized in the same way). Values represent mean ± SE from four biological replicates. Asterisks designate values that were significantly different from control (P<0.05) by Student's t-test.

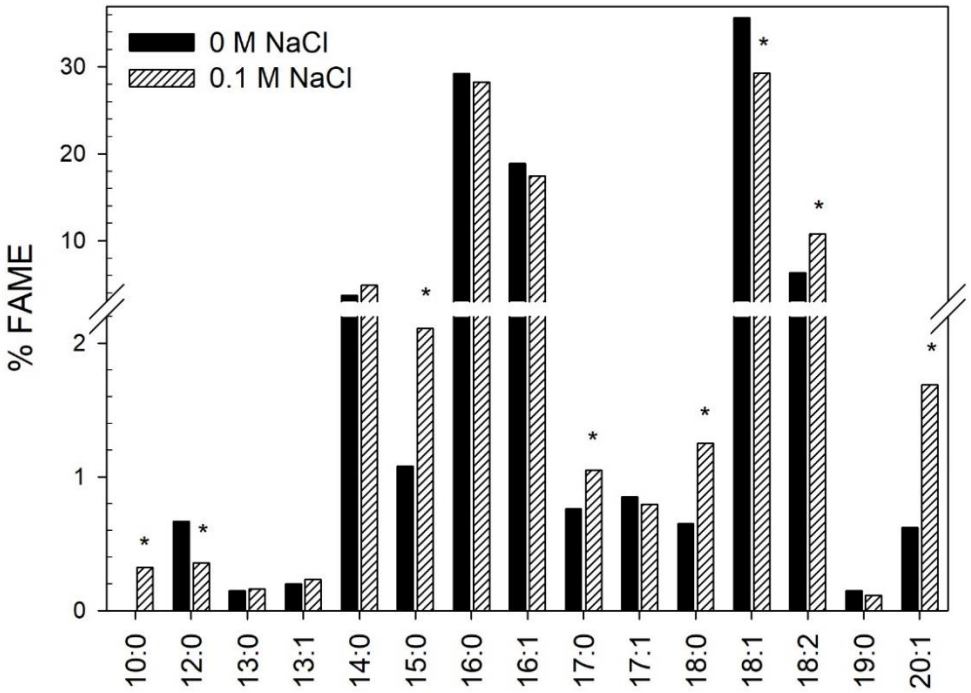

Figure 9: Fatty acid composition of *D. salinum* CCM-UFV059 grown in nitrate-containing BG-11 with and without 0.1 M NaCl. The *y* axis values in % represent the fatty acid level relative to the total levels found in each condition. Values represent % of each FAME in the sample. Values represent mean ± SE from four biological replicates. Asterisks designate values that were significantly different between treatments ($P<0.05$) by Student's *t*-test.

SUPPLEMENTARY MATERIAL

Table 1: Primers used in this work

Primer	Sequence		Reference
16 S rRNA_fw	CCTACGGGAGGCAGCAG	RT-qPCR	Lane, 1991
16 S rRNA_rv	TCTACGCATTTCACCGCTAC	RT-qPCR	Lane, 1991
SPP_fw	CCGCAGACAACTGTTTGTTC	RT-qPCR	This work
SPP_rv	GGCAGCAATACTCCAGATTC	RT-qPCR	This work
TreZ_fw	CCACTCAGAAGCATCTAGTC	RT-qPCR	This work
TreZ_rv	GCTGCATCATACCGAATACC	RT-qPCR	This work
SPP_fw	CTACKGGGCGATCGCC	PCR	This work
SPP_rv	GTGCCACTGGAGTAACTC	PCR	This work
TreZ_fw	GATGGCTATTTCCGCAC	PCR	This work
TreZ_rv	GTCCATTCGTGCCATGTACC	PCR	This work

Table 2: Partial sequence of *D. salinum* CCM-UFV059 genes

Gene	Sequence
TreZ	CANAACAATGGGTTGAAGTCACAGATCCTTATGCCACTGACWTAGATGA AGTAGGTGGAAACGATAACGGTATTGTCCGTATCAAAGATGGGGAAAGA ATTATTGATACTTATGTTTGGCAAAATGATGATAAACCTTTACCTGCTGAC CACGAACTAGTAATTTATGAACTGCATGTTGGTGATTTTTCTGGTGGTGA AGATGACCCTTATGCACGAGGCAAATATAAACATGTTGTTGAAAAATTAR ATTATTTGTCTGAATTAGGAATCAACGCTWTTGAGTTGATGCCAATAAAA GAATATCCTGGCGATCATAGTTGGGGTTATAATCCTCGCTATTTCTTTGCC ACAGAATCTAGTTATGGTTCTACTGCGGGATTGAAAAATTTGATTGATGA ATGTCACGCTAGAGGCATTCGTGTAATTATTGATGGTATTTATAACCACT CAGAAGCATCTAGTCCGTTAACACAAATTGACCACGATTATTGGTATCAT CATTCTCCCCGCGACCCTGATAACAACTGGGGGCCAGAATTTAATTACGA ACATTACGACGAAAATTTAGATGTTTATCCAGCGCGGAAATTTATTGGCG ATACAATCCGCTATTGGATTCAAGAATATCATCTTGATGGTATTCGGTAT GATGCAGCGCGGCAAATTGCCAACTATGATTTTATGCATTGGATTGTGCA AGAAGCCAAAAACACTGCTGGGCCAAAGCCTTTTTATAATGTTGCCGAAC ACATTCCTGAAACCACCAGCATTACTAATGTAGATGGCCCGATGGATGGT TGCTGGCATGACAGTTTTTATCACTGCATTTTAGAACATATCTGTGGGGAT ACCTTTGATTTAGAACGCCTGAAAGATGTTATTGACTGCAAACGTCAAGG CTTTATGGGTGCTACCAATGTGGTAAATTACCTCACCAACCACGACCATC ATCATCTCATGGTAGAAATGGGTAACCGCRRAGATTTTTGATGAAGAAGC CTTTAGACGGATTAAATTAGGAGTAGCTATCCTAATGACTGCTATTGGCG TACCTTTAGT
SPP	GGATTTGTGCCACTGGAGTAACTCTTTTCGAGCATTACCGACTATGATTCC CCTTTCGTTGCCTACAGCAAATAAAGCAATATCATTACCTGAATCACCGC AGACAACTGTTTGTTCTGCTGCAAATTTCCACTTTTGGCGCAAAAATTGC ATTGCTTGACCTTTATCGCTGGTAAGGGGTACAATGTCRAGGTCTATTCC GCTACTGTAGATTAACTTTACATTTAATTTATATTTATCCAACTCTGCCTC AAGTTGCGGWAGAATGCTGACCGCTATTTCTTGAGGAACAAAAAAACTT ACTTTAAAAGCACGCTGTTCTGACTCTGGTTGTAATTTTAATTCAGGGAA AGTCTCAGTTATGGATAAAATGAGTTCGCGATCCCAACCAGGGGAGAGG ATTTCTGACCAACTCGAATCTGGAGTATTGCTGCCATTAAGGTAGATTTCT GTTCCTACAGCAAGGACTAGAGCATCTGGTTGCAAAAGAATCACTAGTGC GGCC

Table 3: Dataset from relative levels of identified metabolites of *D. salinum* CCM-UFV059 or *Nostoc* sp. PCC7120 after exposure to salt stress for 24 h (0M, 0.25M and 0.5 M NaCl).

	PCC7120			**CCM-UFV059**		
Metabolites	**0 M**	**0.25 M**	**0.5 M**	**0 M**	**0.25 M**	**0.5 M**
Aspartate	1.000	0.381	0.725	1.000	0.387	0.440
Serine	1.000	1.354	3.381	1.000	0.964	2.505
Alanine	1.000	1.692	2.696	1.000	1.353	2.398
Glycine	1.000	1.558	3.002	1.000	1.900	5.789
Glutamine	1.000	3.591	6.831	1.000	2.657	3.762
Threonine	1.000	1.231	1.902	1.000	0.787	1.737
Glutamate	1.000	1.596	4.238	1.000	1.361	2.986
Proline	1.000	0.876	5.232	1.000	1.589	4.250
Lysine	1.000	3.784	6.944	1.000	2.211	3.622
Arginine	1.000	1.867	10.843	1.000	1.936	4.634
Valine	1.000	1.993	3.677	1.000	0.980	2.483
Isoleucine	1.000	1.475	4.345	1.000	1.052	3.260
Leucine	1.000	1.747	3.658	1.000	1.021	3.218
Tyrosine	1.000	4.210	9.011	1.000	0.877	3.892
Methionine	1.000	0.743	0.482	1.000	1.596	2.778
Phenylalanine	1.000	1.816	3.039	1.000	0.919	3.221
Tryptophan	1.000	2.485	6.999	1.000	0.825	2.526
Citrate	1.000	1.079	4.670	1.000	0.785	0.834
Succinate	1.000	0.669	3.518	1.000	0.864	2.591
GABA	1.000	1.794	4.759	1.000	2.001	5.523

Table 4: Dataset from relative levels of identified metabolites of *D. salinum* CCM-UFV059 or *Nostoc* sp. PCC7120 after exposure to desiccation stress. Before (BD) and during (DD) desiccation stress as well as after rehydration (AR).

	PCC7120			PCC7120 0.1 M NaCl			CCM-UFV059			CCM-UFV059 0.1 M NaCl		
Metabolites	**BD**	**DD**	**AR**	**BD**	**DD**	**AR**	**BD**	**DD**	**AR**	**BD**	**DD**	**AR**
Aspartate	1.000	1.135	0.102	1.000	1.101	0.086	1.000	1.244	0.289	1.000	1.131	0.246
Serine	1.000	0.377	0.162	1.000	1.014	0.269	1.000	1.275	0.455	1.000	1.209	0.624
Alanine	1.000	0.996	0.402	1.000	1.111	0.064	1.000	1.411	1.032	1.000	0.900	0.935
Glycine	1.000	0.192	0.350	1.000	0.543	0.103	1.000	0.736	0.433	1.000	1.005	0.685
Glutamine	1.000	0.989	0.178	1.000	0.952	0.028	1.000	1.373	0.737	1.000	3.369	2.392
Threonine	1.000	0.495	0.273	1.000	0.984	0.099	1.000	1.605	0.671	1.000	0.864	0.749
Glutamate	1.000	0.574	0.040	1.000	0.598	0.015	1.000	1.185	0.235	1.000	0.862	0.214
Proline	1.000	1.047	0.490	1.000	8.132	0.145	1.000	0.760	0.468	1.000	0.391	0.535
Lysine	1.000	0.949	0.175	1.000	0.818	0.025	1.000	1.337	0.719	1.000	3.056	2.352
Histidine	1.000	0.418	0.853	1.000	1.441	0.297	1.000	1.096	0.779	1.000	0.953	0.574
Arginine	1.000	0.259	0.156	1.000	1.092	0.052	1.000	1.148	0.427	1.000	1.115	0.726
Valine	1.000	0.615	0.407	1.000	1.053	0.119	1.000	0.939	1.028	1.000	0.395	1.098
Methionine	1.000	0.076	0.326	1.000	0.324	0.073	1.000	0.127	0.786	1.000	0.048	1.983
Tyrosine	1.000	0.921	0.134	1.000	1.114	0.041	1.000	0.940	0.290	1.000	0.655	0.867
Isoleucine	1.000	0.490	0.345	1.000	1.611	0.115	1.000	0.660	0.692	1.000	0.314	0.957
Leucine	1.000	0.626	0.539	1.000	1.418	0.106	1.000	0.573	0.736	1.000	0.379	0.905
Phenylalanine	1.000	0.708	0.336	1.000	1.317	0.156	1.000	0.569	0.624	1.000	0.286	0.852
Tryptophan	1.000	1.330	0.740	1.000	1.099	0.125	1.000	1.128	0.653	1.000	0.549	0.685
Pyruvate	1.000	1.249	1.559	1.000	0.871	0.300	1.000	2.152	1.674	1.000	1.882	1.050
Succinate	1.000	0.275	0.525	1.000	1.016	0.175	1.000	2.462	0.925	1.000	1.026	1.966
GABA	1.000	0.716	1.335	1.000	5.202	0.263	1.000	2.437	0.976	1.000	0.655	0.559

COMBINED METABOLIC AND PHYSIOLOGICAL IMPACTS OF LIGHT INTENSITY AND PHOTOPERIOD ON THE HALOTOLERANT *Desmonostoc salinum* CCM-UFV059

Luna Viggiano de Alvarenga, Marcelo Gomes Marçal Vieira Vaz, Alberto Esteves Ferreira, Naira Valle de Castro, Allan Victor Almeida, Adriano Nunes-Nesi and Wagner L. Araújo

To be submitted at **Algal Research**

COMBINED METABOLIC AND PHYSIOLOGICAL IMPACTS OF LIGHT INTENSITY AND PHOTOPERIOD ON THE HALOTOLERANT *Desmonostoc salinum* CCM-UFV059

Luna Viggiano de Alvarenga[1,2], Marcelo Gomes Marçal Vieira Vaz[1,2], Alberto Esteves Ferreira[3], Naira Valle de Castro[1,2], Allan Victor Almeida [1,2], Adriano Nunes-Nesi[1] and Wagner L. Araújo[1,2*]

[1]Departamento de Biologia Vegetal, Universidade Federal de Viçosa, 36570-900, Viçosa, Minas Gerais, Brazil

[2]Max-Planck Partner Group at the Departamento de Biologia Vegetal, Universidade Federal de Viçosa, 36570-900, Viçosa, Minas Gerais, Brazil

[3]National University of Ireland-Galway, Plant Systems Biology Laboratory, Plant and AgriBiosciences Research Centre, School of Natural Sciences, Galway, Ireland

[*]**Corresponding author:** Wagner L. Araújo; Departamento de Biologia Vegetal, Universidade Federal de Viçosa, 36570-900 Viçosa, Minas Gerais, Brazil; Tel: +55 31 3899.2169; Fax**:** +55 31 3899.2580; Email: wlaraujo@ufv.br

Running title: Light responses in *Desmonostoc salinum* CCM-UFV059

Keywords: Stress responses; biomass production, biotechnology, metabolism and storage compounds.

ABSTRACT

Cyanobacteria are autotrophic microorganisms with high photosynthetic efficiency, rapid cell growth, basic nutritional requirements (sunlight, water, and CO_2 mainly) and the possibility of genetic manipulation, and therefore are an excellent resource for industrial applications. In addition, cyanobacterial strains which are able to survive and grow in brackish or saline water might be industrially advantageous by avoiding competition with water resources used for human consumption. Thus, here we characterized the growth responses of the halotolerant cyanobacteria *Desmonostoc salinum* CCM-UFV059 cultivated under different light intensities, photoperiods, and in presence of moderate saline concentrations (NaCl). Our results showed that changes in light intensity altered colony structure and, consequently, biomass composition. The highest biomass was achieved under continuous light with intensity of 70 μmol m^{-2} s^{-1} (24:0_70), yielding a final biomass of 1.6 g L^{-1} (dry weight) after seven days of photoautotrophic growth. Collectively, our results enabled the establishment of optimal conditions (24:0_70) for cultivation of *D. salinum* CCM-UFV059, that allow high increments of both biomass and storage compounds (glycogen and cyanophycin) and optimal conditions for high increments of both biomass and protein (24:0_100).

1. INTRODUCTION

Cyanobacteria are unique prokaryotic microorganisms able to perform oxygenic photosynthesis and in some cases, nitrogen fixation (Steinhauser et al., 2012). During their evolution, these organisms faced environments with varying levels of carbon dioxide (CO_2), nitrogen, light and nutrients (Schopf et al., 1994; Badger et al., 2003). Thus, losses or, especially, gains of genes associated with selective pressures performed by different environmental factors were responsible for an extensive morphological diversification, accompanied by physiological and metabolic divergences within the phylum *Cyanobacteria* (Flores, 2008). As consequence, cyanobacteria can be found in the most extreme, terrestrial and aquatic, environments in Earth including soda lakes (de Alvarenga et al., 2018; Vaz et al., 2015), acidic water (Genuário et al., 2017; Genuário et al., 2019), hot deserts (Fulton et al., 2016; Oren et al., 2017) and polar regions (Chrismas et al., 2015). It is important to mention that cyanobacteria from extreme environments are potential sources of novel genes, products and important targets for biotechnological application (Genuário et al., 2019).

In comparison to land plants, which also rely on sunlight, water, and CO_2 (basic nutritional requirements), cyanobacteria present higher photosynthetic efficiency, rapid cell growth/division and the possibility of genetic manipulation through homologous recombination (Heidorn et al., 2011; Ruffing, 2011). Moreover, cyanobacteria possess high biotechnological potential, being used not only to obtain numerous products, such as biofuels, drugs, biopigments, enzymes, antioxidants, exopolysaccharides used as gellants; but they also display nutritional use as source of vitamins and proteins (Singh et al., 2011, Nowruzi et al., 2018). Considering the multiple uses of cyanobacterial biomass for either biotechnological or food purposes, it is important to highlight the current need of efforts on cyanobacterial cultivation in

non-potable water (probably in saline/brackish waters), avoiding competition with agriculture and human consumption (Pade and Hagemann, 2015). It should be kept in mind, however, that cyanobacterial growth in saline media might affect their cellular metabolism and perhaps negatively the final product yield (Hagemann, 2011). Therefore, a promising step for these purposes is the search of tolerant strains that are able to grow in residual waters and could be used as a source of biomass or metabolites of interest. In this context, *Desmonostoc salinum* CCM-UFV059, a halotolerant filamentous heterocytous strain isolated from a hypersaline environment (de Alvarenga et al., 2018) presents itself as a good candidate for biotechnological application. Coupled to its halotolerance, this strain also performs nitrogen fixation, which could decrease/eliminate the need for using combined nitrogen sources in the culture medium, reducing costs.

Knowledge of the factors acting on cyanobacterial biomass productivity and composition is critical to its biotechnological exploitation as well as to control its growth on the environment. Among these factors are noteworthy those that define an adequate absorption of light energy, allowing cyanobacterial growth and the storage of compounds of interest (Shukla et al., 2016). Light intensity and availability (photoperiod) are the major factors involved in the regulation of the C:N ratio in N-fixing cyanobacteria (Zhang et al., 2006). This ratio should be highlighted due to its influence on the production of cellular components (Otero and Vincenzini, 2004). Thus, it is important to understand the cyanobacterial metabolism and its variation under distinct environmental conditions to optimize the production of biomass and metabolites of interest (Markou et al., 2011). That being said, here, we analyze the physiological and metabolic responses of *Desmonostoc salinum* CCM-UFV059 to different light intensities and photoperiods, as well as to its cultivation under saline

conditions, aiming to find the light regime suitable for maximal biomass production and to better understand how distinct growth conditions interfere within the basal metabolism of this strain. Our results demonstrate that in response to changes in the photoperiod *Desmonostoc salinum* CCM-UFV059 suffer remarkable alterations in the metabolism and, consequently, in its cellular composition. Moreover, slight changes in the light intensity were able to completely change the colony structure of *Desmonostoc salinum* CCM-UFV059. Altogether, the results presented here allowed the establishment of optimal conditions for cultivation of *D. salinum* CCM-UFV059 with different biotechnological applications.

2. MATERIAL AND METHODS

2.1 *Cyanobacterial strain*

The strain *Desmonostoc salinum* CCM-UFV059 (hereafter *D. salinum* CCM-UFV059) used in this study was isolated from a saline-alkaline lake (de Alvarenga et al., 2018), and is currently available at the Collection of Cyanobacteria and Microalgae from Universidade Federal de Viçosa (CCM-UFV). Non-axenic unicyanobacterial cultures of *D. salinum* CCM-UFV059 have been maintained in glass flasks (125 mL) filled with 40 mL of liquid BG-11_0 medium (Rippka et al., 1979), under the following conditions: 24±2 °C, light intensity of 70 μmol·m^{-2}·s^{-1} and photoperiod of 16:8 h (light/dark). When cultured under standard (maintenance) growth conditions *D. salinum* CCM-UFV059 presented a saturation irradiance (I_s) of 100 ± 2 μmol·m^{-2}·s^{-1} and a compensation irradiance (I_c) of 25 ± 5 μmol·m^{-2}·s^{-1}.

2.2 Growth curves and kinetics

To identify the growth phases (lag, log, and stationary) of *D. salinum* CCM-UFV, growth curves were carried out under photoautotrophic growth conditions. Two light regimes were applied: photoperiod of 16:8 h (light/dark) and continuous light (24 h of light), which were conducted in two distinct light intensities namely 70 and 100 $\mu mol \cdot m^{-2} \cdot s^{-1}$. In addition, BG-$11_0$ medium was used with or without 0.1 M of NaCl. The NaCl concentration was chosen following previous studies (de Alvarenga et al. 2018).

Growth curves were performed in 125 mL Erlenmeyer flasks with 40 mL of BG-11_0, which were inoculated with 1 % (v/v) of biomass, taken from cultures at log phase (4-days old). The flasks were maintained at constant shaking (30 × *g*). Growth phases were determined by harvesting samples every day after eight hours of light (middle of the day), up to the third day in which no variation in growth was observed. Growth phases were determined by harvesting samples every day after eight hours of light (middle of the day), up to the third day in which no variation in growth was observed. Growth was evaluated by optical density (OD_{750nm}) and ashes-free dry weight (biomass) in absence of salt. The maximal growth rate (μ_{max}) and generation time (*Gt*) of *D. salinum* CCM-UFV059 were calculated by applying a linear regression of the data within the logarithmic growth period. Dry weight was determined using 5 mL of culture that was filtered on pre-weighed nitrocellulose membranes (0.45 μm porosity - Sartorius Stedim Biotech). The membranes with biomass were dried at 60 °C for 48 h and then weighed. For the determination of ash-free dry weight, the pre-weighed dry matter membranes were calcined in a muffle oven (Fornos Jung Ltda, LF 02312, Brazil) at 550 °C for 30 minutes. After cooling, the porcelain crucibles with the ashes were weighed. The ash-free dry weight was determined by subtraction of the dry

weight by ash weight after calcination and expressed as mg ash-free weight per mL of culture.

2.3 Morphological evaluation

Macroscopic and microscopic morphological observations were conducted on the 7th day of cultivation, during the logarithmic phase, using AxioCam HRc (Zeiss, Göttingen, Germany) and a Zeiss Axioskop 40 optical light microscope equipped with an AxioVision LE 4.6 digital imaging system (Carl Zeiss), respectively. For macroscopic records, colonies were not disrupted while for microscopy records the cultures were slightly homogenized by syringe fluxes.

2.4 ***Physiologic parameters and metabolic profiling***

Both physiological and metabolic evaluations were performed in samples harvested in the middle of the light period (after 8 h of light) of the 7th day of cultivation, allowing to compare their growth, metabolism and physiological performances since cyanobacteria present high growth rates and elevated metabolic activities at logarithmic phase. For biochemical analyses, the samples were harvested and immediately frozen in liquid nitrogen and then stored at -80 °C until further analyses, as described below. In addition, for treatments in which the photoperiod 16:8 h was applied, samples were also harvested in the Beginning of the day (BOD – 0h – start of light phase); Middle of the day (MOD – 8h); End of the day (EOD – 16h); Middle of the night (MON – 20h – middle of dark phase) and End of the night (EON – 24h – with lights still turned off) for analysis of storage compounds.

Briefly, total chlorophyll was extracted in ethanol and quantified according to Porra et al. (1989). Total proteins were determined according to Lowry (1951), with

the Folin-phenol reagent and total amino acids as in Sienkiewicz-Porzucek et al. (2008). Total carbohydrates were determined by using the phenol-sulfuric acid assay according to DuBois (1956), adapted by Masuko et al. (2005) and glycogen content was extracted and quantified using an enzymatic assay with hexokinase (Kirsch et al., 2017).

Cyanophycin content was extracted according to Elbahloul et al. (2005), modified by Trautmann et al. (2016) and quantified according to Messineo et al. (1966). Total neutral lipids were determined according to the modified method of Bligh and Dyer (Chen et al., 2010).

Metabolic profile was performed using an established gas chromatography–mass spectrometry (GC-MS) from fresh cells as described by Krall et al. (2009). Derivatization, standard addition, and sample injection for GC-MS were performed according to Osorio et al. (2012). Chromatograms and mass spectra were evaluated using Chroma TOF 1.0 (Leco, http://www.leco.com/) and TAGFINDER 4.0 software (Luedemann et al., 2008). The mass spectra were cross-referenced with those in the GolmMetabolome Database (Schauer et al., 2005). The amounts of metabolites were determined as relative metabolite abundances, calculated by normalization of signal intensity of ribitol, which was added as an internal standard, and then by dry weight of the material. The treatment 16:8 h (light/dark), 70 $\mu mol \cdot m^{-2} \cdot s^{-1}$ was used as a control to evaluate the changes in metabolite concentration in *D. salinum* CCM-UFV059.

Measurements of net photosynthetic rates and dark respiration were carried out during the logarithmic phase, on day 3 and 7 of each treatment, using a Clark-type electrode connected to an oxygen monitor (Chlorolab 2 System, Hansatech, Norfolk, UK), as previously described (Torzillo et al., 1998, Jeon et al., 2005). The instrument was calibrated using a solution of sodium hydrosulfite and BG-11_0 medium to set 0 %

saturation. Then, 2 mL of culture were inoculated in the electrode chamber and curves of oxygen consumption and evolution, in response to photosynthetically active radiation (PAR), were performed at 25 °C using the light intensity in which the cells were cultured (70 or 100 $\mu mol \cdot m^{-2} \cdot s^{-1}$). The maximum quantum yield of photosystem II (F_v/F_m) was measured with a portable pulse amplitude fluorometer system (PAM-2000, Walz Inc., Germany), after acclimation of cultures for 30 minutes in the dark. The photochemical efficiency of photosystem II adapted to light (ΦPSII) was measured after five minutes of exposure to the light intensities applied in the treatments.

2.5 *Statistical analysis*

The experiments were set in a completely randomized design. Values are presented as the mean ± standard error (SEM) that were obtained from five independent replicates per growth condition and when was the case, over time. ANOVA ($P < 0.05$) was performed to compare the data obtained for the different growth conditions, and the means were compared by the Student's *t*-test test at 5% probability, using the lowest value as a reference. Statistical analysis were performed using the software *Assistat* statistical (version 7.7-http://assistat.com).

3. RESULTS

3.1 *Growth kinetics in response to variations in light intensities*

Regardless the light intensity and/or photoperiod used here, cultures of *D. salinum* CCM-UFV059 presented similar growth patterns in all treatments conducted with BG-11_0, reaching the stationary phase in the 12^{th} day (Fig. 1). Considering the treatments, none of the growth curves displayed lag phases, yet, despite the similar pattern, the

duration of the log phase varied (Table 1). Cells cultivated under the 16:8 h (light/dark), 70 μmol·m^{-2}·s^{-1} (hereafter called 16:8_70) presented an initial log phase of only three days, while cells under 16:8 h (light/dark), 100 μmol·m^{-2}·s^{-1} (16:8_100) presented five days log phase. For both treatments, after the log phase, a non-growth day was observed (between the 3rd and 4th days, as well as 5th and 6th, for the treatments 16:8_70 and 16:8_100, respectively). These phases were followed by a slow resumption of growth, until the cells reached the stationary phase (Fig. 1). The treatments 24/0 h (light/dark), 70 μmol·m^{-2}·s^{-1} (24:0_70) and 100 μmol·m^{-2}·s^{-1} (24:0_100) presented log phases of five days, similar to the treatment 16:8_100, but without the presence of a non-growth day (Fig. 1).

The treatment 16:8_70 had the highest maximum growth rate (μ_{max} - 0.212 d^{-1}) and consequently the lowest generation time (*Gt* - 1.41 d^{-1}) (Table 1). However, due to the shorter log phase, this treatment did not present higher biomass production (Table 1). The highest biomass production was observed for the treatments carried out under continuous light which was almost two times higher than those found in treatments of 16:8 h photoperiod (Table 1). Considering the same photoperiods, similar biomass production was obtained under the different light intensities.

3.2 *Microscopic and macroscopic changes in response to light regimes*

Colonies of *D. salinum* CCM-UFV059 under 16:8_70 showed no clear aggregation pattern, with trichomes homogeneously dispersed into the culture medium (Fig. 2A). Under 16:8_100 trichomes formed conspicuous macroscopic colonies, which were dense and enclosed, presenting some free aggregates of filaments (Fig. 2B). By contrast, cultures under continuous light (24:0_70 and 24:0_100) presented colonies separated into small lumps and heavily aggregated (Fig. 2C and D).

Microscopic pattern of filaments aggregation was also very distinct among the treatments (Fig. 3). Under 70 $\mu mol \cdot m^{-2} \cdot s^{-1}$, regardless of the photoperiod, most of the vegetative trichomes presented heterocytes and were organized in a parallel way (Fig. 3A and C), which is typical of the vegetative stage of *Desmonostoc* strains (Hrouzek et al., 2013). On the other hand, under 16:8_100, hormogonia (motile, non-heterocytic filaments) and non-mature filaments were the predominant type and the parallel organization was partially lost (Fig. 3B). Under 24:0_100, vegetative filaments with heterocytes were predominant and the typical parallel organization of trichomes was completely lost. In addition, the colonies presented a disperse pattern, without conspicuous aggregation, displaying more space between trichomes (Fig. 3D).

3.3 Changes in metabolism in response to light regimes

Among the nitrogen (N) compounds, the amounts of total chlorophyll and proteins presented a similar pattern, with higher levels found in treatments carried out under a photoperiod of 16:8, regardless of the light intensity (Table 2). It is also important to mention that under this photoperiod, higher contents of both metabolites was found at 100 $\mu mol \cdot m^{-2} \cdot s^{-1}$ (Table 2). Total amino acids showed an opposite behavior, with higher contents found under continuous light. Additionally, the lowest level of amino acids was observed at 16:8_100, which yielded the highest protein and chlorophyll contents (Table 2). Cyanophycin, and phycobiliproteins (PBS) content also presented a similar pattern in the treatments 16:8_100, 24:0_70 and 24:0_100 and the lower content was found under 16:8_70 (Table 2).

Regarding carbon (C) compounds, the content of total soluble carbohydrates (hereafter carbohydrates) was nearly conserved among treatments under the same light intensity, independent of photoperiod (Table 2). The highest content of carbohydrates

was found under continuous light and 100 μmol·m^{-2}·s^{-1}. Curiously, the amounts of glycogen followed a similar pattern also observed for cyanophycin, and PBS, for which higher levels were observed among the treatments 16:8_100, 24:0_70 and 24:0_100 (Table 2). Contrary to the other storage compounds, neutral lipids content showed a higher level under 16:8_70 (Table 2).

We also analyzed the metabolite contend under 16:8 h during a complete light/dark cycle after seven days of growth (Fig. 4). Total protein contents were higher under 16:8_100 regardless the sampling point (Fig. 4A), as observed also for the analysis on the 7th day (Table 2). In addition, total protein contents showed no differences over the diurnal light/dark cycle (Fig. 4A). Oppositely, and as expected, cyanophycin showed clear variations on its diurnal levels, although the peak of accumulation differed between both treatments (Fig. 4B). In cells cultured under 16:8_100 the highest level of cyanophycin was found in the middle of the day (after 8 h of light), decreasing from this point. However, under 16:8_70 the highest level was achieved only at the end of day (16 h of light). The patterns of carbohydrates and glycogen accumulation were similar. Under 16:8_70, both metabolites did not show any significant change along the diurnal cycle, while under 16:8_100 their content increase over the day and decrease during the night (Fig. 4C and D).

Considering the growth conditions, the net photosynthetic rates (*A)* showed no variation, after three days of cultivation, with an average value of ~ 4.0 nmol O_2 min^{-1} mg^{-1} dry mass (Table 3). After seven days of growth, *A* was reduced by more than 50 % in all conditions, with the exception of the treatment 16:8_70, which sustained a higher *A* (2.98 nmol O_2 min^{-1} mg^{-1} dry mass) (Table 3). By contrast, the respiratory rates at the 3rd day of growth were distinct between the photoperiods. Cells grown under continuous light presented higher respiratory rates compared with cells under

16:8 h. At the 7th day of growth, the respiratory rates decreased for all treatments, reaching as much as only 20% for those cells cultured under continuous light. F_v/F_m values were similar among the treatments, while the quantum yield of photochemical energy conversion in PSII (ΦPSII) was higher under 16:8_70 (0.44), reducing with increased light availability, and reaching the lowest value under 24:0_100 (0.2) (Table 2).

Under continuous light, increased amounts of sugars (maltose, glucose, trehalose, maltotriose), aspartate, alanine, tyrosine, ornithine, putrescine and spermidine were observed when compared with treatments under 16:8 h. Moreover, ascorbic acid and galactose were significantly increased reaching values more than five times higher compared with the 16:8 h treatments (Fig. 5).

3.4 Response to light under saline conditions

To evaluate the effects of light intensities and photoperiods on the growth of *D. salinum* CCM-UFV059 under saline conditions, cells from BG-11_0 supplemented with 0.1 M NaCl were also analyzed. Under 16:8 h, biomass production in cells grown without or with 0.1 M NaCl was similar. Furthermore, under continuous light, the biomass production in the BG-11_0 medium with salt was significantly reduced in comparison to control conditions (Fig. 6).

On the 3rd day of cultivation, under saline conditions *A* was higher in the treatments under 100 $\mu mol \cdot m^{-2} \cdot s^{-1}$, regardless the photoperiod. However, at the 7th day of growth, the treatments under 16: 8 h presented the highest *A* (Table 4). This pattern of higher *A* after seven days of growth was also observed under 16:8_70 without salt. Under saline conditions, the respiratory rate on the 3rd day of cultivation was more than five times higher under continuous light, compared to treatments 16:8 h; under

continuous light in medium without salt higher respiratory rates on the 3rd day was also observed. On the 7th day of cultivation, this pattern was modified and became similar to the growth without salt, with the highest respiratory rate was observed under 16:8 h photoperiod (Table 4).

Surprisingly, opposite to the situation observed under non-salt conditions, almost no changes were detectable in the metabolism of *D. salinum* CCM-UFV059 in response to light intensities while growing under saline conditions. It seems reasonable to assume that, due to the great metabolic readjustment in response to the saline conditions (Fulda et al., 2000), *D. salinum* CCM-UFV059 cells did not display significant metabolic reprogramming in response to the light treatments.

4. DISCUSSION

An association between the macroscopic colony architecture of *D. salinum* CCM-UFV059 and its predominant cellular/filament types was observed considering both macroscopic and microscopic patterns found for the different growth conditions (Figs. 2 and 3). Colonies with loose pattern presented vegetative cells as the most abundant cell type (16:8_70, 24:0_70 and 24:0_100), whereas highly aggregated colonies (16:8_100) had a higher abundance of hormogonia, indicating the occurrence of cellular differentiation in dense colonies (Figs. 1 and 2). Hormogonia are specialized filaments that enter in a non-growth state, showing gliding motility and are distinguishable from mature trichomes mainly by reduced cell size and absence of heterocytes (Khayatan et al., 2017). In filamentous heterocytous cyanobacteria the spectral quality of light greatly affects the differentiation of hormogonia, being possibly the best-understood factor as an inductor of the formation of this specialized cell type (Li et al., 2005). The enrichment of the inward of the colony with long and

less energetic wavelengths, known as selective filtration of light, leads to the preferential excitation of the PSI and to an oxidation of the pool of plastoquinones, triggering the process of hormogonia differentiation (Campbell et al., 1993; Afonso et al., 2001). It is likely possible that the dense and enclosed macroscopic pattern presented by the colonies in the treatment 16:8_100 is associated with the enrichment of low energetic wavelengths, and consequently, the abundance of hormogonia. Moreover, metabolic and biochemical analysis were performed on the 7th day, after the non-growth day displayed by the cells under 16:8_100 (Fig. 1). Another feature observed under this growth condition was a high content of chlorophyll and total protein per dry weight. Although no significant synthesis of DNA, proteins or chlorophyll occur during the hormogonia cycle (Meeks et al., 2002), the higher amount of protein and chlorophyll per dry weight (Table 2) found in these colonies could be a reflection of the reduction of other cellular components, resulting in a higher proportion per biomass.

Variations in light intensity seems to modulate the storage metabolism of *D. salinum* CCM-UFV059 without reflecting on the final biomass production. Under 70 $\mu mol \cdot m^{-2} \cdot s^{-1}$ in the 16:8 h photoperiod the lowest amounts of storage compounds such as glycogen and cyanophycin (Table 1) was observed; however, the total final biomass were similar as observed under 16:8_100. Phycobiliproteins (PBS), light-harvesting water-soluble proteins, which also work as nitrogen storage compounds (Grossman et al., 2001), showed an accumulation pattern similar to glycogen and cyanophicin, with lowest amounts under 16:8_70. Neutral lipids were the only reserve with increased contents in this treatment (16:8_70). Due to the importance of the C:N ratio in cyanobacteria biomass, especially among nitrogen-fixing species (Zhang et al., 2006), it is reasonable to assume that under 16:8_70 a misbalance in this ratio likely occurs,

resulting in the accumulation of storage compounds lacking nitrogen, such as neutral lipids. The accumulation of neutral lipids in response to nitrogen starvation has been widely studied in microalgae (Breuer et al., 2012; Singhasuwan et al., 2015; Benvenuti et al., 2015; Machado et al., 2016). Moreover, the availability of ATP and reduced coenzymes are important to define the metabolism direction in response of a C:N misbalance (Xiong et al., 2017) and consequently, the preferable storage compounds accumulated. This could explain, at least partially, the accumulation of lipids over glycogen in the treatment 16:8_70. Accordingly, the reduced amount of storage compounds for 16:8_70 allowed the cells to sustain high photosynthetic rates on the 7th day of growth (Table 3), most likely due to a lower limitation of the photosynthetic rate by the end product. Under 100 μmol·m^{-2}·s^{-1}, especially under continuous light, high soluble carbohydrate contents, including exopolysaccharides (EPS), were found. Moreover, cells under continuous light produced high amounts of galactose (Fig. 5), one of the main substrates for EPS biosynthesis in cyanobacteria (Liu et al., 2017). Accordingly, several studies have reported the importance of EPS under stress tolerance, including light stress (Ehling-Schulz et al., 1999; Tamaru et al., 2005 and Ozturk et al., 2010; Kehr & Dittmann, 2015). Higher content of EPS may indicate export of carbon to the cell exterior, also due to a misbalance in the C:N ratio. This coupled with high amounts of ascorbic acid, a metabolite with an important role in the prevention of reactive oxygen species accumulation (He et al., 2012; Cheloni & Slaveykova, 2018), indicates that under continuous light, cyanobacterial metabolism is likely adjusted to avoid light stress. Despite the similar F_v/F_m observed in all growth conditions investigated here, ΦPSII was severely reduced under continuous light, especially under 100 μmol·m^{-2}·s^{-1} (Table 3). Regardless these slight indications of light stress, *D. salinum* CCM-UFV059 was able to most likely adjust their cellular

metabolism to cope with high light availability, as depicted by the higher biomass production under continuous light.

After seven days of growth, *D. salinum* CCM-UFV059 biomass production was similar under the same photoperiod, regardless light intensity (Fig. 1 and Table 1). Nevertheless, under continuous light higher final biomass after 7 days of growth (~1.6 $g \cdot L^{-1}$) was observed. Similar biomass production was also observed after seven days under mixotrophic conditions (medium supplemented with 1 % sucrose) by *Nostoc flagelliforme*, a cyanobacteria daily used in Chinese cuisine with a much consolidated market (Yu et al., 2009). By cultivating *D. salinum* CCM-UFV059 under mixotrophic conditions a 10-x fold higher biomass was observe in a pilot experiment (data no shown). Moreover, the higher biomass produced by *D. salinum* CCM-UFV059 is similar to values presented by *Spirulina platensis* under laboratory conditions (Coca et al., 2015; Celekli et at., 2016; Shao et al., 2018). By comparing the growth of *D. salinum* CCM-UFV059 with cyanobacteria already available on the market, it seems reasonable to suggest that the cultivation of this strain aiming at biomass production for commercial use is most likely possible.

The ability to sustain photosynthetic rates and produce biomass without impairments under moderate saline conditions and long day photoperiods (16:8 h) indicates the possibility of cultivation of *D. salinum* CCM-UFV059 in brackish or wastewater. Further research using large scale cultivation is clearly required to proper evaluate the biomass production of this strain for biotechnological purposes. Nevertheless, *D. salinum* CCM-UFV059 seems to possess a highly plastic metabolism and the ability to sustain grow under different of light regimes, possibly allowing its outdoor cultivation and commercial use.

ACKNOWLEDGEMENTS

This work was supported by funding from the Max Planck Society, the National Council for Scientific and Technological Development (CNPq-Brazil) and the Foundation for Research Assistance of the Minas Gerais State, Brazil (FAPEMIG, Grants APQ-01106-13, and APQ-01357-14) to W.L.A. L.V.A. was supported by scholarship from the Foundation for Research Assistance of the Minas Gerais State, Brazil (FAPEMIG). M.G.M.V.V. is supported by scholarship from the Brazilian Federal Agency for Support and Evaluation of Graduate Education (CAPES, Grant PNPD-1638006). N.V.C. and A.V.A. were supported by student fellowships from CNPq and CAPES, respectively. Research fellowships granted by CNPq-Brazil to A.N-N and W.L.A. are also gratefully acknowledged.

CONFLICTS OF INTEREST

The authors declare no conflicts of interest.

AUTHOR CONTRIBUTION

LVA and WLA designed the work. LVA, AVMA and NVC carried out the experiments. LVA wrote the manuscript. AAFE and MGGVV gave scientific inputs for improvement of the manuscript. WLA and ANN edited and approved the final manuscript.

STATEMENT OF INFORMED CONSENT

No conflicts, informed consent, human or animal rights applicable.

AUTHOR DECLARATION

All the authors agree to the authorship and submission of the manuscript to the peer review process.

REFERENCES

Alfonso, M., Perewoska, I., & Kirilovsky, D. (2001) Redox control of ntcA gene expression in Synechocystis sp. PCC 6803. Nitrogen availability and electron transport regulate the levels of the NtcA protein. Plant Physiology, 125(2), 969-981.

Anderson, J. M., Chow, W. S., & Park, Y. I. (1995) The grand design of photosynthesis: acclimation of the photosynthetic apparatus to environmental cues. Photosynthesis Research, 46(1-2), 129-139.

Badger, M. R., & Price, G. D. (2003) CO_2 concentrating mechanisms in cyanobacteria: molecular components, their diversity and evolution. Journal of Experimental Botany, 54(383), 609-622

Beck C., Knoop H., Axmann I. M. & Steuer R. (2012) The diversity of cyanobacterial metabolism: genome analysis of multiple phototrophic microorganisms. BMC Genomics 13(1): 56.

Benvenuti, G., Bosma, R., Cuaresma, M., Janssen, M., Barbosa, M. J., & Wijffels, R. H. (2015) Selecting microalgae with high lipid productivity and photosynthetic activity under nitrogen starvation. Journal of Applied Phycology, 27(4), 1425-1431.

Bhadauriya, P., Gupta, R., Singh, S., & Bisen, P. S. (2009) NaCl induced metabolic changes in the diazotrophic cyanobacterium Anabaena cylindrica. World Journal of Microbiology and Biotechnology, 25(2), 341.

Breuer, G., Lamers, P. P., Martens, D. E., Draaisma, R. B., & Wijffels, R. H. (2012) The impact of nitrogen starvation on the dynamics of triacylglycerol accumulation in nine microalgae strains. Bioresource Technology, 124, 217-226.

Campbell, D., Houmard, J., & De Marsac, N. T. (1993) Electron transport regulates cellular differentiation in the filamentous cyanobacterium Calothrix. The Plant Cell, 5(4), 451-463.

Çelekli, A., Topyürek, A., Markou, G., & Bozkurt, H. (2016) A multivariate approach to evaluate biomass production, biochemical composition and stress compounds of spirulina platensis cultivated in wastewater. Applied Biochemistry and Biotechnology, 180(4), 728-739.

Cheloni, G., & Slaveykova, V. (2018) Photo-oxidative stress in green algae and cyanobacteria. React. Oxyg. Species, 5, 126-133.

Chen, P., Min, M., Chen, Y., Wang, L., Li, Y., Chen, Q. & Deng, S. (2010) Review of biological and engineering aspects of algae to fuels approach. International Journal of Agricultural and Biological Engineering, 2(4), 1-30.

Chrismas, N. A., Anesio, A. M., & Sánchez-Baracaldo, P. (2015) Multiple adaptations to polar and alpine environments within cyanobacteria: a phylogenomic and Bayesian approach. Frontiers in Microbiology, 6, 1070.

Coca, M., Barrocal, V. M., Lucas, S., González-Benito, G., & García-Cubero, M. T. (2015) Protein production in Spirulina platensis biomass using beet vinasse-supplemented culture media. Food and Bioproducts Processing, 94, 306-312.

Damerval, T., Guglielmi, G., Houmard, J., & De Marsac, N. T. (1991) Hormogonium differentiation in the cyanobacterium Calothrix: a photoregulated developmental process. The Plant Cell, 3(2), 191-201.

de Alvarenga, L.V., Vaz, M.G.M.V., Genuário, D.B., Esteves-Ferreira, A.A., Almeida, A.V.M., Castro, N.V., Lizieri, C., Souza, J.J.L.L., Schaefer, C.E.G.R., Nunes-Nesi, A., Araújo, W.L. (2018) Extending the ecological distribution of Desmonostoc genus: proposal of Desmonostoc salinum sp. nov., a novel Cyanobacteria from a saline–alkaline lake. Int. J. Syst. Evol. Microbiol. 68, 2770–2782.

Ding Z., Jia S., Han P., Yuan N. & Tan N. (2013) Effects of carbon sources on growth and extracellular polysaccharide production of *Nostoc flagelliforme* under heterotrophic high-cell-density fed-batch cultures. Journal of Applied Phycology 25(4): 1017-1021.

Ehling-Schulz, M., & Scherer, S. 1999. UV protection in cyanobacteria. European Journal of Phycology, 34(4), 329-338.

Elbahloul, Y., Krehenbrink, M., Reichelt, R., & Steinbüchel, A. (2005) Physiological conditions conducive to high cyanophycin content in biomass of *Acinetobacter calcoaceticus* strain ADP1. Applied and Environmental Microbiology, 71(2), 858-866.

Flores, F. G. 2008. The cyanobacteria: molecular biology, genomics, and evolution. Horizon Scientific Press.

Fulda S., Huang F., Nilsson F., Hagemann M., Norling B. (2000) Proteomics of Synechocystis sp. strain PCC 6803. Identification of periplasmic proteins in cells grown at low and high salt concentrations. Eur J Biochem 267: 5900–7.

Fulton, J. M., & Van Mooy, B. A. (2016) Microbial Response to UV Exposure and Nitrogen Limitation in Desert Soil Crusts. In AGU Fall Meeting Abstracts.

Genuário, D. B., Andreote, A. P. D., Vaz, M. G. M. V., & Fiore, M. F. (2017) Heterocyte-forming cyanobacteria from Brazilian saline-alkaline lakes. Molecular Phylogenetics and Evolution, 109, 105-112.

Genuário, D. B., Vaz, M. G., Santos, S. N., Kavamura, V. N., & Melo, I. S. (2019) Cyanobacteria from Brazilian extreme environments: toward functional exploitation. in microbial diversity in the genomic era (pp. 265-284). Academic Press

Grossman A. R., Bhaya D. & He Q. (2001) Tracking the light environment by cyanobacteria and the dynamic nature of light harvesting.Journal of Biological Chemistry,276(15): 11449-11452.

Hagemann M. (2011) Molecular biology of cyanobacterial salt acclimation. FEMS Microbiology Reviews 35(1): 87-123.

He, Y. Y., & Häder, D. P. (2002) UV-B-induced formation of reactive oxygen species and oxidative damage of the cyanobacterium *Anabaena* sp.: protective effects of ascorbic acid and N-acetyl-L-cysteine. Journal of Photochemistry and Photobiology B: Biology, 66(2), 115-124.

Heidorn T., Camsund D., Huang H-H., Lindberg P., Oliveira P., Stensjo K., Lindblad P. (2011) Synthetic biology in cyanobacteria: Engineering and analyzing novel functions. In C Voigt, ed, Methods in Enzymology, vol 497: Synthetic Biology, methods for part/device characterization and chassis engineering, pp 539-579

Hrouzek, P., Lukešová, A., Mareš, J., & Ventura, S. (2013) Description of the cyanobacterial genus *Desmonostoc* gen. nov. including *D. muscorum comb*. nov. as a distinct, phylogenetically coherent taxon related to the genus *Nostoc.* Fottea, 13(2), 201-213.

Jeon, Y. C., Cho, C. W. & Yun, Y. S. (2005) Measurement of microalgal photosynthetic activity depending on light intensity and quality. Biochem Eng J, 27, 127-131.

Karandikar M., Kawadkar N., & Wandre S. (2016) scientific cultivation and quality control system for futuristic super food-SPIRULINA. International Journal of Scientific Research,5(1).

Kehr, J. C., & Dittmann, E. (2015) Biosynthesis and function of extracellular glycans in cyanobacteria. Life, 5(1), 164-180.

Khayatan, B., Bains, D. K., Cheng, M. H., Cho, Y. W., Huynh, J., Kim, R., & Splitt, S. D. (2017) A putative O-linked β-N-acetylglucosamine transferase is essential for hormogonium development and motility in the filamentous cyanobacterium *Nostoc punctiforme*. Journal of Bacteriology, JB-00075.

Kirsch, F., Pade, N., Klähn, S., Hess, W. R., & Hagemann, M. (2017) The glucosylglycerol-degrading enzyme GghA is involved in acclimation to fluctuating salinities by the cyanobacterium *Synechocystis* sp. strain PCC6803. Microbiology, 163(9), 1319-1328.

Krall, L., Huege, J., Catchpole, G., Steinhauser, D., & Willmitzer, L. (2009) Assessment of sampling strategies for gas chromatography–mass spectrometry (GC–MS) based metabolomics of cyanobacteria. Journal of Chromatography B, 877(27), 2952-2960.

Liu, W., Cui, L., Xu, H., Zhu, Z., & Gao, X. (2017) The flexibility-rigidity coordination of dense exopolysaccharide matrix in terrestrial cyanobacteria acclimated to periodic desiccation. Applied and Environmental Microbiology, AEM-01619.

Lowry O., Rosebrough N., Farr A. & Randall R. (1951) Protein measurement with the Folin phenol reagent. The Journal of Biological Chemistry 193(1):265-275.

Luedemann A., Strassburg K., Erban A. & Kopka J. (2008) TagFinder for the quantitative analysis of gas chromatography-mass spectrometry (GC-MS)-based metabolite profiling experiments. Bioinformatics 24(5): 732–737.

Machado, M., Bromke, M., Júnior, A. P. D., Vaz, M. G. M. V., Rosa, R. M., Vinson, C. C., ... & Willmitzer, L. (2016) Comprehensive metabolic reprogramming in freshwater Nitzschia palea strains undergoing nitrogen starvation is likely associated with its ecological origin. Algal Research, 18, 116-126.

Masuko, T., Minami, A., Iwasaki, N., Majima, T., Nishimura, S. I., & Lee, Y. C. (2005) Carbohydrate analysis by a phenol–sulfuric acid method in microplate format. Analytical Biochemistry, 339(1), 69-72.

Mateo P., Perona E., Berrendero E., Leganés F., Martín M. & Golubić S. (2011) Life cycle as a stable trait in the evaluation of diversity of *Nostoc* from biofilms in rivers. FEMS Microbiology Ecology 76(2): 185-198.

Meeks J. C., Campbell E. L., Summers M. L., & Wong F. C. (2002) Cellular differentiation in the cyanobacterium *Nostoc punctiforme*. Archives of Microbiology 178(6): 395-403.

Messineo, L. (1966) Modification of the Sakaguchi reaction: spectrophotometric determination of arginine in proteins without previous hydrolysis. Archives of Biochemistry and Biophysics, 117(3), 534-540.

Nowruzi, B., Haghighat, S., Fahimi, H., & Mohammadi, E. (2018) Nostoc cyanobacteria species: a new and rich source of novel bioactive compounds with pharmaceutical potential. Journal of Pharmaceutical Health Services Research, 9(1), 5-12.

Otero, A., & Vincenzini, M. 2004. Nostoc (Cyanophyceae) goes nude: extracellular polysaccharides serve as a sink for reducing power under unbalanced C/N metabolism. Journal of Phycology,40(1), 74-81.

Ozturk, S., & Aslim, B. (2010) Modification of exopolysaccharide composition and production by three cyanobacterial isolates under salt stress. Environmental Science and Pollution Research, 17(3), 595-602.

Pade N & Hagemann M. (2015) salt acclimation of cyanobacteria and their application in biotechnology. Life 5(1): 25-49.

Parmar A., Singh N. K., Pandey A., Gnansounou E., Madamwar D. (2011) Cyanobacteria and microalgae: A positive prospect for biofuels. Bioresource Technology 102(22): 10163–10172.

Porra, R.J., Thompson W.A., and Kriedemann P.E. (1989) Determination of accurate extinction coefficients and simultaneous equations for assaying chlorophylls a and b extracted with four different solvents: verification of the concentration of chlorophyll

standards by atomic absorption spectroscopy. Bioch et Biophys Acta. 975(3): p. 384-394.

Rigonato, J., Gama, W. A., Alvarenga, D. O., Branco, L. H. Z., Brandini, F. P., Genuário, D. B., & Fiore, M. F. (2016) *Aliterella atlantica* gen. nov., sp. nov., and *Aliterella antarctica* sp. nov., novel members of coccoid cyanobacteria. International Journal of Systematic and Evolutionary Microbiology, 66(8), 2853-2861.

Rippka R., Deruelles J., Waterbury J. B., Herdman, M., & Stanier, R. Y. (1979) Generic assignments, strain histories and properties of pure cultures of cyanobacteria. Microbiology,111(1), 1-61.

Ruffing A.M. (2011) Engineered cyanobacteria: Teaching an old bug new tricks. Bioengineered Bugs 2: 136-149

Schauer N., Steinhauser D., Strelkov S., Schomburg D., Allison G., Moritz T., Lundgren K., Roessner-Tunali U., Forbes M. G., Willmitzer L. & Fernie, A. R. (2005) GC–MS libraries for the rapid identification of metabolites in complex biological samples. FEBS letters,579(6), 1332-1337.

Schopf, J. W. (1994) Disparate rates, differing fates: tempo and mode of evolution changed from the Precambrian to the Phanerozoic. Proceedings of the National Academy of Sciences, 91(15), 6735-6742.

Shao, W., Ebaid, R., Abomohra, A. E. F., & Shahen, M. (2018) Enhancement of Spirulina biomass production and cadmium biosorption using combined static magnetic field. Bioresource technology.

Shi, W. Q., Li, S. D., Li, G. R., Wang, W. H., Chen, Q. X., Li, Y. Q., & Ling, X. W. (2016) Investigation of main factors affecting the growth rate of Spirulina. Optik-International Journal for Light and Electron Optics, 127(16), 6688-6694.

Shukla, M., Tabassum, R., Singh, R., & Dhar, D. W. (2016). Influence of light intensity, temperature and CO_2 concentration on growth and lipids in green algae and cyanobacteria. Indian Journal of Experimental Biology 54, 482-487.

Sienkiewicz-Porzucek, A., Nunes-Nesi, A., Sulpice, R., Lisec, J., Centeno, D. C., Carillo, P., ... & Fernie, A. R. (2008) Mild reductions in mitochondrial citrate synthase activity result in a compromised nitrate assimilation and reduced leaf pigmentation but have no effect on photosynthetic performance or growth. Plant Physiology, 147(1), 115-127.

Singh R. K., Tiwari S. P., Rai A. K. & Mohapatra T. M. 2011. Cyanobacteria: an emerging source for drug discovery. The Journal of Antibiotics, 64(6): 401-412.

Singhasuwan, S., Choorit, W., Sirisansaneeyakul, S., Kokkaew, N., & Chisti, Y. (2015) Carbon-to-nitrogen ratio affects the biomass composition and the fatty acid profile of heterotrophically grown Chlorella sp. TISTR 8990 for biodiesel production. Journal of Biotechnology, 216, 169-177.

Tamaru, Y., Takani, Y., Yoshida, T., & Sakamoto, T. (2005) Crucial role of extracellular polysaccharides in desiccation and freezing tolerance in the terrestrial cyanobacterium Nostoc commune. Applied and Environmental Microbiology, 71(11), 7327-7333.

Torzillo, G., Bernardini, P. & Masojidek, J. (1998) On-line monitoring of chlorophyll fluorescence to assess the extent of photoinhibition of photosynthesis induced by high oxygen concentration and low temperature and its effect on the productivity of outdoor cultures of Spirulina platensis (Cyanobacteria). J Phycol, 34, 504-510.

Trautmann, A., Watzer, B., Wilde, A., Forchhammer, K., & Posten, C. (2016) Effect of phosphate availability on cyanophycin accumulation in Synechocystis sp. PCC 6803 and the production strain BW86. Algal Research, 20, 189-196.

Walters, R. G. (2005) Towards an understanding of photosynthetic acclimation. Journal of Experimental Botany, 56(411), 435-447.

Xiong, W., Cano, M., Wang, B., Douchi, D., & Yu, J. (2017). The plasticity of cyanobacterial carbon metabolism. Current Opinion in Chemical Biology, 41, 12-19.

Xu, K., Jiang, H., Juneau, P., & Qiu, B. (2012) Comparative studies on the photosynthetic responses of three freshwater phytoplankton species to temperature and light regimes. Journal of Applied Phycology, 24(5), 1113-1122.

Zhang, C. C., Laurent, S., Sakr, S., Peng, L., & Bédu, S. (2006) Heterocyte differentiation and pattern formation in cyanobacteria: a chorus of signals. Molecular Microbiology, 59(2), 367-375.

Zhang, C. C., Zhou, C. Z., Burnap, R. L., & Peng, L. (2018) Carbon/Nitrogen Metabolic Balance: Lessons from Cyanobacteria. Trends in Plant Ccience.

Zhang, L., Chen, L., Wang, J., Chen, Y., Gao, X., Zhang, Z., & Liu, T. (2015) Attached cultivation for improving the biomass productivity of Spirulina platensis. Bioresource Technology, 181, 136-142.

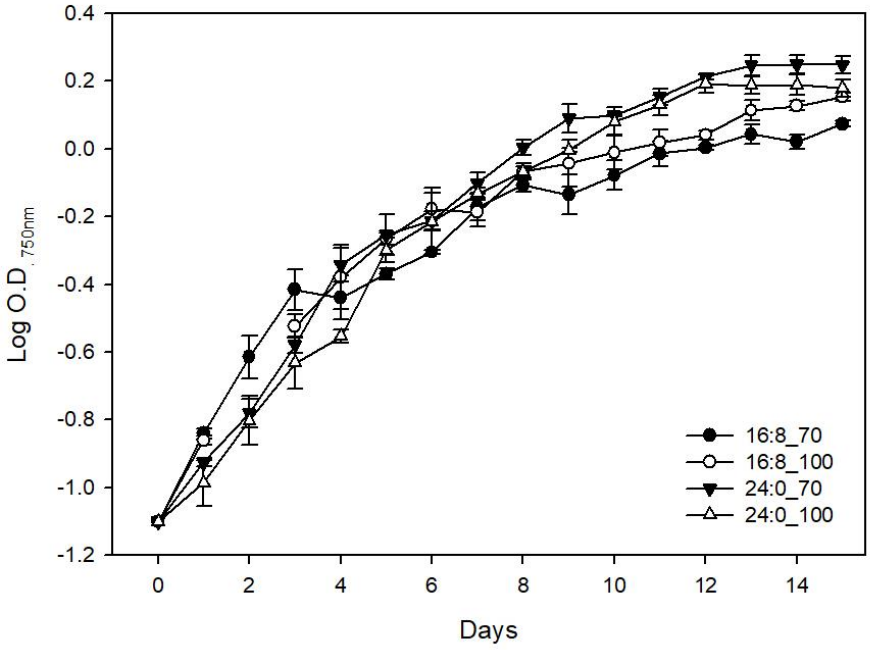

Figure 1: *Desmonostoc salinum* CCM-UFV059 growing under distinct photoperiods and light intensities. The growth was measure daily in response to increases in the optical density ($O.D._{750\ nm}$). (16:8_70) Photoperiod of 16:8 h, light intensity of 70 $\mu mols \cdot m^{-2} \cdot s^{-1}$. (16:8_100) Photoperiod of 16:8 h, light intensity of 100 $\mu mols \cdot m^{-2} \cdot s^{-1}$. (24:0_70) Photoperiod of 24:0 h, light intensity of 70 $\mu mols \cdot m^{-2} \cdot s^{-1}$. (24:0_100) Photoperiod of 24:0 h, light intensity of 100 $\mu mols \cdot m^{-2} \cdot s^{-1}$.

Table 1: Growth parameters and biomass production of *Desmonostoc salinum* CCM-UFV059 grown under distinct photoperiods and light intensities. Maximum growth rate (μ_{max}) and Generation time (*Gt*) were measured considering the log phase; Biomass production was determined after seven days of exposure to the treatments. Values represent mean ± SE from five biological replicates. For biomass production, means followed by the same letter were not significantly different (P<0.05) by Student's *t*-test.

	16:8_70	**16:8_100**	**24:0_70**	**24:0_100**
μ_{max}	0.212 d^{-1}	0.138 d^{-1}	0.153 d^{-1}	0.155 d^{-1}
Gt	1.41 d^{-1}	2.17 d^{-1}	1.96 d^{-1}	1.93 d^{-1}
Log phase*	3 days	5 days	5 days	5 days
Biomass production#	0.74 ± 0.02 **b**	0.68 ± 0.01 **b**	1.62 ± 0.04 **a**	1.58 ± 0.01 **a**

*Log phase duration; # ($g.L^{-1}$)

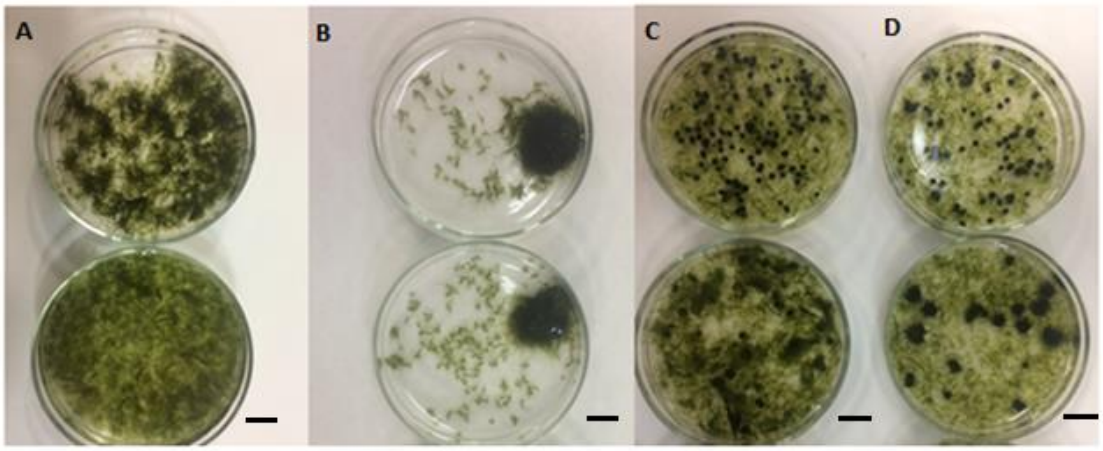

Figure 2: Macroscopic aspect of *Desmonostoc salinum* CCM-UFV059 grown in liquid BG-11_0 culture medium, under distinct photoperiods and light intensities. The pictures were taken on the 7^{th} day of growth without disrupted the colony structure. (A) Photoperiod of 16:8 h, light intensity of 70 µmols·m^{-2}·s^{-1}. (B) Photoperiod of 16:8 h, light intensity of 100 µmols·m^{-2}·s^{-1}. (C) Photoperiod of 24:0 h, light intensity of 70 µmols·m^{-2}·s^{-1}. (D) Photoperiod of 24:0 h, light intensity of 100 µmols·m^{-2}·s^{-1}. Scale bar = 1 cm.

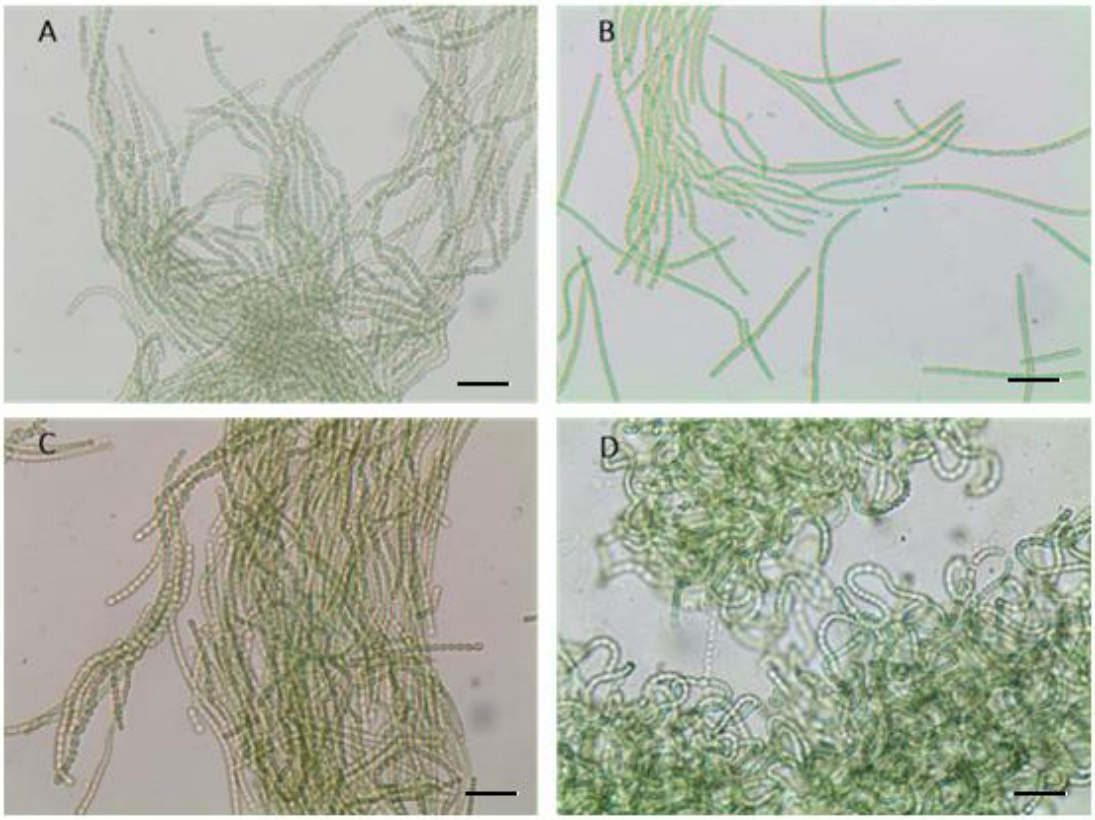

Figure 3: Microscopic aspect of *Desmonostoc salinum* CCM-UFV059 cultured in liquid BG-11_0 culture medium, under distinct photoperiods and light intensities. The pictures were taken on the 7^{th} day of growth. The pictures represent the predominant aspect of the colonies after softly homogenization with syringe. (A) Photoperiod of 16:8 h, light intensity of 70 µmols·m^{-2}·s^{-1}. (B) Photoperiod of 16:8 h, light intensity of 100 µmols·m^{-2}·s^{-1}. (C) Photoperiod of 24:0 h, light intensity of 70 µmols·m^{-2}·s^{-1}. (D) Photoperiod of 24:0 h, light intensity of 100 µmols·m^{-2}·s^{-1}. Scale bar = 40 µm.

Table 2: Biochemical parameters of *Desmonostoc salinum* CCM-UFV059 grown under distinct photoperiods and light intensities. The sampling point was in the middle of the 7th day of growth. The values are expressed in $\mu g \cdot mg^{-1}$ dry weight. Values represent mean ± SE from five biological replicates. Means, in the same line, followed by the same letter were not significantly different (P<0.05) by Student's *t*-test.

Metabolite	**16:8_70**	**16:8_100**	**24:0_70**	**24:0_100**
Chlorophyll	15.0 ± 0.04 **b**	21.35 ± 1.2 **a**	5.71 ± 0.7 **c**	6.04 ± 1.0 **c**
Amino acids	2.8 ± 0.3 **b**	2.03 ± 0.4 **c**	3.09 ± 0.2 **a**	3.75 ± 0.4 **a**
Soluble carbohydrates	206.2 ± 6.5 **c**	236.3 ± 8.7 **b**	201.75 ± 7.0 **c**	263.84 ± 5.9 **a**
Total proteins	151.2 ± 6.0 **b**	208.3 ± 8.5 **a**	130.47 ± 2.5 **c**	131.59 ± 4.1 **c**
Phycobiliproteins	15.7 ± 3.4 **b**	23.81 ± 3.2 **a**	22.53 ± 3.2 **a**	22.87 ± 2.0 **a**
Glycogen	1.9 ± 0.2 **b**	3.23 ± 0.2 **a**	3.13 ± 0.6 **a**	3.66 ± 0.06 **a**
Cyanophycin	6.2 ± 0.5 **c**	12.84 ± 0.8 **a**	10.43 ± 0.4 **b**	12.59 ± 0.6 **a**
Neutral lipids	19.5 ± 2.9 **a**	7.74 ± 1.1 **b**	7.8 ± 1.0 **b**	3.8 ± 0.7 **c**

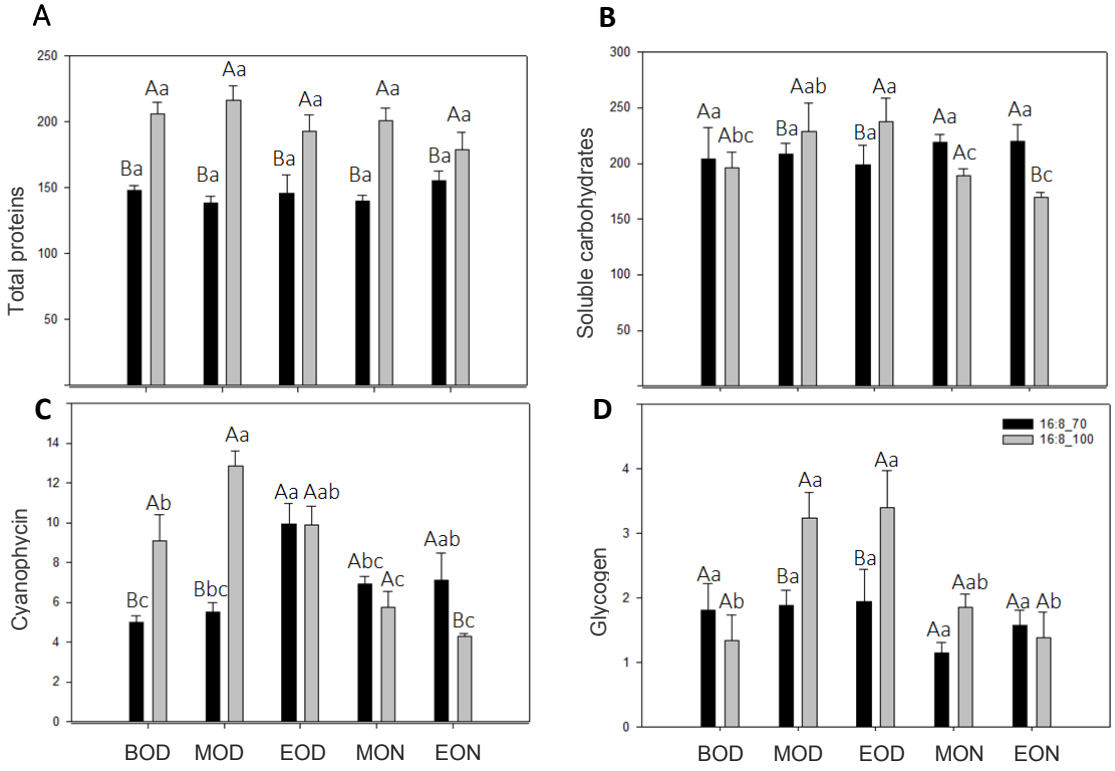

Figure 4: Biochemical parameters of *Desmonostoc salinum* CCM-UFV059 grown under the treatments 16:8 h_70 µmol·m^{-2}·s^{-1} and 16:8 h_100 µmol·m^{-2}·s^{-1}. The sampling points correspond to BOD (0 h): Beginning of the day; MOD (8 h): Middle of the day; EOD (16 h): End of the day; MON: Middle of the night (20 h); EON: End of the night (24 h), totalizing 24 hours. (A) Total protein; (B) Soluble carbohydrates; (C) Cyanophycin; and (D) Glycogen, expressed in µg.mg dry weight^{-1}. Values represent mean ± SE from five biological replicates. Means, in the same line, followed by the same letter were not significantly different (P<0.05) by Student's *t*-test. Low case letter: comparison between averages in the same treatment. Uppercase letter: comparison between averages of different treatments at the same time.

Table 3: Gas exchange measurements and chlorophyll fluorescence parameters of *Desmonostoc salinum* CCM-UFV059 grown under distinct photoperiods and light intensities. Photosynthetic (*A*) and respiratory (*Rd*) measurements were performed on the 3rd and 7th days of growth. The maximum quantum yield of photosystem II (F_v/F_m) and the photochemical efficiency of photosystem II adapted to light (ΦPSII) were measured in the 7th day of growth. Values represent mean ± SE from five biological replicates. Means, in the same line, followed by the same letter were not significantly different ($P<0.05$) by Student's *t*-test.

	16:8_70	**16:8_100**	**24:0_70**	**24:0_100**
A (Day 3)	4.35 ± 0.35 **a**	4.05 ± 0.42 **a**	4.42 ± 0.14 **a**	4.66 ± 0.45 **a**
A **(**Day 7)	2.98 ± 0.14 **a**	1.88 ± 0.13 **b**	1.89 ± 0.02 **b**	2.01 ± 0.03 **b**
Rd (Day 3)	0.84 ± 0.07 **b**	0.98 ± 0.05 **b**	1.70 ± 0.02 **a**	1.55 ± 0.11 **a**
Rd (Day 7)	0.57 ± 0.06 **a**	0.59 ± 0.04 **a**	0.32 ± 0.01 **b**	0.30± 0.01 **b**
F_v/F_m	0.47 ± 0.009 **a**	0.46 ± 0.01 **a**	0.42 ± 0.006 **a**	0.46 ± 0.02 **a**
ΦPSII	0.44 ± 0.009 **a**	0.37 ± 0.01 **b**	0.35 ± 0.008 **b**	0.2 ± 0.02 **c**

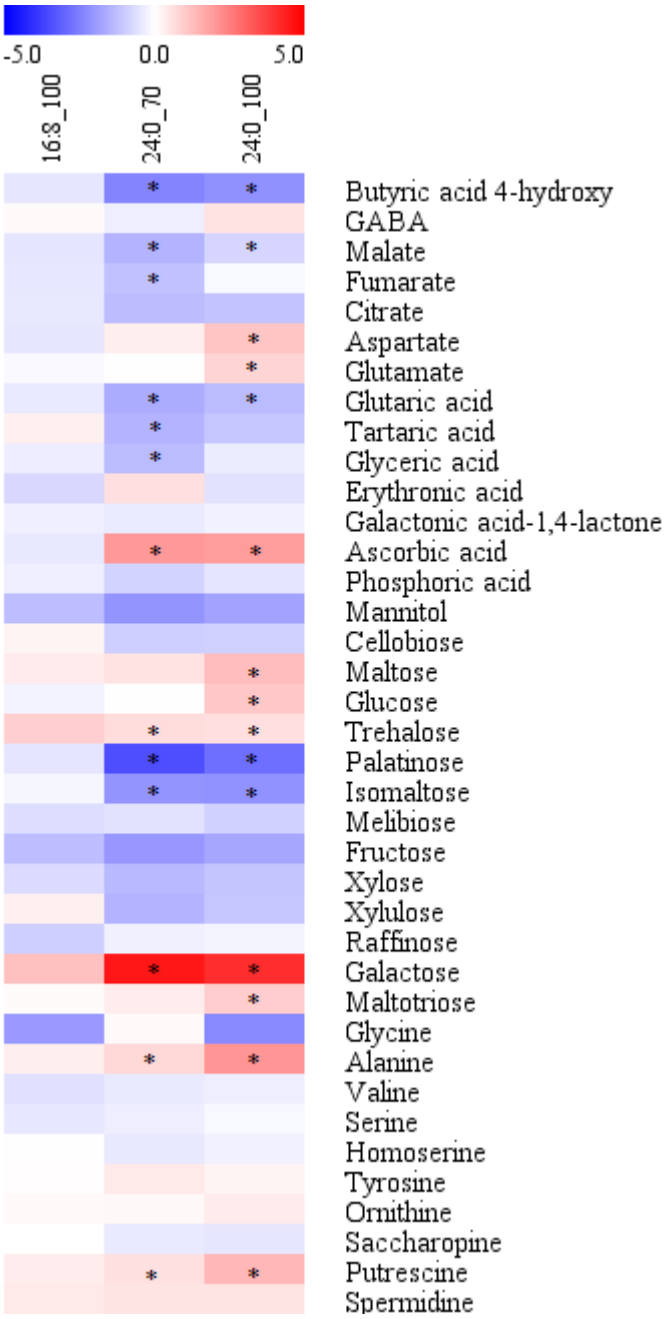

Figure 5: Metabolic profile of *Desmonostoc salinum* CCM-UFV059 grown under distinct photoperiods and light intensities in BG-11_0 medium. The sampling point was on the 7th day of growth. The full datasets from these metabolic profiling studies are additionally available in Supplementary Table 1. The colour code of the heat map is given as the X-fold changes. Data are normalized with respect to the mean response calculated for the control (16:8_70) of each strain (to allow statistical assessment, individual replicates from this set were normalized in the same way). Values represent

mean ± SE from five biological replicates. Asterisks designate values that were significantly different from control (P<0.05) by Student's t-test. (16:8_70) Photoperiod of 16:8 h, light intensity of 70 µmols·m^{-2}·s^{-1}. (16:8_100) Photoperiod of 16:8 h, light intensity of 100 µmols·m^{-2}·s^{-1}. (24:0_70) Photoperiod of 24:0 h, light intensity of 70 µmols·m^{-2}·s^{-1}. (24:0_100) Photoperiod of 24:0 h, light intensity of 100 µmols·m^{-2}·s^{-1}.

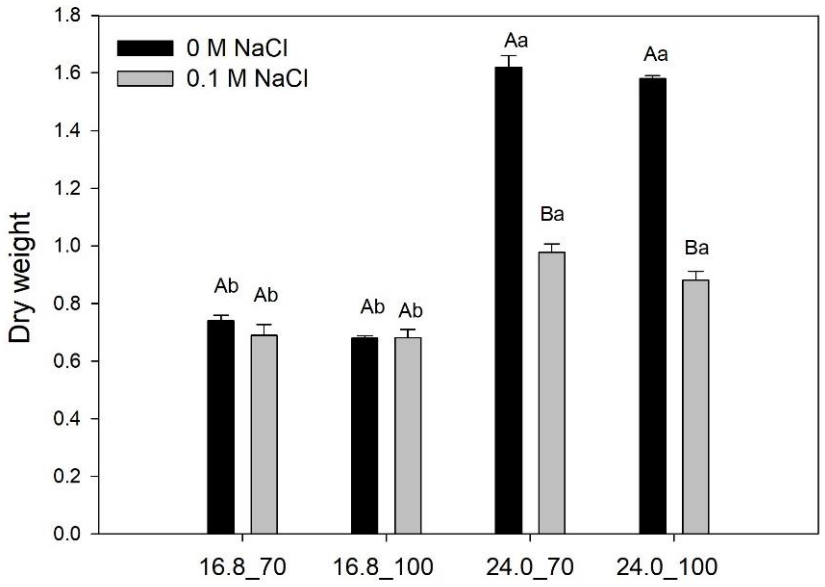

Figure 6: Biomass production of *Desmonostoc salinum* CCM-UFV059 grown in BG-11_0 supplemented with and without 0.1 M NaCl, during seven days, applying distinct photoperiods and light intensities. Biomass production expressed in dry weight (mg/mL). Values represent mean ± SE from five biological replicates. Means followed by the same letter were not significantly different (P<0.05) by Student's t-test. Low case letter: comparison between averages in the same treatment. Uppercase letter: comparison between averages of different treatments at the same time.

Table 4: Gas exchange measurements of *Desmonostoc salinum* CCM-UFV059 grown in BG-11_0 supplemented with 0.1 M NaCl under distinct photoperiods and light intensities. Values represent mean ± SE from five biological replicates. Means, in the same line, followed by the same letter were not significantly different (P<0.05) by Student's *t*-test.

	16:8_70	**16:8_100**	**24:0_70**	**24:0_100**
A (Day 3)	1.79 ± 0.20 **b**	1.95 ± 0.16 **a**	1.24 ± 0.52 **b**	2.24 ± 0.40 **a**
A **(**Day 7)	2.43 ± 0.32 **a**	3.64 ± 0.31 **a**	1.39 ± 0.11 **b**	1.80 ± 0.45 **b**
Rd (Day 3)	0.16 ± 0.03 **b**	0.16 ± 0.09 **b**	1.01 ± 0.26 **a**	1.01 ± 0.19 **a**
Rd (Day 7)	0.42 ± 0.03 **b**	0.72 ± 0.09 **a**	0.29 ± 0.01 **c**	0.42 ± 0.03 **b**

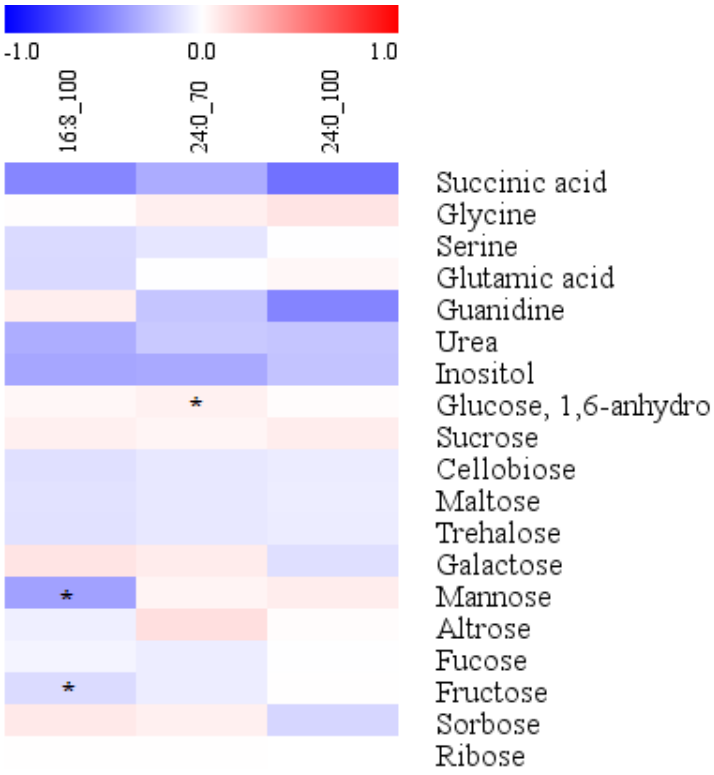

Figure 7: Metabolic profile of *Desmonostoc salinum* CCM-UFV059 grown in BG-11_0 supplemented with 0.1 M of NaCl under distinct photoperiods and light intensities. The sampling point was on the 7th day of growth. The full datasets from these metabolic profiling studies are additionally available in Supplementary Table 1. The colour code of the heat map is given as the x-fold changes. Data are normalized with respect to the mean response calculated for the control (16:8_70) of each strain (to allow statistical assessment, individual replicates from this set were normalized in the same way). Values represent mean ± SE from five biological replicates. Asterisks designate values that were significantly different from control (P<0.05) by Student's *t*-test. (16:8_70) Photoperiod of 16:8 h, light intensity of 70 µmols·m^{-2}·s^{-1}. (16:8_100) Photoperiod of 16:8 h, light intensity of 100 µmols·m^{-2}·s^{-1}. (24:0_70) Photoperiod of 24:0 h, light intensity of 70 µmols·m^{-2}·s^{-1}. (24:0_100) Photoperiod of 24:0 h, light intensity of 100 µmols·m^{-2}·s^{-1}.

SUPPLEMETARY DATA

Table 1: Dataset from relative levels of identified metabolites of *D. salinum* CCM-UFV059 grown in BG-11_0 exposure to distinct photoperiods and light intensities. . (16:8_70) Photoperiod of 16:8 h, light intensity of 70 µmols·m^{-2}·s^{-1}. (16:8_100) Photoperiod of 16:8 h, light intensity of 100 µmols·m^{-2}·s^{-1}. (24:0_70) Photoperiod of 24:0 h, light intensity of 70 µmols·m^{-2}·s^{-1}. (24:0_100) Photoperiod of 24:0 h, light intensity of 100 µmols·m^{-2}·s^{-1}.

	16:8		**24:0**	
Metabolites	**70**	**100**	**70**	**100**
Butyric acid 4-hydroxy	1.000	0.718	0.189	0.223
GABA	1.000	1.081	0.800	1.478
Malate	1.000	0.704	0.358	0.568
Fumarate	1.000	0.731	0.431	0.914
Citrate	1.000	0.737	0.406	0.444
Aspartate	1.000	0.712	1.266	2.256
Glutamate	1.000	0.925	1.017	1.805
Glutaric acid	1.000	0.745	0.327	0.398
Tartaric acid	1.000	1.236	0.357	0.466
Glyceric acid	1.000	0.787	0.398	0.780
Erythronic acid	1.000	0.592	1.554	0.676
Galactonic acid-1,4-lactone	1.000	0.809	0.770	0.832
Ascorbic acid	1.000	0.732	4.086	3.859
Phosphoric acid	1.000	0.804	0.550	0.707
Mannitol	1.000	0.411	0.234	0.287
Cellobiose	1.000	1.162	0.521	0.528
Maltose	1.000	1.330	1.497	2.476
Glucose	1.000	0.852	1.022	2.138
Trehalose	1.000	1.935	1.602	1.563
Palatinose	1.000	0.708	0.091	0.140
Isomaltose	1.000	0.888	0.236	0.227
Melibiose	1.000	0.632	0.676	0.537
Fructose	1.000	0.408	0.243	0.300
Xylose	1.000	0.617	0.387	0.449
Xylulose	1.000	1.236	0.357	0.466
Raffinose	1.000	0.523	0.817	0.868
Galactose	1.000	2.377	23.581	17.505
Maltotriose	1.000	1.068	1.278	1.992
Glycine	1.000	0.251	1.077	0.204

Alanine	1.000	1.270	1.708	4.261
Valine	1.000	0.671	0.758	0.801
Serine	1.000	0.722	0.804	0.913
Homoserine	1.000	1.014	0.734	0.833
Tyrosine	1.000	1.042	1.358	1.172
Ornithine	1.000	1.086	1.102	1.329
Saccharopine	1.000	1.012	0.749	0.715
Putrescine	1.000	1.300	1.542	2.689
Spermidine	1.000	1.364	1.448	1.460

Table 2: Dataset from relative levels of identified metabolites of *D. salinum* CCM-UFV059 grown in BG-11_0 supplemented with 0.1 M of NaCl and exposure to distinct photoperiods and light intensities. . (16:8_70) Photoperiod of 16:8 h, light intensity of 70 µmols·m^{-2}·s^{-1}. (16:8_100) Photoperiod of 16:8 h, light intensity of 100 µmols·m^{-2}·s^{-1}. (24:0_70) Photoperiod of 24:0 h, light intensity of 70 µmols·m^{-2}·s^{-1}. (24:0_100) Photoperiod of 24:0 h, light intensity of 100 µmols·m^{-2}·s^{-1}.

	16:8		**24:0**	
Metabolites	**70**	**100**	**70**	**100**
Succinic acid	1.000	0.336	0.473	0.279
Glycine	1.000	1.024	1.166	1.279
Serine	1.000	0.717	0.802	0.992
Glutamic acid	1.000	0.710	1.000	1.083
Guanidine	1.000	1.173	0.595	0.332
Urea	1.000	0.479	0.616	0.596
Inositol	1.000	0.450	0.461	0.585
Glucose, 1,6-anhydro	1.000	1.078	1.140	1.035
Sucrose	1.000	1.151	1.103	1.181
Cellobiose	1.000	0.758	0.817	0.843
Maltose	1.000	0.772	0.814	0.854
Trehalose	1.000	0.768	0.819	0.849
Galactose	1.000	1.279	1.189	0.756
Mannose	1.000	0.430	1.107	1.180
Altrose	1.000	0.870	1.336	1.031
Fucose	1.000	0.910	0.856	0.999
Fructose	1.000	0.727	0.855	1.015
Sorbose	1.000	1.225	1.150	0.696
Ribose	1.000	1.011	1.011	1.005

CONCLUDING REMARKS

The presented study consisted of the analysis of a newly isolated cyanobacterium by using several distinct but complementary experimental approaches. *Desmonostoc salinum* CCM-UFV059 was isolated from the Laguna Amarga, a harsh environment with high pH and salinity. Noteworthy, the characterization of a cyanobacteria species from the *Nostocales* family in such environment instigated the development of this research initiative since heterocytous cyanobacteria are rarely found in saline ecosystems. Moreover, cyanobacteria from such extreme environments are potential sources of novel genes and products and important targets for biotechnological applications. As such, after the polyphasic identification a novel species, named *Desmonostoc salinum* sp. nov., with *Desmonostoc salinum* CCM-UFV059 as reference strain, was erected. The proposal was given under the provisions of the International Code of Nomenclature for algae, fungi and plants and this finding extends the ecological coverage of the genus *Desmonostoc*, contributing to a better understanding of its diversity and systematic. Remarkably, this was the first report of a *Desmonostoc* in a saline environment. Interestingly, we could observe the remarkable salt and desiccation tolerance displayed by *Desmonostoc salinum* CCM-UFV059 when compared with the Nostocales model strain to stress response, *Nostoc* sp. PCC7120. The results obtained here indicate that the tolerance toward both stresses is most likely an adaptation feature to the environment of Laguna Amarga. This was obtained by the combination of different mechanisms including the maintenance of low cellular Na^+ concentrations associated with the accumulation of high amounts of sucrose and to a lower extent trehalose as well as the presence of highly unsaturated lipids in the membrane. We postulate that following the complete genome sequencing of strain, a fact already under

development, *Desmonostoc salinum* CCM-UFV059 presents itself as a new heterocytous cyanobacteria model for environmental stress response. Further investigations on the mechanisms allowing this strain to cope with distinct environmental constraint would help clarify how the rapid evolution of salt-resistance occurred in this ubiquitous cyanobacterial strain.

Our hope is that the results presented within this thesis will introduce the strain *D. salinum* CCM-UFV059 to researchers beyond the ecology and cyanobacterial physiology (e.g. molecular biologists, biochemists, stress biologists, evolutionary biology), who may have interest in using this wonderful and versatile model to address several long-standing questions in cyanobacterial stress physiology.

To further define possible biotechnological applications of *Desmonostoc salinum* CCM-UFV059 we analyzed the biomass production in response to light availability. We observed that changes in light intensity altered the cellular type, the colony structure and, consequently, the biomass composition of *Desmonostoc salinum* CCM-UFV059. Moreover, it was possible to correlate different light regimes with changes in the metabolism and in the production of specific metabolites. It seems reasonable to suggest that the ability of *Desmonostoc salinum* CCM-UFV059 to growth in saline/brackish water opens possibilities to produce cyanobacterial biomass with a reduced cost. This is even more important in regions that comprise large brackish water aquifers that cannot be used for agriculture and/or human consumption, such as in the northeast of Brazil. It is important to mention that such brackish water usually contains high content of calcium and magnesium besides sodium, similarly to the conditions found in the Laguna Amarga environment. *Desmonostoc salinum* CCM-UFV059 biomass could be also used to feed animals, such as fish or even swine, since it was not detected the presence of any cyanotoxin or gene from cyanotoxin production

pathways in this strain. On top of that, the relatively high amount of protein observed in *Desmonostoc salinum* CCM-UFV059 provide further support to the usage of this strains as food for animals. Nevertheless, further research is clearly required in order to enable the large scale cultivation *Desmonostoc salinum* CCM-UFV059 aiming at its commercial use; it is important to mention, however, that this application mean the utilization of an abundant and inexpensive resource, such as brackish water, to generate food and stimulate regional economy.

Overall, this research initiative is of crucial importance for the bioprospection of genes, pathways and products that may be used for biotechnological purposes in the future. Further analysis using genomics and transcriptomics approaches will aid to our understanding of the physiological plasticity and adaptive strategies of *Desmonostoc salinum* CCM-UFV059. The results presented here coupled with the current knowledge over salt tolerance in cyanobacteria allow us to conclude that *Desmonostoc salinum* CCM-UFV059 present a great biotechnological potential that must be explored in the future.